

**A HIGH RESOLUTION DIGITAL SYSTEM FOR AUTOMATED AERIAL  
SURVEYING**


**Andrew Stuart Coleman**

Submitted in partial fulfilment of  
the requirements for the degree of  
MSc Eng

School of Bioresource Engineering and Environmental Hydrology  
University of Natal  
Pietermaritzburg  
South Africa

December 2000

I wish to certify that the work reported in this dissertation is my own unaided work except where specific acknowledgement is made.

Signed:   
A.S. Coleman

## ACKNOWLEDGEMENTS

Prof AC Hansen, Professor, School of Bioresource Engineering and Environmental Hydrology, University of Natal, for supervising this project and for his invaluable assistance, guidance and support throughout.

Prof PWL Lyne, Head of Department, School of Bioresource Engineering and Environmental Hydrology, University of Natal, for his guidance and support during this project.

MBB Consulting Engineers, Inc., for providing the opportunity and financial support to develop the system for my MScEng project. In particular, Messrs James Brodie and Kevin Meier are to be thanked for their continuous assistance and input during this project. Mr Alick Rennie also provided useful input for the pre-flight planning software and gave up his time to fly an initial test flight.

Messrs Rob and Hal Wooding of Rob Wooding and Associates for kindly lending me their Kodak DCS420 digital camera and associated computer peripherals for my project.

Dr Gavin Hough and the staff at Techtrix International for their assistance and ideas regarding the computer programming aspects of this project.

Mr S Lynch, School of Bioresource Engineering and Environmental Hydrology, University of Natal, for his guidance during the computer programming and debugging aspects of this project.

Mr CC Tredrea, senior technician, School of Bioresource Engineering and Environmental Hydrology, University of Natal, for his help in interfacing with the GPS.

Mr Rob North, chief technician, School of Bioresource Engineering and Environmental Hydrology, University of Natal, for his assistance in building a camera mount.

The University of Natal and the Foundation for Research Development for financial support.

Jeff of Light Flight, Cato Ridge for offering his time and Jabiru light aircraft for flying the official test flight of the system.

The staff at the Geographical Information Management Systems' (GIMS) Photogrammetry lab for kindly offering their time and Orthobase software to process my digital images. In particular, Dirk Craigie is to be thanked for his time, expertise and valuable input.

A special thanks to my fiancée Aukje and my family for all their support, patience and understanding while I was trying to complete my Msc. Their backing was invaluable.

## TABLE OF CONTENTS

|  | Page |
|--|------|
| <b>1. INTRODUCTION</b> .....   | 1    |
| <b>2. EXISTING AERIAL VIDEOGRAPHY SYSTEM</b> .....                                     | 5    |
| 2.1 Pre-flight Planning .....  | 5    |
| 2.1.1 Procedure .....  | 5    |
| 2.1.2 Limitations .....  | 6    |
| 2.2 Image Acquisition .....  | 8    |
| 2.2.1 Equipment .....  | 9    |
| 2.2.2 Limitations .....  | 16   |
| 2.3 Post-flight Image Processing and GIS Input .....                                   | 16   |
| 2.3.1 Equipment .....  | 17   |
| 2.3.2 Procedure .....  | 19   |
| 2.3.3 Limitations .....  | 21   |
| <b>3. DIGITAL STILL CAMERAS: STATUS AND APPLICATIONS</b> .....                         | 23   |
| 3.1 Characteristics and Operation .....  | 23   |
| 3.2 Advantages .....   | 25   |
| 3.3 Disadvantages .....  | 28   |
| 3.4 Applications .....   | 30   |
| 3.4.1 Vegetation monitoring and mapping .....  | 31   |
| 3.4.2 Land use mapping, environmental analyses and resource database<br>updating ..... | 36   |
| 3.4.3 DEM and orthophoto generation .....  | 38   |
| 3.4.4 Other .....  | 41   |

|  | <b>Page</b> |
|--|-------------|
| <b>4. PRE-FLIGHT PLANNING IMPROVEMENTS</b> .....         | 46          |
| 4.1 Program Inputs .....                                 | 46          |
| 4.1.1 Camera and lens parameters .....                   | 47          |
| 4.1.2 Ground pixel size .....                            | 47          |
| 4.1.3 Catchment generate file .....                      | 47          |
| 4.1.4 Digital elevation model .....                      | 47          |
| 4.1.5 Overlap requirements .....                         | 49          |
| 4.2 Program Outputs .....                                | 49          |
| 4.2.1 Flight line spacing .....                          | 49          |
| 4.2.2 Flight strip way point coordinates .....           | 53          |
| 4.2.3 Flying time summary .....                          | 56          |
| 4.2.4 Photograph/image positions .....                   | 57          |
| 4.2.5 GPS way point file .....                           | 61          |
| <br>   |             |
| <b>5. IMAGE ACQUISITION SYSTEM</b> .....                 | 62          |
| 5.1 The Sensor .....                                     | 62          |
| 5.1.1 Cost-benefit analysis .....                        | 70          |
| 5.2 Camera Mount .....                                   | 83          |
| 5.3 Global Positioning System (GPS) .....                | 84          |
| 5.3.1 Standard GPS errors .....                          | 84          |
| 5.3.2 Differential GPS .....                             | 85          |
| 5.3.3 Carrier-phase GPS .....                            | 87          |
| 5.3.4 Further considerations .....                       | 88          |
| 5.3.5 The Trimble Pro-XRS GPS .....                      | 89          |
| 5.4 GPS Interface .....                                  | 91          |
| 5.5 Camera Control Interface .....                       | 94          |
| 5.6 In-flight Graphical User Interface and Program ..... | 95          |

|  | <b>Page</b> |
|--|-------------|
| <b>6. SYSTEM VERIFICATION</b> .....                  | 98          |
| 6.1 Initial Qualitative Testing and Refinement ..... | 98          |
| 6.2 Quantitative Testing .....                       | 102         |
| 6.3 Test Flight .....                                | 106         |
| 6.4 Image Spatial Accuracy Assessment .....          | 107         |
| 6.4.1 Rubbersheeting and mosaicing .....             | 107         |
| 6.4.2 Aerotriangulation and bundle adjustment .....  | 109         |
| 6.4.3 Camera calibration .....                       | 113         |
| 6.4.4 GCP survey .....                               | 117         |
| 6.4.5 Photogrammetric process .....                  | 121         |
| 6.4.6 Bundle block adjustment results .....          | 126         |
| <br>   |             |
| <b>7. DISCUSSION AND CONCLUSION</b> .....            | 135         |
| <br>   |             |
| <b>8. REFERENCES</b> .....                           | 145         |

## LIST OF FIGURES

| Figure | Page   |
|--------|--|
| 1      | Example 1 of the potential for data loss at the start or end of flight strips ..... 7  |
| 2      | Example 2 of the potential for data loss at the start or end of flight strips ..... 7  |
| 3      | The existing airborne videography image acquisition system ..... 9   |
| 4      | Flowchart of post-flight mapping process ..... 19  |
| 5      | The pre-flight planning graphical user interface ..... 46  |
| 6      | Flowchart depicting procedure for reading a DEM ..... 48   |
| 7      | Flowchart of algorithm for calculating the flight strip spacing ..... 50   |
| 8      | The altitude percentiles form ..... 52   |
| 9      | Flowchart of algorithm to determine initial flight line way point coordinates ..... 54   |
| 10     | Flow diagram of algorithm to ensure no loss of data at the ends of flight strips ..... 55  |
| 11     | The program summary of flying times ..... 56   |
| 12     | Flowchart of algorithm for calculating photograph positions ..... 59   |
| 13a    | Example of photograph or image that would be excluded ..... 60   |
| 13b    | Example of photograph or image that would be included ..... 60   |
| 14     | The Kodak DCS420 digital camera ..... 66   |
| 15     | Algorithm used in cost-benefit analysis spreadsheet to calculate flying time and total<br>number of photographs/images to be captured. .... 74 |
| 16     | Cost (R/ha) vs survey area (km <sup>2</sup> ) for different systems at 1m ground pixel resolution.<br>..... 75                                 |
| 17     | Cost (R/ha) vs survey area (km <sup>2</sup> ) for different systems at 0.5m ground pixel resolution.<br>..... 77                               |
| 18     | Cost (R/ha) vs survey area (km <sup>2</sup> ) for different systems at 2m ground pixel resolution.<br>..... 78                                 |
| 19     | Total processing time per survey (days) vs survey area (km <sup>2</sup> ). .... 79   |
| 20     | Cost (R/ha) vs survey area (km <sup>2</sup> ) for varying numbers of surveys per year. .... 81   |
| 21     | Flowchart of OnTriggerData event for reading the GPS NMEA strings and triggering the<br>camera ..... 92  |



| <b>Figure</b>   | <b>Page</b> |
|---|-------------|
| 22 The in-flight GUI .....  | 96          |
| 23 Revised algorithm for OnTrigger event .....  | 100         |
| 24 Flow chart of aerotriangulation process .....  | 110         |
| 25 Camera calibration grid layout .....   | 115         |
| 26 Example of desired GCP position .....  | 118         |
| 27 Example of completed GCP locality plot. ....   | 119         |
| 28 Example of perspective distortion between two images from different flight lines.<br>..... | 122         |
| 29 Orthobase GCP measurement window. ....   | 123         |
| 30 Incorrect measurement of GCP number 1. ....  | 127         |
| 31 Image 4-13 showing the distortion due to the incorrect measurement of GCP 1.<br>.....      | 128         |
| 32 Example 1 of cadastral boundaries overlaid on digital camera orthophotographs.<br>.....    | 130         |
| 33 Example 2 of cadastral boundaries overlaid on digital camera orthophotographs.<br>.....    | 131         |
| 34 Example 3 of cadastral boundaries overlaid on digital camera orthophotographs<br>.....     | 132         |
| 35 Example 4 of cadastral boundaries overlaid on digital camera orthophotographs.<br>.....    | 133         |

## LIST OF TABLES

| Table |   | Page |
|-------|---|------|
| 1     | Panasonic WV-CL352 video camera specifications . . . . .                            | 10   |
| 2     | Panasonic AG-5700 video cassette recorder specifications . . . . .                  | 13   |
| 3     | Panasonic WV-BM900 video monitor specifications . . . . .                           | 14   |
| 4     | Panasonic TC-1470Y video monitor specifications . . . . .                           | 18   |
| 5     | Garmin GPS way point coordinate file . . . . .                                      | 61   |
| 6     | Summary of characteristics of available digital cameras . . . . .                   | 63   |
| 7     | Kepner-Tregoe decision analysis for digital cameras . . . . .                       | 64   |
| 8     | Kodak DCS420 and DCS460 digital camera specifications . . . . .                     | 67   |
| 9     | Costs and times used in the cost-benefit analysis . . . . .                         | 73   |
| 10    | Summary of GPS error sources . . . . .  | 85   |
| 11    | RMS errors for averaged GPS positions and instantaneous GPS positions . . . . .     | 103  |
| 12    | Maximum errors for averaged GPS positions and instantaneous GPS positions . . . . . | 104  |
| 13    | Maximum triggering errors of in-flight system. . . . .                              | 105  |
| 14    | Camera calibration results . . . . .  | 116  |
| 15    | Exterior orientation parameters. . . . .  | 126  |

## ABSTRACT

Resource managers frequently require moderate to high resolution imagery within short turn-around periods for use in a GIS-based management system. These spatial data can greatly enhance their ability to make timely, cost-saving decisions and recommendations.

MBB Consulting Engineers, Inc., of Pietermaritzburg, South Africa had for many years made use of airborne videography to provide the imagery for several resource-based applications. Applications included detailed land use mapping in various South African river catchments and identification, density classification and mapping of alien vegetation. While the system was low cost and easy to operate, MBB had found that their system was inherently limited, particularly by its lack of automation and poor spatial resolution. This project was started because of a need to address these limitations and provide an airborne remote sensing system that was more automated and could produce higher resolution imagery than the existing system. In addition, the overall cost and time required to produce a map of the resource of interest needed to be reduced.

The system developed in this project aimed to improve upon the pre-flight planning and in-flight image acquisition aspects of the existing system. No new post-flight image processing procedures were developed, but possible future refinement of the post-flight image processing routine was considered throughout the development of the system. A pre-flight planning software package was developed that could quickly and efficiently calculate the positions of flight lines and photographs or images with a minimum of user input. The in-flight image acquisition setup developed involved the integration of a high resolution digital still camera, a Global Positioning System (GPS), and camera control software. The use of the rapidly developing and improving technology of a digital still camera was considered to be a better alternative than a videographic or traditional film camera system for a number of reasons. In particular, digital still cameras produce digital imagery without the need for development and scanning of aerial photographs or framegrabbing of video images. Furthermore, the resolution of current digital still cameras is already significantly better than that of video cameras and is rivalling the resolution of 35mm film.

The system developed was tested by capturing imagery of an urban test area. The images obtained were then rectified using photogrammetric techniques. Results obtained were promising with planimetric accuracies of 5 to 10m being obtained. From this test it was concluded that for high

accuracy applications involving numerous images, use would be made of softcopy photogrammetric software to semi-automatically position and rectify images, while for applications requiring fewer images and lower accuracy, images could be rectified using the simpler technique of assigning GCPs for each image from scanned orthophotos.

## 1. INTRODUCTION

Natural resource managers are frequently in need of moderate to high resolution digital imagery within a short period of time for updating and complementing existing spatial databases of natural resources. Such imagery, particularly if it can be coupled with the convenience and powerful processing and analysis capabilities of the contemporary Geographical Information System (GIS), can greatly enhance a resource manager's ability to make timely, cost-saving and defensible decisions and recommendations. Imagery of this kind can also greatly improve the communication between a resource manager and his client by providing easily accessible and understood visual information about an area. For the past 10 to 15 years airborne videography has provided a means of obtaining this imagery.

While videography cannot be viewed as a replacement for aerial photography or satellite remote sensing, there are several reasons why airborne videography has been considered as an alternative to these more traditional and frequently used remote sensing alternatives. Some of the advantages of video which are commonly recognised by researchers are near-real-time availability of imagery for visual assessment or computer image processing, low running costs relative to aerial photography, and availability of a 'live' image during flight as assurance that a particular site is being covered and as an aid in navigating along narrow, winding flight lines. Researchers also indicate that video can be obtained under high overcast or broken cloud conditions whereas photographic imagery cannot (Pywell and Myhre, 1992). This is due to video's provision for real time adjustment of camera gain settings and iris control (Brownlie *et al.*, 1996). The fact that a PAL video image is acquired every 1/25 of a second is a further advantage of video. This is important where narrow biological windows are involved since it allows multiple images of a scene or target to be produced thereby ensuring that vital information will not be lost (Mausel *et al.*, 1992).

MBB Consulting Engineers, Inc., Pietermaritzburg, South Africa recognised the benefits of airborne videography and developed a video-based aerial survey system in 1992. Their system has since been widely applied in the mapping and management of natural resources. Some of the applications of the system include:

- 1) Detailed land use mapping in various South African river catchments for the purposes of hydrological modelling. Catchments surveyed include the upper Mvoti, upper Tugela and Lovu river catchments in the Kwazulu-Natal province, South Africa.
- 2) The combining of airborne video and ground survey data of McGregor village, which is situated near Cape Town in the Cape Province of South Africa, to establish whether the existing water resources were being effectively and efficiently used. This study was conducted with a view to building a new dam to provide additional water to allow expansion of the village and local farming ventures.
- 3) Identification, density classification and mapping of alien vegetation in the upper Tugela, upper Lovu and upper Mvoti river catchments. For the upper Lovu and upper Mvoti catchments, the information contained in the maps produced was used to assess whether the cost of clearing the alien vegetation from the riparian zones of rivers could be offset by the potential benefits of increased water yield. In all studies, the maps derived were used in the planning and implementation stages of the process of clearing the alien vegetation.

MBB found their video system to be a very low cost, low maintenance and easily manageable unit. They were able to produce maps that were suitably accurate for the applications outlined above within a short period of time and at a fraction of the cost of photographic or satellite-derived information. They did, however, emphasise that their airborne survey system could be improved as there were several shortfalls or limitations of the system. These limitations, which included a lack of automation and poor spatial resolution, are described in detail in Chapter 3. This project was begun to address these limitations and improve MBB's airborne remote sensing system.

The objective of this project was to develop an airborne survey system that was more effective than MBB's airborne videography system. The system developed had to take into consideration the pre-flight planning, image acquisition and post-flight processing aspects of an airborne survey mission. Furthermore, the following basic requirements of the system had to be met:

- 1) The system had to be considerably more automated than the present videography system.
- 2) The system had to produce images of equal or improved spatial resolution when compared with the present system.

- 3) The overall cost of performing a survey and producing maps of the resource of interest should be reduced by implementing the system.
- 4) Mapping of the resource of interest should be made easier and more timely by implementing the system. The spatial accuracy of the mapping should also be improved.

Initially it was envisaged that MBB's video-based system would be maintained and improvements would be made to it. One of the possible improvements identified was to employ the Society of Motion Picture and Television Engineers (SMPTE) time code specification to facilitate frame registration of Global Positioning System (GPS) data with video data. This specification is explained in detail by Graham (1993) and Linden *et al.* (1996). This improvement would have permitted easy retrieval of the positional data relating to a specific video frame and introduced the possibility of connecting a VCR to the RS-232 port of a computer and being able to instruct the VCR to position itself at a specific frame, using the SMPTE time code. Being able to control the VCR in this manner would have been a significant step in automating both the geo-location of frames and actual mapping of natural resources.

It was evident during the early stages of research, however, that there were several advantages to moving away from a video-based system to a system based on a digital still or frame camera. Advances in standard video technology were unlikely to produce imagery with more than twice the resolution of current video systems due to the limitations in terms of resolution of the Video Cassette Recorders (VCRs). Even by utilising the Digital Video (DV) recording format, which is a unified standard that has been adopted by many companies around the world, an increase of only 100 lines horizontal resolution from the 400 lines of the more common Super-VHS (S-VHS) recording format was likely to be possible. On the other hand, digital still cameras have in the last decade been receiving increasing attention from researchers in remote sensing as they continuously increase in resolution and decrease in price. Sensors with image formats of up to 5k by 5k pixels - an approximate equivalent resolution of 5000 lines, have been developed while 3k by 2k sensors are commercially available today (Maas and Kersten, 1997; Kodak, 1998) and are becoming common as alternatives to 35 mm film. According to King *et al.* (1995), the higher resolution cameras are likely to begin replacing standard 23cm format photography in the near future. Fraser (1997) substantiates this statement by commenting that digital imaging sensors are rendering film cameras obsolete for all but the niche domain of extreme high accuracy photogrammetry.

In this dissertation an analysis of MBB's airborne videography system is made and its limitations are identified. The pre-flight planning, image acquisition and post-flight image processing and mapping systems are all analysed. This is followed by a review of the technological status of digital still cameras and some of the current applications of such cameras. The following two chapters discuss the improvements that were made to the pre-flight planning and image acquisition systems. Descriptions of the algorithms implemented are included. The test procedures which were used to verify the system and the results obtained are then documented and discussed. A comparison of two methods for geographical referencing of a set of images is provided and the results of the application of one of these methods to images obtained during the test flight over an urban test area are included. The dissertation is concluded with the main findings of the project as well as some recommendations for any further developments and improvements to the system that were not highlighted in the preceding chapters.



## 2. EXISTING AERIAL VIDEOGRAPHY SYSTEM

The complete MBB videography system consisted of three distinct sub-systems, namely the pre-flight planning system, the in-flight image acquisition system and the post-flight image processing and GIS system in the office. These three systems are described below.

### 2.1 Pre-flight Planning

For the purposes of the discussion of the pre-flight planning procedure that was employed by MBB Consulting Engineers, Inc., the example will be used where the area of interest is a quaternary catchment. This is a suitable example since a large proportion of their aerial videographic work involved the survey of quaternary catchments.

#### 2.1.1 Procedure

The planning of a videographic survey involved the use of four separate software packages. Firstly, the flying altitude, flight strip spacing and swath width were determined using a Quattro Pro spreadsheet (Corel, 1997). This spreadsheet allowed the user to enter the view angle of the lens to be used, the desired ground pixel size and the average catchment altitude, from which the flying altitude above sea level and flight strip spacing were calculated. Then, after first creating a data transfer format file (\*.dxf) of the catchment boundary from an Arcview shape file (\*.shp) in Arcview 3.0a (ESRI, 1998), the data transfer format file was opened in a CAD drafting package. The CAD drafting package was used to draw in the flight lines as a series of parallel lines with a calculated flight strip spacing. Allowance was also made for a five kilometre 'run-in' and 'run-out' at the ends of each flight strip. These allowances were made to provide the pilot with sufficient time to position the aircraft along the flight strip.

Once the flight line positions had been established the coordinates of the endpoints of each flight strip, in other words the way points, were entered into a separate DOS-based program to convert the way point coordinates from their original coordinates in metres to geographic coordinates. An estimate of the time for turns and total flying time was an additional useful output of this program. The coordinates were then printed out and the latitude and longitude of each way point were

manually input into the GPS that was used for in-flight navigation. This GPS is described in detail in Section 2.2.1. A 1:250 000 plot of the catchment boundary and flight strips was also made onto transparent film. This plot was overlaid on a 1:250 000 topographical map to serve as a reference during the flying of a survey.

### 2.1.2 Limitations

The main limitation of the pre-flight planning setup was that it involved the use of several different software programs to obtain the desired way point coordinates. Files had to be repeatedly converted to the correct format, saved and exported, and then re-opened in the applicable program. This process was time-consuming and cumbersome. The development of a single program which could calculate the flight strip spacing and flying altitude for any combination of camera, lens and ground pixel size, and that could produce the desired way point coordinate outputs with a minimum of user effort, was therefore considered to be very important.

There were also limitations of the procedure relating to the determination of the flight line positions. These were that the effect of changes in altitude within a catchment on the overlap of imagery was not accounted for in the calculation of the flight strip spacing, and unusual situations, such as the situations illustrated in Figure 1 and Figure 2, were ignored. In the situation depicted in Figure 1 as an example, the endpoints of the flight lines were calculated by simply extending the flight lines 5 km beyond where they cross the catchment boundary. The capturing of video data would then start at or just after point A. By calculating the flight line way points in this manner, no account is taken of the possibility that although the aircraft may be flying outside of the catchment boundary, video data still needs to be captured since part of the catchment may fall within the swath width or field of view of the camera. Consequently there is the potential for lost data, as shown in Figures 1 and 2. To avoid the loss of data, video footage should be captured from point B which is the point where the edge of the previous or next flight line's swath width crosses the catchment boundary. The flight line starting position should then be extended 5km back from this point. It was seen as important that such situations, as well as the effect of catchment topography on flight line spacing, be addressed in the new system.

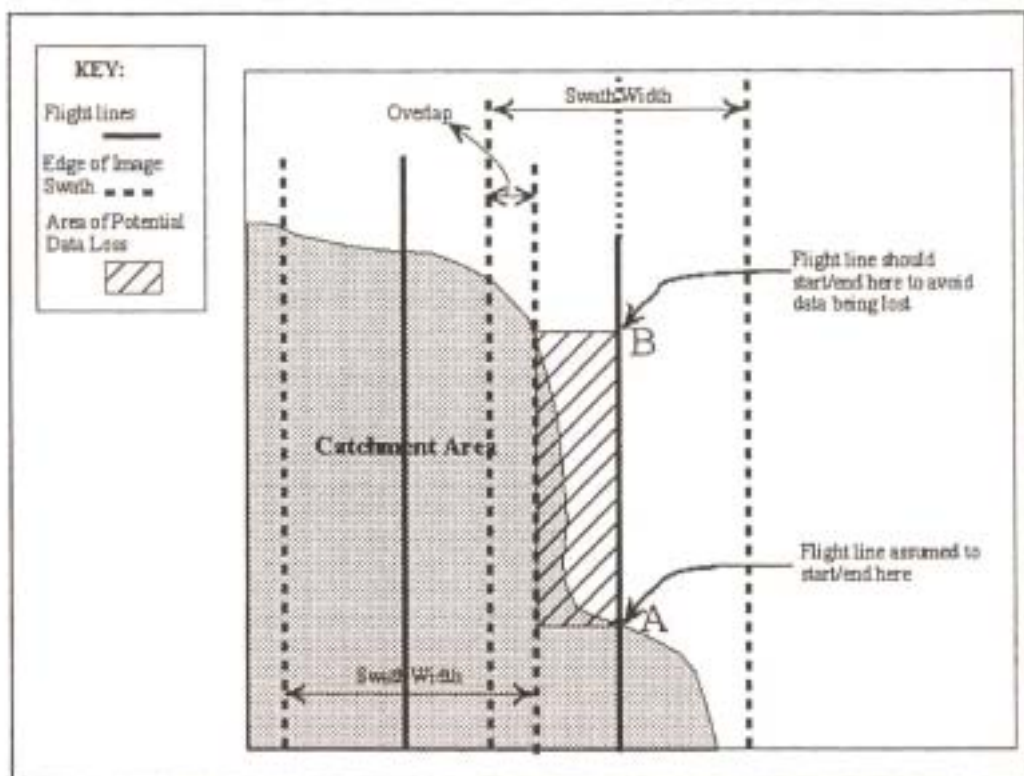


Figure 1: Example 1 of the potential for data loss at the start or end of flight strips

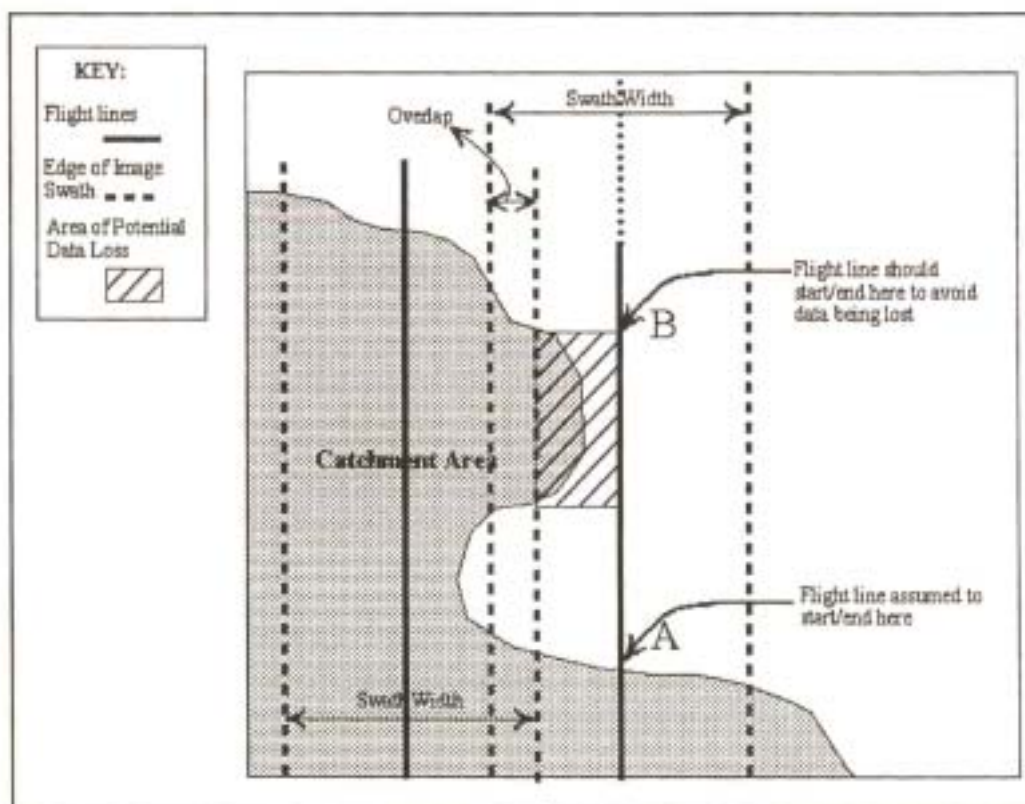


Figure 2: Example 2 of the potential for data loss at the start or end of flight strips

Considering the input of way point coordinates into the GPS, it was felt that this procedure needed to be automated if possible. The option to input the coordinates directly from the program into the GPS or GPS software needed to be explored. The use of a different GPS needed to be considered here, since previous attempts at automating the input of the way point coordinates into the Garmin GPS (Garmin, 1999) used had failed.

## 2.2 Image Acquisition

The basic MBB image acquisition setup consisted of 8 components. These were a video camera, video recorder (VCR), camera mount, video monitor, GPS video titler unit, 24V to 12V DC-DC converter, DC-AC inverter and a GPS receiver. A twin engine, four seater Piper Comanche aircraft was the aerial platform utilised. Figure 3 on the following page shows how the various components were integrated to produce the basic in-flight system. Each of these components is described in the section following the diagram.

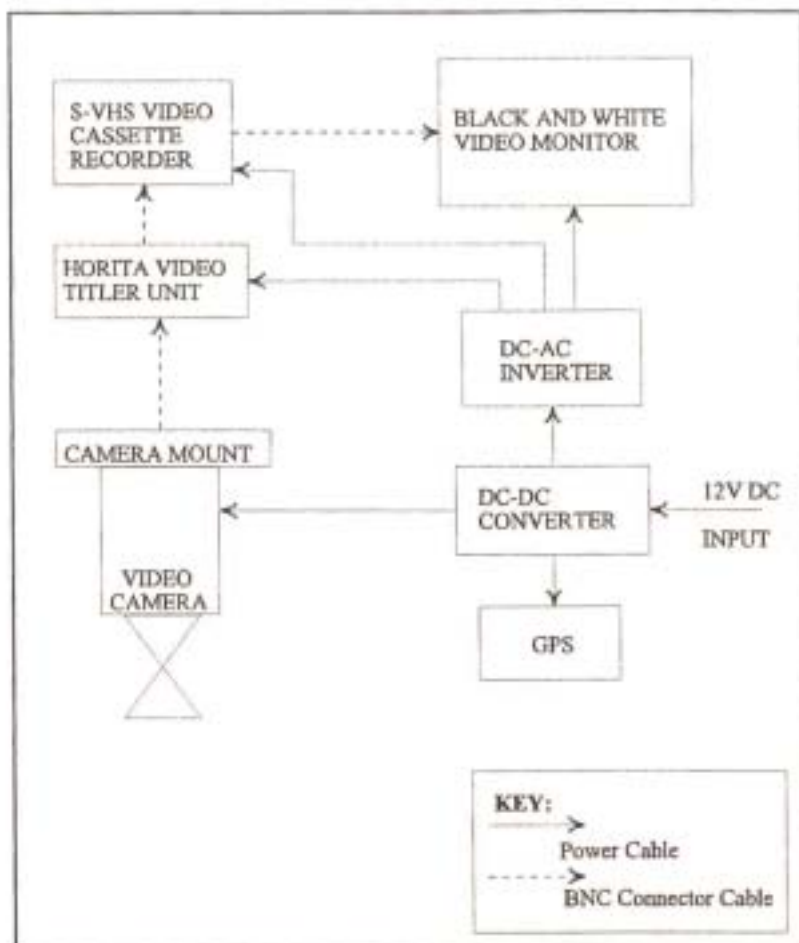


Figure 3: The existing airborne videography image acquisition system

### 2.2.1 Equipment

The video camera utilised was a Panasonic WV-CL352 colour Closed Circuit TeleVision (CCTV) camera. The camera specifications are listed in Table 1. This camera was chosen for its compactness, ruggedness and low cost versus resolution when compared with other cameras. A compact, rugged and durable camera was required when considering the limited space and harsh environment of an aircraft cockpit.

Table 1: Panasonic WV-CL352 video camera specifications

|                               |   |
|-------------------------------|---|
| Power Source                  | 220-240 V AC, 50Hz/12 V DC, 2A                    |
| Power Consumption             | Approx. 29W                                       |
| Screen Size                   | 8-9/16" (diagonal actual measured) 90° deflection |
| Video Input Impedance         | 75Ω or high impedance                             |
| Video Input Level             | 1.0V <sub>p-p</sub>                               |
| Horizontal Resolution         | More than 750 lines (Horizontal at centre)        |
| Horizontal Scanning Frequency | 15.625kHz   |
| Vertical Scanning Frequency   | 50Hz  |
| Sweep Linearity               | Horizontal: Less than 5%                          |
|                               | Vertical: Less than 5%                            |
| Ambient Operating Temperature | -10°C to +50°C                                    |
| Dimensions                    | 220(W) x 227.5(H) x 259(D) mm                     |
| Weight                        | 4.5 kg  |

There were several other important features of the camera which made it ideal for integration in the airborne videography system. The camera's digital signal processing of the colour signal limited the creation of colour noise by the camera and allowed for a variety of picture enhancement functions to be performed, while its local on-screen menu allowed for convenient setup and adjustment of light control, shutter speed, auto gain control and white balance. The camera required a 12V DC power source which could be provided by the plane's battery, and it had easy system integration capabilities. Furthermore, the camera was designed to accept a broad range of lenses which was important for allowing the acquisition of a range of aerial video coverages and resolutions, depending on the level of detail and accuracy required, and it incorporated a character generator which was useful for labelling images of interest.

The camera contained a solid-state chip sensor consisting of three charge-coupled device (CCD) sensors. These three CCD's were responsive to the red, green and blue (RGB) portions of the electromagnetic spectrum, respectively. The exact electromagnetic sensitivity of the CCD's was not specified by the manufacturer. The camera also included a high speed electronic shutter

offering exposures as fast as 1/10 000 of a second. This speed allowed the reduction of image motion and resultant blurring of images.

For alien vegetation studies use was also made of a second Sony black and white video camera mounted alongside the first camera. This camera was fitted with a zoom lens to provide a high resolution sample image of the Panasonic camera's image. This zoomed sample image was extremely useful for identifying the presence of individual specimens of alien vegetation, particularly in the riparian zones of rivers, as well as for correctly classifying the density of the alien vegetation infestation. To ensure that the system could still be operated easily and efficiently when this camera was used, some additional components were required. These were not shown in Figure 3 for clarity. A second VCR was added to record the zoomed imagery, and two switch boxes were added. The first switch box was introduced between the cameras and the Video Cassette Recorders (VCRs), after the video titler unit. When this box was in the off position no signal was sent to the VCRs, while when it was switched to the on position, the two video signals from the cameras were sent concurrently to their respective VCRs. By combining this switch box with the 'sensor' recording feature of the VCRs, as described later, the two video recorders were synchronised to begin and end the recording of their respective video signals.

The second switch box was positioned in the system between the VCRs and the small video monitor. This switch box took video signal inputs from both VCRs and provided a single video signal output to the monitor. By switching the box's switch either left or right, the operator was able to view the zoomed out or zoomed in video signal, respectively.

To mount one or both of the cameras, a basic, custom built camera mount which was deemed to be sufficient for maintaining the camera upright and stable for obtaining aerial video imagery was used. It was constructed of sheet steel with a small, rivet-connected L-section to which one of the video cameras could be bolted by utilising the existing bolt holes in the camera. The second camera was then secured to the first using cable ties. The mount was designed to be positioned and fixed in the place of a removable floorboard between the pilot and front passenger seats of the aircraft. Removing this floorboard provided access to a small port suitable for a clear, unobstructed view of the ground below.

To record the imagery captured by these video cameras, the Panasonic Model AG-5700 portable Super-VHS video cassette recorder with Panasonic remote control unit AG-A11 was chosen. This unit was fully compatible with the WV-CL352 camera. It was chosen for its compact size, light weight, ruggedness, and for its ability to record in the Super-VHS format.

The S-VHS format was particularly desirable as it allowed the recording of at least 400 lines of horizontal resolution compared to the 240 lines for the standard VHS format. This is achieved by recording the colour signals independently of the luminance signals, thereby avoiding the need to combine them into a composite standard VHS signal. This recording format ensured that the loss of resolution during the recording of imagery on to video tape was kept to a minimum.

Other features of the VCR which were considered useful were the provision of an RS-232 port to allow communication and control from a PC or editing controller if desired, and the audio dubbing features which would permit the recording of time signals on the second audio channel by connecting a SMPTE time-code generator.

For operating the two-camera system, two such VCRs were operated in their 'sensor' recording mode. When in this mode, the VCR is able to identify the presence of a second VCR in the system, and it will not record unless the second VCR in the system is also receiving and recording a signal.

The VCRs were powered by 220-240V AC necessitating the inclusion of a DC-AC inverter which is described later. The remote control unit allowed for control of the playback and recording features of the VCR from a distance, which was a beneficial feature in the confined environment of an aircraft cockpit. The complete VCR specifications are listed in Table 2.



Table 2: Panasonic AG-5700 video cassette recorder specifications

|                             |   |
|-----------------------------|---|
| Power Source                | 220-240V AC, 50-60Hz  |
| Power Consumption           | 27W   |
| Television System           | CCIR Standard (625 lines, 50 fields)<br>PAL colour signal   |
| Video Playback System       | 2 head-helical scanning, azimuth recording, S-VHS/VHS   |
| Heads                       | Video: 4 rotary heads, Audio: 2 rotary heads (Hi-Fi 2ch),<br>Erase: 1 full track erase  |
| Tape Format                 | S-VHS tape, VHS tape  |
| Tape Speed                  | 23.39mm/s   |
| Recording Time              | 180 minutes (with NV-E180)  |
| Playback Time               | 180 minutes (with NV-E180)  |
| FF/REW Time                 | Less than about 2.5 minutes (with NV-E180)  |
| Operating Temperature       | 5°C - 40°C  |
| Operating Humidity          | 35% to 80%  |
| Weight Dimensions           | Approx 5.7kg  |
| <b>VIDEO</b>                |   |
| Input/Output                | Line (BNC); 1.0V <sub>p-p</sub> , 75Ω<br>S-Video (4P); Y: 1.0V <sub>p-p</sub> , 75Ω<br>C: 0.3V <sub>p-p</sub> , burst level 75Ω |
| Video Horizontal Resolution | S-VHS; 400 lines (B/W, colour)<br>VHS; 240 lines (B/W, colour)  |
| Signal-to-Noise Ratio       | VHS; 45dB (B/W, colour)   |
| <b>AUDIO</b>                |   |
| Input Level                 | Audio; AUDIO IN (PHONO), -8dBv, 47Ω unbalanced<br>Mic; Mini-Jack, -60dB, 60Ω unbalanced   |
| Output Level                | Audio; AUDIO OUT (PHONO), -8dBv, 1kΩ unbalanced<br>Headphones; M3, -65--30dB, 8Ω  |
| Channels                    | 3 channels (Hi-Fi: 2 ch, normal: 1 ch)  |
| Hi-Fi Audio                 | Frequency response; 20Hz to 20 kHz<br>Dynamic Range; 90dB   |
| Normal Audio                | Frequency response; 80Hz to 10 kHz  |
| S/N Ratio                   | 45dB (Normal Audio)   |

To provide assurance to the pilot and camera operator that a particular area was being fully covered and to allow focussing of the camera/s prior to the commencement of a survey, use was made of a small, inexpensive black and white Panasonic WV-BM900 video monitor in the cockpit of the aircraft. A black-and-white monitor was chosen as it was less expensive than a colour monitor at the time of purchase, and it was deemed to be unnecessary to use a colour monitor for the purposes set out above. Its size made it ideal for use in the aircraft and the brightness and contrast controls allowed the operator to obtain clear, crisp images. The monitor was fully compatible with the video camera and VCR. The complete specifications of the monitor are shown in Table 3.

Table 3: Panasonic WV-BM900 video monitor specifications

|                               |   |
|-------------------------------|---|
| Power Source                  | 220-240 V AC, 50Hz/12 V DC, 2A                    |
| Power Consumption             | Approx. 29W                                       |
| Screen Size                   | 8-9/16" (diagonal actual measured) 90° deflection |
| Video Input Impedance         | 75Ω or high impedance                             |
| Video Input Level             | 1.0Vp-p   |
| Horizontal Resolution         | More than 750 lines (Horizontal at centre)        |
| Horizontal Scanning Frequency | 15.625kHz   |
| Vertical Scanning Frequency   | 50Hz  |
| Sweep Linearity               | Horizontal: Less than 5%                          |
|                               | Vertical: Less than 5%                            |
| Ambient Operating Temperature | -10°C - +50°C                                     |
| Dimensions                    | 220(W) x 227.5(H) x 259(D) mm                     |
| Weight                        | 4.5 kg  |

A Horita video titler unit (Horita, 1998) was used to annotate the video imagery with user-defined information such as date, time and flight strip numbers on the video tape. Unlike other available Horita data encoding equipment where the information is stored on the second audio track of the

video using SMPTE time codes, this unit uses the NMEA 0183 protocol to display and record information directly on the video track.

The Piper Comanche aircraft used for aerial surveys was fitted with a 12V supply cable from the aircraft's battery. However, other aircraft have a 24V supply which would not have been suitable for powering the 12V DC-powered components of the system mentioned above. In the event of the Piper Comanche being grounded for repairs or maintenance it was necessary to include a 24V to 12V DC converter unit to ensure that the system would still be operational even if an aircraft with a 24V power supply was used.

The converter offered three separate 12V DC sockets. One was fitted with an on-off switch and the video monitor was connected to this socket so that it could be switched on only when required. This was done because the power consumption of the monitor was relatively high, and it was found that there was insufficient power to operate the two VCRs in 'sensor' mode unless the video monitor was switched off prior to the commencement of recording at the start of a flight strip. The remaining sockets were used to power the GPS unit and for 12V DC input into the DC-AC inverter, respectively. The DC-AC inverter was required in order to power the VCRs, Horita titler unit and Sony zoomed camera. The 24V to 12V DC converter unit was also provided with a switch to alternate between 12V and 24V supply as required.

A Garmin GPS100 aviation kit was used as the GPS unit for navigating along flight lines during aerial video surveys. While it was not an integral part of the aerial videographic system in that its output was not used for geo-referencing imagery with SMPTE time coding, it was a vital component which insured a complete coverage of an area. Having manually input and stored all way points in the GPS prior to a survey, the corresponding pairs of way points could be quickly called up and entered as a route. The GPS then provided the pilot and video operator with information regarding distance right or left of the flight strip, and distance to the end of the flight strip. The GPS also had a simple graphical display depicting the aircraft's position relative to the flight strip. This display and the accompanying information was considered very useful for navigational purposes.

### 2.2.2 Limitations

As with many videographic systems described in the literature, the dominant limitation of the image acquisition system was the VCR. The resolution of the system was limited to 400 lines of horizontal resolution even when the S-VHS recording format was used. This limited resolution meant that the system was not well suited to vast area coverage since, to obtain a ground pixel resolution suitable for land use mapping and other resource management applications, it was necessary to fly at relatively low altitudes above ground level compared to photographic surveys and hence the area coverage per flight strip was small. This resulted in a direct increase in flying and processing costs, and highlighted the need for a system that could provide higher resolution imagery.

While the use of the Horita titler unit was suitable for most of MBB's applications, it removed the possibility of placing the video recorders under computer control for easy frame location and editing using SMPTE time codes, as Graham (1993) and Linden *et al.* (1996) had done. A preliminary investigation into the feasibility and ease of incorporating an SMPTE time-code generator and reader, such as the one described and used by Linden *et al.* (1996), into MBB's system had been performed prior to this project, but the time required to develop such a system and the cost of purchasing a complete system had been seen as prohibitive.

Vibration of the camera mount was a further problem which required attention. No sorbothane or similar dampening material was incorporated into the mount to reduce the vibrations and shock forces associated with flying. It was felt that these would be insufficient to prevent the acquisition of good videographic data. However, it was found during flying that vibration of the camera and mount was occasionally a problem, particularly when using the zoomed camera since any vibration of the mount was accentuated when viewing the zoomed image. This indicated that some dampening material or an improved mount design may have been required.

### 2.3 Post-flight Image Processing and GIS Input

The office-based post-flight sub-system allowed the processing and synthesis of the collected aerial video data into useful information. This information could be used by the resource manager or

engineer to make informed decisions and recommendations. The equipment used in the office, the procedure employed to map the resource of interest and the limitations of the office setup are described below.

### 2.3.1 Equipment

The office setup utilised the same VCR as the aerial system, as well as several other components. These were a scanner, colour TV monitor, video editing controller, and image processing and GIS software.

A flatbed Hewlett Packard Scanjet 4c scanner was used for the scanning of 1:50 000 topographic maps and orthophotos for use as base maps in a GIS. This scanner was able to scan a maximum document size of 216mm by 356mm and offered scanning resolutions from 12 to 2250 dpi at 100% scaling, as well as various scanning modes, including 4, 8, 10, 24 and 30-bit. Further features included image processing options of colour correction, thresholding and filtering.

To rectify and mosaic these scanned orthophotos and topographical maps, the ERDAS IMAGINE software package was used. This system incorporates the functions of both image processing and geographic information systems. These functions include importing of various image formats, viewing and altering images, and analysing both raster and vector data sets.

To allow viewing of the captured video imagery in the office, a 37cm Panasonic TC-1470Y colour video monitor was used. This monitor was chosen as it was capable of displaying both VHS and S-VHS video signals. It could also accept two video and two audio lines which allowed the operator to quickly alternate between two video or audio signals. This was particularly useful when the zoomed camera was used, since the operator was able to quickly alternate between the zoomed out and zoomed in video signals. A colour monitor was chosen since colour is crucial for the identification of, and distinguishing between, different crop types, tree species, and many other land uses. The full specifications of this video monitor are shown in Table 4 below.

Table 4: Panasonic TC-1470Y video monitor specifications

|   |  |
|---|--|
| System                                      | Interlaced, PAL / SECAM / NTSC 3.58 / NTSC 4.43  |
| Power Source                                | 220-240 V AC, 50Hz   |
| Power Consumption                           | 85 W   |
| Picture Tube                                | 14" (36cm) diagonal  |
| Speaker Output                              | 1.5 W  |
| Video/Audio Terminals:<br>(LINE A / LINE B) |  |
| Video Input                                 | 1.0Vp-p, 75Ω or high impedance (Auto), BNC type connector  |
| Video Through Out                           | Automatic termination opener, BNC type connector   |
| Audio Input                                 | 0.5Vrms, 22 kΩ or more, phono type connector   |
| Audio Through Out                           | Phono type connector   |
| S-Video Input                               | Y signal 1.0Vp-p, C signal 0.285Vp-p, 75Ω or high impedance (manual), MINI DIN 4p type connector |
| VTR Terminal:                               |  |
| Video Input                                 | 1.0Vp-p, 75Ω   |
| Audio Input                                 | 1.0Vrms, 22kΩ or more, 8 pin connector   |
| Resolution                                  | 420 TV lines (horizontal)  |
| Dimensions                                  | 14" (356mm) W x 16-1/2" (419mm) D x 13-3/8" (341mm) H  |
| Weight                                      | 31-15/16 lbs (14.5 kg)   |
| Operating Temperature                       | 32°F to 104°F (0°C to +40°C)   |
| Operating Humidity                          | 20% to 80%   |
| Warm Up                                     | 30 min to meet specifications  |
| Accessory                                   | TSX3104  |
| Option:                                     | Rack mounting kit  |

During the viewing and mapping of the video imagery it was important that the operator was able to quickly move to video frames of interest. Once at a particular frame, the video needed to be paused or played at a slower speed, in order for the features of interest to be identified and mapped. While a standard VCR remote control was able to fulfill many of these functions, the use of such a remote was seen as cumbersome and difficult. A Panasonic AG-A570 editing controller was thus incorporated into the system. This editing controller, which is connected to the VCR via

an RS-232C port, allows the operator to play the video forward or backward at playback speeds from still picture to 7 times normal tape speed, by operating a single shuttle dial. This greatly improved the efficiency of the mapping operation.

For the mapping of the natural resource of interest the ArcView 3.0a GIS software package was used. It provides all the necessary tools required to produce high quality, accurate maps and coverages suitable for use in resource management and as input into hydrological models. The procedure used to produce these maps and coverages using the equipment described above is detailed in the following section.

### 2.3.2 Procedure

The procedure used in the office to produce the required information for resource management was typically as shown in the flowchart in Figure 4 below.

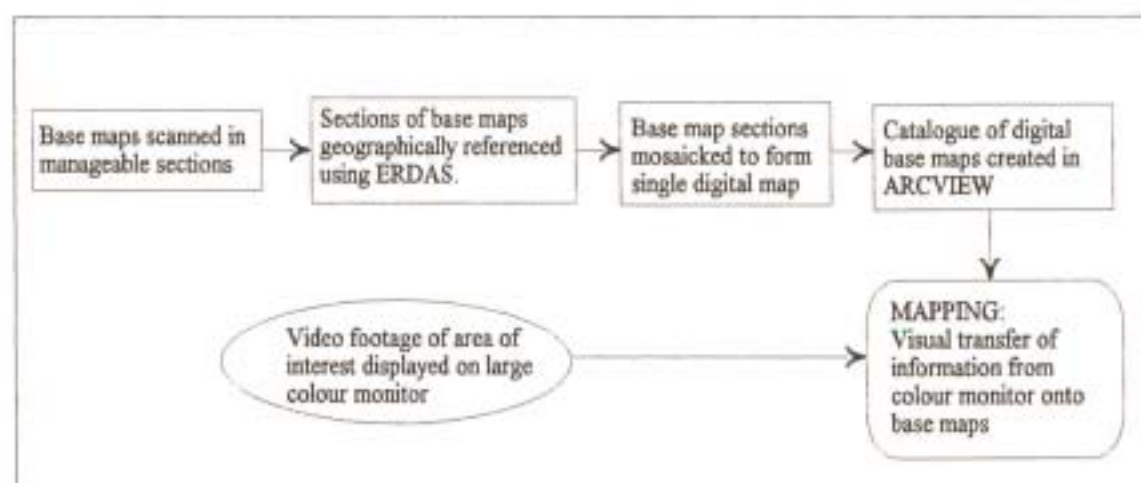


Figure 4: Flowchart of post-flight mapping process

Before mapping begins, digital base maps covering the area of interest are created, and geographically referenced. The images are then imported into ArcView 3.0a and displayed as themes.

The base maps typically used are 1:50 000 topographical maps for land use mapping and 1:10 000 orthophotos for alien vegetation mapping. Due to the limit on the size of the document that could

be scanned, manageable sections of these maps or orthophotos are scanned at a time using a HP Scanjet 4c scanner. They are typically scanned at a resolution of 100dpi. This resolution was chosen as it provides a balance between resolution and computer memory capacity. The resultant images are saved and then imported into ERDAS IMAGINE so that they can be geographically referenced.

The procedure used to geographically reference the scanned sections of orthophotos or topographic maps using ERDAS was then as follows:

- 1) Import the scanned image.
- 2) Assign Ground Control Points (GCPs) to the image. GCPs are identifiable points or objects in an image at which the coordinates are precisely known.
- 3) Check that the Root-Mean-Square (RMS) error, defined as the difference between the desired output coordinate for a GCP and the actual output coordinate for the same point when the image is transformed, is within reasonable bounds.
- 4) Resample/transform the image to conform to the new coordinate system. First or second order polynomials are used to convert from the initial coordinate system to the rectified map coordinates.
- 5) Save the resampled image.

Once the individual sections of the map or orthophoto are geo-referenced, ERDAS IMAGINE is used to mosaic the individual sections to create a single image which is a digital representation of the original hardcopy map or orthophoto. This procedure is repeated for each map making up a coverage.

The digital base maps are then imported into Arcview and a catalogue of these maps is created. By creating a catalogue, the time-consuming activation and de-activation of these base map themes is avoided, as only the images relevant to a particular view are automatically activated.

The methodology most often adopted for the actual mapping of natural resources, involves the visual transfer of information from a video monitor to the base maps in Arcview. For viewing the video and mapping the relevant features, the colour video monitor and a computer monitor



displaying the base maps in ArcView are set up alongside one another. The pre-planned flight strips are overlaid as a theme on the base maps to assist the technician in establishing where the 'live' video image and base maps coincide. The technician then uses road intersections, farm boundaries, river courses and other distinguishable features to assist in correctly scaling and positioning landuse and other polygons and line features. On completion of mapping, Arcview provides the means to create meaningful land use maps with the base maps overlaid with the themes of interest and produce tables showing summaries of, for example, different land use areas or lengths of river encroached by alien vegetation.

### 2.3.3 Limitations

The maximum document size which the scanner was able to accept meant that orthophotos and 1:50 000 maps had to be scanned in sections. This was seen as a disadvantage as it introduced the extra image processing step of mosaicing the sections of a map in order to produce a complete geographically referenced base map.

The process of assigning GCPs to each section of a map or orthophoto, resampling the image to fit these GCPs and then mosaicing these sections to form a complete map was a time-consuming and expensive process. It was therefore imperative that this process of geographically referencing the base maps be automated as much as possible.

The 'indirect' nature of mapping from the video imagery also introduces errors in terms of spatial accuracy. The estimated spatial accuracy was between 20 and 50 metres, and while this was adequate for the mapping of land uses and alien vegetation infestation, it removed the possibility of using this methodology for applications requiring greater spatial accuracy. Such applications would include town planning and conflict resolution relating to the use or exploitation of natural resources. Furthermore, the indirect nature of the mapping process made it a limiting factor in achieving a rapid turn-around time between acquiring the video data and providing the client with useful information required for decision making and planning.

It was observed that if rectified digital images of the area of interest could replace the topographic or orthophoto base maps in the GIS, the time required for mapping could be significantly reduced,

and the spatial accuracy of the map produced would in all likelihood be improved. The process of scanning and rectifying base maps could be eliminated altogether, and mapping could be as simple as digitising polygons of the resource of interest directly on to the geographically referenced digital image in a GIS. While this project did not include the development of procedures for automated post-flight geographical referencing of imagery, the possibility of purchasing software that was able to do this at a later stage had to be considered when deciding on the components of the new system. During the testing of the system as described in Chapter 6, one such method for semi-automated geographically referencing of imagery was tested.

There is evidence from the above discussion of the three sub-systems which comprised MBB's aerial videography system that several problems and bottlenecks existed. While such a system was able to provide resource managers with information at a greatly reduced cost when compared with aerial photography and satellite remote sensing, it was evident that by replacing certain components of the system and automating some of the cumbersome and time-consuming procedures the turn-around time between acquiring aerial imagery and providing the client with the information he/she required could be greatly decreased. By later reducing the amount of processing required, the overall cost of the system could also be reduced and this reduced cost could offset the capital cost of any new components.

The following chapter discusses an alternative to video technology that was identified as having the greatest potential to produce higher resolution, lower cost imagery in a digital format. The chapters thereafter discuss the system which was developed with the aim of producing a rapid turn-around, low-cost digital aerial survey system with improved spatial resolution and accuracy.

### 3. DIGITAL STILL CAMERAS: STATUS AND APPLICATIONS

The single component of a remote sensing system which can have the greatest influence on the quality of the resulting information is the image sensor. The image sensor determines the resolution of the image data from the outset and this has widespread implications in terms of the area that can be covered, the information that can be extracted from the imagery, and the spatial accuracy of the maps produced from the images.

While aerial photographic remote sensing can still produce the highest resolution imagery, King (1995) and King *et al.* (1995) believe that digital frame cameras can be considered as an alternative to expensive photographic and high resolution solid-state linear array image sensors for providing a simple means for both multispectral imaging and mapping. Combined, these activities can significantly improve the capabilities of resource and environmental spatial analysis in a GIS environment. Digital frame cameras also offer several benefits in relation to other remote sensing alternatives. These advantages cannot be fully understood, however, unless the characteristics and operation of such a camera are outlined.

#### 3.1 Characteristics and Operation

King *et al.* (1995) provide a simple clear discussion of how a digital image is formed within a digital frame camera. Readers requiring a more detailed explanation of the performance characteristics and applications of digital frame cameras should refer to King (1995).

Solid-state digital frame cameras consist of a two-dimensional array of photosites embedded in a substrate material. The most common substrate material is silicon. In very basic terms, the method by which an image is formed is that incident photons excite electrons in each photosite resulting in a charge developing which can be converted to an analog signal in direct linear proportion to the incident radiation. Depending on how the charge developed at each photosite is accumulated in the chip, the sensor array can be known as a charge coupled device (CCD), which is the most common and least costly type of chip, or a charge injection device (CID) (King, 1995). These two sensor types have slightly different signal generation and processing features, which are beyond the scope of this review. The analog signal generated is then digitised within

the camera (hence, the term digital camera) by an A/D converter in a format which usually matches the photosite format. This means that the same number of digital pixels are produced as there are photosites in the array. This digitisation is most commonly 8-bit, such that the sensor output voltage is divided into 256 possible grey levels. However, most solid-state arrays allow for 10, 12, 14 or 16-bit digitisation, providing up to 64000 grey levels at correspondingly greater cost. Unlike video, the actual spatial format of the photosites is not standard. Chips in the 1k by 1k range have typically been developed with a 1280 by 1024 pixel format (King, 1995), but a camera with a format of 1500 by 1024 photosites has also been developed by Eastman Kodak, Inc. (Kodak, 1998).

There are two basic digital frame camera designs used to create colour digital images. These are documented by King (1995) and Hoppus and Evans (1997). The first camera design is the beamsplitting camera. This camera passes incident radiation through a system of dichroic mirrors and splits the radiation into the red, green and blue (RGB) bands, each band being directed to a separate CCD. The RGB outputs from each CCD are usually combined to produce a true colour image, although some cameras can produce separate RGB analog or digital outputs that can be fed to a computer for simplified spectral analysis (King, 1995). This camera design results in excellent colour reproduction and spatial resolution, but is expensive and the recycle time between the capturing of images is slow (Hoppus and Evans, 1997). King (1995) also identifies the disadvantage of sensor modification by an applications user being difficult because optical modifications are required.

The second camera design makes use of a single CCD chip and a colour filter array. Essentially this filter array, described by King (1995) as a visible spectrum striping filter, allows the transmission of only a single band of the RGB spectrum to each photosite. An RGB signal for each photosite is then derived by using a weighted average to interpolate the other two required bands from the neighbouring photosites. According to Hoppus and Evans (1997) these cameras are relatively inexpensive and they have faster recycle times. The disadvantage of such cameras is that the interpolation process tends to reduce the spatial resolution somewhat (King, 1995). Kodak Inc. have developed such single chip sensors that are able to produce 36-bit colour images (Mason *et al.*, 1997).

The materials used in solid-state sensors have differing spectral sensitivities. Silicon's spectral sensitivity generally spans the visible and near-IR ranges of the light spectrum between about 400nm and 1000nm, peaking between 700nm and 800nm. Importantly, almost one-half the response of silicon is in the near-IR, thereby providing excellent potential for colour infrared (CIR) composite imaging and vegetation studies, while the blue response is very poor (King, 1995). The low signal-to-noise ratio in the blue reduces the clarity of the images. Other more expensive materials have been manufactured to respond to other wavelengths, such as mid-infrared and thermal-infrared, but their efficiency at converting incident photons to an image signal is much lower than for silicon (King, 1995). The response of silicon sensors to radiance is linear in all spectral bands. This means that the analog voltage amplitude and/or the digital grey level is directly proportional to the target radiance (King, 1995).

Although some digital cameras allow manual triggering by the operator, the control of exposure of a digital frame camera is most commonly computer-based. Exposure time, the interval between exposures, the number of exposures, camera gain, read-out rates and image size are all examples of imaging variables which can be controlled via a keyboard. Computer control of a system in as many ways as possible is important if a system is to be flexible for many applications, according to King (1995).

Having outlined the more pertinent characteristics and operational issues relating to the use of digital frame cameras in airborne surveying, the advantages and disadvantages of such cameras can be discussed. The benefits and limitations of digital frame cameras are reviewed below.

### 3.2 Advantages

The single characteristic of a digital frame camera that results in several advantages is the digital format of the imagery that it produces. The direct acquisition of digital image data means that processing costs are considerably reduced in relation to photography since film development is eliminated and no scanning is required (Light, 1996; Mills and Newton, 1996; Positive Systems, 1996; King *et al.*, 1997; Mason, 1997). By eliminating the scanning of photographs the distortions innate in such a process are reduced (Mills and Newton, 1996), and the accuracy potential of the imagery is improved (Maas and Kersten, 1997). Maas and Kersten (1997) found that in close-

range applications with signalized targets, well-defined edges or good texture on flat surfaces, precision of the order of 1/50 of a pixel ( $0.2\mu\text{m}$ ) in image space could be regularly achieved. Eliminating film development and scanning also substantially reduces turnaround time with weekly fly-overs being possible and information being available within two or three days of the flight (Oltman, 1996a). For immediate assessment of the impacts of catastrophic events, resource managers can reduce the turn-around time even further by making use of the digital camera's inherent electronic capability to transmit its digital image from the aircraft to the ground (Light, 1996). Alternatively, the images can be viewed in the cockpit of the aircraft (Light, 1996; Positive Systems, 1996; Mason *et al.*, 1997). This would serve a further purpose of allowing the evaluation of exposure and focus parameters, and would provide verification that the targets are being acquired. This would avoid costly return flights to a site.

Digital format imagery is also more suited to image processing for improvement of radiometric characteristics, such as noise reduction and reduction of brightness variations with view angle, geometrical warping and to quantitative image analysis (King *et al.*, 1994). In particular, a higher signal-to-noise ratio is achievable under conditions of low scene contrast and low light levels in comparison with film-based systems. This higher ratio is possible due to the ease of digital contrast enhancement (Light, 1996). Such image processing is also easier since having digital images allows easy integration with softcopy<sup>1</sup> image processing systems (Toth, 1997). Furthermore, by having a digitally based system, different sets and different kinds of data can be integrated, merged, intersected and compared, resulting in wider and more flexible operations within and beyond the field of mapping (Ackermann, 1996).

The higher resolution of Digital Frame Camera (DFC) imagery when compared with video and satellite is another advantage. Unlike standard videography, which can already provide an order of magnitude better resolution than satellite remote sensing, DFC's are not confined to National Television Standards Committee (NTSC) or other television scanning specifications (King *et al.*, 1994). As a result, sensors have been developed which contain many more photosites per unit sensor dimension than video sensors (King *et al.*, 1994), thereby providing a vast improvement

---

1

Softcopy refers to the fact that the original hard copy or print of the photograph is not processed, but rather a digital representation or softcopy of the photograph is used

in resolution. DFC's, with their current resolutions, could therefore be considered as a substitute for photography where the needs do not demand the very high quality and resolution of photography. Further advantages of still cameras over analogue video are their greater flexibility since no on-board power supply and computer are necessarily required, and their higher mapping accuracy potential since the effects of framegrabbing analogue video images to produce digital imagery are avoided (Mason *et al.*, 1997).

Being able to control the camera via a computer is a further benefit, since it affords the opportunity to automate the in-flight image acquisition process. Computer-based control also facilitates the performing of some real-time processing of the imagery. This could include correcting for lens distortions and lens vignetting, reducing image noise through use of image filtering, and adjusting for non-uniform radiometric response of the CCD array. King (1995) provides a review of research into these aspects of image processing.

The digital nature of the data acquired also introduces the vast potential for automation of post-flight image processing. Heipke (1995), Ackermann (1996), Schenk (1996), and Toth and Krupnik (1996) all identify the potential of automating photogrammetric procedures through the use of digital imagery, thereby providing quick response times. The prime examples identified by Ackermann (1996) were aerial triangulation, generation of digital elevation models and production of digital orthophotos. The use of digital still camera imagery for some of these applications will be reviewed later in this chapter.

In terms of the other characteristics of the imagery, King *et al.* (1997) states that digital cameras produce frame exposures with geometric characteristics as good or better than film and much better than line scanner images. Airborne line scanner imagery typically suffers from line-to-line geometric variability (Monday *et al.*, 1994; King *et al.*, 1994), particularly under turbulent flying conditions where roll, pitch and yaw are unstable. This results in severe image reconstruction problems (Light, 1996) and makes photogrammetric analysis and geometric transformations more difficult. Radiometric performance of CCD sensors is also often significantly better when compared to scanned film (King *et al.*, 1994; Maas and Kersten, 1997). The spectral fidelity of the imagery is also excellent, and there are no problems associated with film emulsion batches, temperature and humidity (Positive Systems, 1996).

There are, however, some disadvantages relating to the use of DFC's which currently prevent them from becoming the sensor of choice for all aerial imaging applications. These disadvantages are described in the following section.

### 3.3 Disadvantages

The three main limitations of current digital cameras which have hindered their widespread use in mapping and monitoring are their small sensor (imaging chip) size, lower resolution and relatively slow data transfer and storage rates (Mason *et al.*, 1997).

Sensors are typically in the range of 19 x 19 mm for 2000 by 2000 pixel format cameras (King *et al.*, 1997). Such array sizes produce total view angles of between  $10^{\circ}$  and  $50^{\circ}$  for the variety of focal length lenses available for them (King, 1995), resulting in small ground coverage per frame in comparison with photography. The coverage can be improved by flying at higher altitudes using a short focal length, wide angle lens, but these options introduce further complications. Flying higher results in an increase in the ground pixel resolution and atmospheric effects on the imagery (King, 1995), while employing a short focal length, wide angle lens introduces geometric distortions that require the use of an expensive calibrated lens and/or geometric calibration (King *et al.*, 1997). Larger CCD sensors can be manufactured, but there are economic and technical constraints which limit their use in commercial cameras (Maas and Kersten, 1997). It is estimated that the production cost of CCD sensors grows with the fifth power of the area of the sensor. Also, pixel sizes cannot be arbitrarily reduced due to the light sensitivity characteristics of silicon. These constraints also explain why the resolution of commercially available digital cameras is limited.

The maximum resolution of current commercially available DFC's is approximately 3k by 2k (Kodak, 1998; Maas and Kersten, 1997). A 9216 by 7168-pixel sensor has been developed by Philips (Maas and Kersten, 1997), but even the resolution of this sensor, which cannot be considered ready for practical use yet, is modest in comparison with the equivalent resolution of in excess of 20k by 20k of high quality 23 by 23 cm format aerial cameras (Light, 1996; Toth, 1997). In conventional terms of frequency response, the resolution for digital camera sensors with the smallest photosites of 6.8 microns is a maximum (for high contrast targets) of about 55 line-



pairs/mm. This compares with film resolution which is generally in the range of 80-100 line-pairs/mm for high contrast imaging (King *et al.*, 1997), and with Super VHS video's horizontal resolution of 25 line pairs/mm (King, 1995). Consequently, digital frame camera imaging, as is the case with aerial videography, will generally have a much narrower width of coverage than photographic film for the same spatial resolution. This limits the potential of DFC's for regional mapping, which has been a primary application of photography, since the number of flight lines and images required to produce a suitable resolution coverage of an area is too high to be economically competitive with large format aerial photography (Light, 1996; King, 1995). Consequently, as King *et al.* (1995) suggest, the greatest potential for DFC's for mapping is currently in local site-specific mapping, or in linear/transect mapping.

A third limitation of high resolution DFC's in particular, is the rate at which data can be transferred and stored (King *et al.*, 1994; Light, 1996; Hoppus and Evans, 1997). For example, a compressed 3k by 2k DFC image consists of over 4 Mb of information (Kodak, 1998) and requires a storage time of 8 seconds per image (Maas and Kersten, 1997; Kodak, 1998). Data transfer of even lower resolution imagery to an inexpensive tape drive or disk is thus slow and relatively slow aircraft velocities are required. As King *et al.* (1994) states, this does not permit large image overlap as in NTSC video where a complete image is acquired every 1/30 s. Consequently, they believed that use of these sensors was limited to non-continuous data acquisition with some capability for image overlap. Mason *et al.* (1997) believed that the problem of image overlap could be overcome by flying each strip a number of times. Unfortunately this solution increases the complexity of both the flight planning and execution.

Further disadvantages of digital still cameras are documented by Fraser (1997). Unstable interior orientation and focal plane unflatness of the cameras, which are designed more for the mass consumer market than for photogrammetry, are primary factors limiting the photogrammetric potential of large-area CCD digital cameras. Digital still cameras, such as the Kodak DCS series, make only modest concessions in their design for a stable interior orientation. Error sources include movement of the CCD sensor with respect to the camera body, movement of the c-mount lens also with respect to the body, and differential movement of lens elements. Both Mason *et al.* (1997) and Maas and Kersten (1997) identified this as a potential problem in their research.

In terms of focal plane unflatness, any departure from planarity of the chip results in the image being displaced. This invariably leads to significant accuracy degradation in the object space. Unfortunately, manufacturers do not readily provide information regarding chip topography, and there is no satisfactory alternative to measuring the surface topography.

From the above discussion there is evidence that most of the DFC's currently available will not replace aerial photography for large-scale mapping applications, mainly due to the limitations of resolution and image chip size. Some researchers (Maas and Kersten, 1997; Light, 1996) believe that this will be the case for a long time to come. Light (1996) expects the foreseen transition from film cameras to digital sensors to be gradual since film cameras will also improve with computer designed lenses, forward motion compensation and angular motion stabilisation. Nevertheless, all researchers agree that as costs continue to decrease and some of the problems associated with digital cameras are solved, the digital sensor format will compete with and replace standard airborne videography and small format photography. In fact, some researchers and organizations have already realised that the development or leasing of digital frame cameras is a cost-effective and advantageous alternative to buying data and have begun using them mostly for reconnaissance work, in localised studies, and in situations where photography and higher resolution line scanning cameras provide too much detail (King, 1995). Despite the belief that digital still cameras are not suited to large-area mapping, some research and commercial work has also been done into such applications with promising results. The following section provides a review of potential applications of a digital frame camera system.

### 3.4 Applications

The main thrust of current research and commercial ventures incorporating digital frame cameras is in the monitoring and mapping of vegetation, and in topographic mapping. Other applications are documented and these are also detailed below.

### 3.4.1 Vegetation monitoring and mapping

The two main types of vegetation which have been remotely sensed using digital frame cameras are forestry and agricultural crops. They have received greater attention probably due to their commercial value and consequent need for regular monitoring and inventory.

King (1997) summarises various research initiatives conducted with digital camera sensors for development of models to quantitatively map forest ecosystem characteristics. This includes summaries of the research by King *et al.* (1997) and Seed and King (1997). These research efforts form part of an integrated research program in airborne multispectral digital camera imaging for use in environmental analysis and mapping.

In terms of forest health modelling, research has concentrated on relating the spectral, textural and structural characteristics of digital frame camera imagery to various physical responses of forestry to stress. These physical responses are often evident in the upper tree crowns and the forest canopy. This work has all been done along a chosen transect of forest within an abandoned acid mine site near Timmins, Ontario, Canada where drainage and airborne contaminants from an area of heavy metal tailings are transported into the adjacent forest. This transect is divided into 15 plots of 20m by 20m.

Seed and King (1997) used digital imagery generated in the green, red and near IR bands from the Kodak DCS420 Colour Infra-Red (CIR) camera to define three spectrally unique shadow fractions and their relative areal proportions within a mixed boreal forest. The details of how these shadow fractions were determined are not of importance in this discussion and interested readers should refer to Seed and King (1997). These shadow fractions were used in a correlation analysis to find any significant relations which existed between potential combinations of the three shadow fractions and the biophysical variables of effective LAI, stand basal area, and crown closure. These biophysical variables were estimated for each plot by performing field-based measurements. From multiple regression analysis it was found that effective leaf area index (LAI) could be predicted with a  $r^2$  of 0.90 and standard error of 0.34 in all study plots, canopy closure with  $r^2$  of 0.90 and standard error of 10% in dominantly conifer plots, and basal area with a  $r^2$  of 0.80 and standard error of 10.9 m<sup>2</sup>/ha in dominantly deciduous plots. Seed and King (1997) concluded that low cost,

high resolution airborne digital imaging coupled with linear regression modelling of image structure was a viable alternative to more expensive multiband remote sensors and sophisticated spectral modelling for determination of mixed boreal forest stand structure.

Olthof and King (1997) hoped to improve on the results achieved by Seed and King (1997) by utilising textural information to improve the estimation of LAI using high resolution digital imagery captured with the same camera. They made use of the red band of imagery to derive six separate texture measures from the co-occurrence matrix of a moving window. Co-occurrence matrices are frequency tables whose entries represent the number of times that pixels of two possible grey level combinations occur at a specified distance and direction from each other. These co-occurrence matrices were then used to generate texture channel histograms which allowed the determination of the texture mean and standard deviation in each plot.

The relationship between the average texture for each of the six texture measures and LAI was evaluated using a correlation analysis. The texture measure with the highest correlation coefficient was then used in conjunction with other image information to see if the relationship between image variables and LAI could be improved. Additional image information was spectral information extracted from the red and near IR bands, including combinations of these two bands.

Results showed that the contrast texture measure consistently had the most significant relationship with LAI ( $r=0.64$ ) for the window sizes and sampling distances chosen. In terms of the spectral measures, the individual near IR band produced the most significant correlation coefficient with LAI of 0.56. By combining these two measures the correlation improved significantly ( $r = 0.70$ ), while further addition of the variation in texture, measured by the texture standard deviation, improved the correlation to  $r = 0.81$ . These results showed that spectral measures should be combined with textural information such as frequency distribution of texture and texture standard deviation when high resolution digital imagery is being used for estimation of forest structure parameters.

King (1997) also documents research which had just begun into developing a forest health index. This health index will combine soils data, forest and individual tree structure variables, and a field-based visual health index with digital image spectral, textural and structural measures developed

in research as described above, in order to provide quantitative and complementary information on forest health characteristics. In yet another study, the expansion of the mine's tailing and consequent degradation of the surrounding forest is being monitored and modelled with the help of digital still imagery. An individual tree segmentation methodology is combined with overlays of archived aerial photography and more recent digital imagery to assess and predict the state of the forest boundary at various times in the near future.

Other research by King and his fellow researchers has looked at the potential of low cost airborne digital imaging in the automatic identification of conifer crop species for various densities of competing vegetation (King *et al.*, 1997). This was done to establish whether digital cameras could replace photography in assessing forest regeneration.

Two study sites were included in this research. The first was a tree seedling nursery which was divided into three randomized complete block experiments. Each experiment block was identical in layout and plant setup, with 11 plots in each block containing jack pine (*Pinus banksiana*) and black spruce (*Picea mariana*) plus one competition species. Within the plot, there were 12 experimental units of 7m by 7m, each containing jack pine or black spruce and one competition species at a specific density. The other site was a natural clear cut setting consisting of four 28m by 28m plots with ten 7m by 7m experimental units. Each of the units contained four conifer species, namely red pine (*Pinus resinosa*), white pine (*Pinus strobus*), jack pine, and black spruce. The units were subject to different herbaceous vegetation removal treatment, thereby producing different densities of competing vegetation in each unit.

Having obtained vegetation measurements including conifer survival, vegetation cover, height, stem diameter, crown width, leaf area index, and biomass at the two sites, digital imagery of the sites was obtained using the Kodak DCS420 CIR camera. Analysis of these images began by evaluating the statistical separability of the conifers and competition species as a function of competition density. Results showed that good separabilities could be obtained for some competition species when they were not in direct competition with the conifers. Spectral separabilities of the conifers with the other competition species were poor even when not in direct competition with each other. Jack pine and black spruce also produced poor spectral separability even when not in competition with each other. This decrease in separability was found to be a near

linear function of the increase in density of competition. King *et al.* (1997) provide several explanations for these poor results.

Following the separability analysis, King *et al.* (1997) performed some initial classifications of the data using a maximum likelihood classifier. Although they were expecting poor classification accuracy for the conifers due to the poor separability results, this was not the case. They found that the planting patterns of the conifers was generally quite visible and that when all but the conifer class was re-classified to black, the conifer crowns were almost perfectly classified as entities. Despite these results being inaccurate on a pixel-by-pixel basis since pixels which fell on conifer branches that overlapped with the competition's branches were mis-classified, King *et al.* (1997) concluded that such methods could be useful for tree counting. For automated discrimination of conifers from competition and for automated tree size measurement, they suggested that more advanced classifiers be tested and that stereo imaging be investigated as a tool for measuring tree height and crown diameter, respectively.

These research efforts described above show the tremendous potential of digital frame cameras for use in forestry management. Research and commercial ventures have not been limited to forestry applications though. Remote sensing for the monitoring and management of agricultural crops is another area where digital frame cameras have been applied.

Remotely sensed imagery, particularly multispectral imagery, can provide insight into crop growth patterns and plant stress levels which would not be detectable from ground level or with the naked eye. This advantage allows growers and farmers to analyse their crops and then make cost saving, timely decisions that can prevent the loss of yield and income.

Oltman (1996a) provides a practical review of work being performed by Datron Inc.'s imaging systems division of Milipitas. They have been conducting fly-overs of agricultural areas in California and Arizona in the United States of America to compile data on a variety of crops. The system they operate consists of four digital cameras, each equipped with a 20mm lens and a different filter to record reflected energy in the blue, green, red and near IR portions of the spectrum. A GPS is also included to provide the latitude and longitude of each image centre.

The four digital spectral bands are used individually or combined to provide different information relating to the crops and fields. The red band (622 - 780nm), green band (492 - 577nm) and blue band (455 - 492nm) are combined to produce a "true colour" image which provides an intuitive, easily understood reference image. The blue band is used to provide information relating to soil types and conditions. The near IR band (780 - 1100nm) is the most useful for identifying plants that are stressed due to over-watering, under-watering, insect activity or disease infestation. This multispectral capability of the system has made it a very useful tool in a variety of situations, which are documented by Oltman (1996a).

The system was used to identify and solve a specific problem relating to drip irrigation in a lettuce field. Multispectral imagery clearly highlighted a particular strip in the field. On further investigation, it was found that there was a restriction in the drip tapes irrigating the beds that showed up in the images. This problem could not have been identified visually. In another irrigation related problem, the unevenness in a sprinkler irrigation pattern was identified using the airborne digital imagery.

The ability of the system in revealing different soil types within a particular field is also discussed by Oltman (1996a). The position and extent of a particular soil type can be established by geographically referencing the imagery and importing it into a GIS. Then, although the soils cannot be physically changed, the farmer may be able to apply varying amounts of irrigation water depending on the soil type.

Other applications documented by Oltman (1996a) have included using the imagery to monitor the growth and health of permanent crops. Information gathered on citrus orchards has allowed growers to pinpoint trees which are performing badly. This is achieved by examining the trees' chlorophyll or green spectral band reflectance. Trees that are healthy and therefore photosynthetically active will have a higher concentration of chlorophyll and reflect more radiation in the green band. In vineyards, the four-band multispectral digital imagery has proved effective for the early detection, monitoring, and mapping of the extent of *phylloxera*, a vine-destroying root louse. Oltman (1996b) provides a detailed report on this research.

According to Oltman (1996b), this project was a success, not because researchers found a specific spectral signature for *phylloxera*, but rather, by combining the use of a false colour image, which is created from the near IR (780-1100nm), red (622-780nm) and green (492-577nm) spectral bands, and a Normalized Difference Vegetation Index (NDVI), which is based upon near IR reflectance and red reflectance, areas of stress and differing vine sizes could be highlighted. These two characteristics are a good indication that phylloxera may be present in a vineyard. Advantages of the system, which are identified by Oltman (1996b), include the ability to compare imagery from year to year in order to track the spread of phylloxera and the fact that a decline in vine vigour is often more easily detected using the digital imagery than from the ground or using normal infrared photography. Furthermore, by being able to identify areas of strength and weakness in a vineyard, a grower can use the imagery to help in harvest planning.

Lang (1996) documents a similar application of a four-band multispectral digital camera system in monitoring vineyard health and vigour. The imagery, which was flown by Positive Systems Inc. of Whitefish, Montana, U.S.A., was similarly processed to produce a NDVI. This data was to be tied back to a GIS and overlaid with soils and yields to determine the overall health and productivity of the vineyard. This information is important for estimating replanting costs and identifying potential problems early.

Other vegetation mapping applications are mostly related to updating existing natural resource databases, environmental analyses, and land use mapping for various resource management applications.

#### 3.4.2 Land use mapping, environmental analyses and resource database updating

Positive Systems, who claim to be the leaders in digital aerial photography, have since 1991 been involved in several natural resource-based applications. They have developed a comprehensive and versatile family of Airborne Data Acquisition and Registration (ADAR) digital aerial photography systems. Positive Systems (1996;1997) provide brief descriptions of a selection of the projects the ADAR systems have been used in. The diverse nature of these projects clearly demonstrates the tremendous potential and versatility that digital frame camera systems are already showing in a variety of applications.



The Positive Systems' ADAR units have been used in various animal habitat mapping projects. Digital photographs from the ADAR System 5500, which is the digital four band multispectral system used by Datron Inc., were used within an ongoing research study of grizzly bear habitat and stream side ecology. In another study, ADAR system imagery has been used by the U.S. Army Corps of Engineers to classify and map the habitat of the endangered desert tortoise. Imagery of the Blackfoot river was analysed to develop GIS basemaps of river habitat and riparian conditions, and was to be integrated with telemetry observations for the endangered bull trout. Reptile and mammal habitat studies in southern California have also benefitted from quarter metre and two metre resolution imagery captured with an ADAR system.

The use of ADAR digital camera imagery in hydrological studies is also documented. Imagery was used as part of a study to evaluate the long term effect of cattle grazing in arid riparian zones, while NASA and San Diego State University are utilising an ADAR system in a long term project to monitor the restoration of California coastal wetlands. Multispectral digital aerial photos have also assisted in wetlands analysis within a 90 mile rail corridor to review the potential environmental impacts relating to a planned railway expansion.

Further digital frame camera projects described in Positive Systems (1996;1997) include:

- 1) mapping of noxious weeds in agricultural and rangeland areas by the University of Idaho,
- 2) wetlands delineation, development of a detailed vegetation map, fire modelling and verification of the status of plant communities from imagery of the Vandenberg Air Force Base,
- 3) mapping of 200 square miles of Willapa Bay, Washington as part of a community-based environmental analysis and GIS project,
- 4) analysis of multispectral ADAR aerial photographs in a study of wildfire impact on forest succession in the Sequoia National Park, and
- 5) use of georeferenced, mosaicked multispectral digital imagery in evaluation of environmental characteristics for changing rural and suburban service areas.
- 6) the cost-effective updating of a forest resource aerial photography database for an area encompassing almost 1200 square miles. The specific objective relating to the capture

of digital frame camera imagery was to obtain a mosaic of the individual photographs, thereby providing a contiguous image data layer for use with various GIS vector layers already compiled for the area.

The final project listed above is described in some detail in Positive Systems (1997). The success of this project clearly indicates that although many researchers believe that digital frame cameras are only suitable for localised, site-specific studies, the potential is there for the use of DFC's in large area mapping.

The use of DFC's for topographic mapping and other photogrammetric applications, has also been researched. The following section examines the possibility of utilising overlapping digital frame camera images for generating DEM's and creating orthophotos.

#### 3.4.3 DEM and orthophoto generation

Digital elevation models (DEM's) are the primary data used in the analysis of catchment topography (Moore *et al.*, 1991) and are thus important information layers in a GIS. While stereoscopic aerial photography has been the main means of deriving DEM's in the past, the advent of modern computer-based image processing and transformation packages has meant that procedures which are analogous to photogrammetric techniques are now being applied to raster based digital images.

The reason that height information can be obtained from overlapping pairs of images is simply due to the fact that changes in ground elevation produce changes in photo scale and these in turn produce measurable relative displacements of objects within the pairs of images (Burnside, 1979, p93). Points that are higher than the image nadir are displaced outward from the centre of the image and points that are lower in elevation are displaced inward from their true position.

King *et al.* (1994) selected a single pair of 0.7 m pixel digital frame camera images which overlapped by 60 percent to evaluate the potential of using the 1340 by 1037 pixel Kodak MEGAPLUS 1.4 black-and-white digital camera for elevation determination. The test site chosen was in the east end of Toronto, Canada. This area had a very small elevation variation and

consisted mainly of residential and small commercial land uses. Municipal survey control points were thus abundant.

An edge-enhancing algorithm was first applied to improve pixel identification of suitable control and test points, after which three points were chosen as control points. This small number of control points was chosen in order to simulate an operational situation where only a few control points can be measured because of cost or difficulty in identification. These three points were used in a bundle adjustment<sup>2</sup> program to perform relative and absolute orientation of the images. The accuracy of elevations of other test points in the imagery were then evaluated by comparing their elevations with those obtained in a ground based survey using standard levelling and traversing techniques. Results showed that despite no rigorous sensor calibration having been performed, the method had potential for elevation determination, with elevation RMS being about 2.3% of the total variation in topography within the scene. This was similar in dimension to the pixel size. They considered the method to be applicable to obtaining large-scale elevation models.

Subsequent to this research, the same camera was evaluated for use in DEM generation in natural terrain where survey control was not abundant or evenly distributed across airborne imagery. This study is documented by King *et al.* (1995). The study area in this case was the Gatineau Park in Quebec, just north-west of Ottawa, Ontario. This park had rugged terrain and was mostly forested with only a few roads crossing its interior.

Digital elevation models of the area were automatically created using a photogrammetric software package. This package used an iterative area-based matching process to determine conjugate pixels in stereo image pairs. The elevation for each matching pixel was computed using the parallax equation, following which the elevation of points between the conjugate pairs was interpolated to fill in the rest of the raster DEM. Finally, the DEM was absolutely referenced to the ground reference system using the existing control points in the imagery. In comparing the photographic and DFC imagery for elevation modelling accuracy by relating the elevations derived from the imagery to those obtained from a field survey using static differential GPS techniques,

---

2

Bundle or block adjustment is the final step in a process that is known in photogrammetry as aerotriangulation. Aerotriangulation and bundle adjustment are complex processes. The interested reader should refer to Chapter 6 for a detailed explanation.

the DFC model was found to produce mean differences closer to zero than the photographic model. King (1995) indicated that this may have been due to a systematic error in the photography such as greater influence of vegetation. Unfortunately, the precision associated with the DFC model was lower than in the previous urban study. The standard deviation of the elevation differences was 4 times the ground pixel dimension compared to 2.14 times for the photography. King (1995) provided several possible explanations for this poor result and concluded that the potential of the sensor used was in low cost acquisition of medium accuracy DEMs for custom applications.

Maas and Kersten (1997) have performed similar research to establish the potential of digital cameras for photogrammetric applications. They made use of two test areas. The first area was an alpine village with an area of 520 by 500 m where the use of digital photogrammetry was of interest for cadastral applications and for orthophoto generation. The second area was a 900 by 300 m landslide area consisting of lightly forested meadows over a steep rock slope. In this case, the focus was on measuring deformations and generating a DTM.

Imagery for the two pilot studies was captured using a 1524 by 1012 pixel Kodak DC5000 digital camera. The imagery of the two areas was then semi-automatically aerotriangulated using hand-signalized control points in the form of white plastic plates and additional measured natural points. Results of this aerotriangulation were considered to be reasonably good with accuracies of 2 cm and 5 to 6 cm being achieved for the planimetry coordinates and height, respectively.

Based on the results of aerotriangulation, DTM's were derived from the two image datasets. Multi-image feature-based matching, which is characterised by its high reliability, was applied to automatically derive the DTM's. Following this, orthophoto mosaics were computed for the two regions. For the alpine village study, the average standard deviation of the reconstructed points was 0.027, 0.027 and 0.109 m in X, Y, and Z, respectively. For the landslide site, the average standard deviations in the X, Y, and Z coordinates were 0.023, 0.023 and 0.095 m, respectively. In both cases these standard deviations were 0.03 percent of the flying height above ground.

The results achieved by King *et al.* (1995), King (1995) and Maas and Kersten (1997) show promise for the use of digital still cameras for DTM generation and aerotriangulation. Importantly,

both sets of researchers state that newer generation DFCs with higher resolutions would be expected to produce much better results.

There are also a few applications of DFC's which cannot easily be categorised. These include the use of DFC's in informal settlement planning, urban run-off determination, precise mapping of hydro towers and lines, pipeline rights-of-way management and for verification and revision of large-scale mapping.

#### 3.4.4 Other

Spatial information is fundamental to a range of informal settlement management tasks and imagery is a means of providing this information. At a very coarse level, imagery can be used to detect informal settlements and delineate boundaries (Mason, 1997). At the individual shack level, imagery is very useful for a variety of reasons. It can be invaluable in response to emergencies, and can provide an important communication tool in encouraging and enabling community participation in planning. Furthermore, it assists greatly in social surveys of the number of shacks for census purposes and facilitates detailed mapping for upgrading services and developing a settlement GIS of shack boundaries and facilities (Mason, 1997; Mason *et al.*, 1997). With these potential uses in mind, Mason *et al.* (1997) looked at the possibility of using the Kodak DCS460 digital camera, in place of more conventional large format aerial photography, for mapping of informal settlements. This remote sensing option was considered to be cheaper and more appropriate in terms of spatial accuracy for the contained and dynamic environment of an informal settlement.

Imagery of the approximately 7.8 ha Marconi Beam settlement in Cape Town, South Africa was captured at a ground pixel resolution of 0.3 to 0.4 m. The imagery was then triangulated in a bundle block adjustment using the measured coordinates of well-defined roof corners and ground features as both control and external check points. This bundle adjustment yielded accuracies in the order of 0.2 m in planimetry and 0.6 m in elevation. This was considered sufficient to meet the requirements for detailed mapping for most informal settlement applications. For applications in which only low to medium accuracy is required and scene interpretation is more important, Mason (1997) and Mason *et al.* (1997) suggest that geo-referencing the imagery using less rigorous and

inexpensive techniques of warping or 'rubber-sheeting' the images to fit a set of ground control points (GCPs) should be considered. Accuracies of between 1 and 5m are commonly achieved which is sufficiently accurate for most informal settlement planning applications. Digital cameras can also be used in urban mapping applications and can provide accuracies sufficient for thematic mapping applications.

Monday *et al.* (1994) describe the use of four-band ADAR 5000 imagery of a 16 square mile (41.4 km<sup>2</sup>) test area in the city of Irving, Texas, to classify and quantify impervious versus pervious areas in order to determine the storm water run-off within each ownership land parcel. This was done to comply with U.S. Environmental Protection Agency (EPA) urban water quality management guidelines.

The areas of pervious and impervious surfaces were classified by using the Normalized Difference Vegetation Index (NDVI), which compares data in the near infrared and red spectral bands of imagery. By using the NDVI, vegetation covered areas appeared bright in the NDVI image, while streets and other bare areas appeared dark. This made the general classification of pervious and impervious areas relatively simple through image thresholding, leaving only the "ambiguous" areas to be accounted for. These "ambiguous" areas were classified by applying a more rigorous classification utilising all four spectral bands. These classified raster data were then overlaid with existing vector data of the city's existing property parcels to create reports on the number and type of classified pixels within each parcel.

Preliminary results were considered to be excellent with surface areas determined using the classified image data showing a correlation of better than 99 percent with the city's area calculations. Although the image acquisition costs were approximately one-third higher than for conventional orthophotography, the advantages of spectral analysis, timeliness of results, and simplified and cost-effective updates ultimately reduced the overall project cost. The success of this project prompted the city to utilise this technology to map the entire city of Irving and it was envisaged that the data would be used by other departments for specific projects such as flood plain evaluation, comprehensive planning, parks management, and hazardous material monitoring.

Jadkowski *et al.* (1994) document the use of a 1320 by 1035 pixel Kodak Megaplug 1.4 CCD camera to cost-effectively acquire up-to-date aerial imagery of pipeline rights-of-way corridors. Their research was initiated because pipeline companies were facing increasing regulatory pressures, operating issues, and were needing to remain ahead in a competitive market. Digital cameras were identified as economic and versatile alternatives to traditional aerial photography and satellite remote sensing for providing aerial image data that would allow regular monitoring of pipelines. Monitoring applications described by Jadkowski *et al.* (1994) included general map updating, marketing, pipeline updating and inventories, locating environmentally sensitive areas such as wetlands, and planning access and boom placement in the event of a pipe rupture. The main use, however, was in providing the data to allow pipeline companies to perform mandatory annual dwelling surveys to determine the dwelling density within 200 metres of each pipeline. The density of dwellings determines the stress level in a pipeline which in turn determines whether or not the movement of gas in a pipeline should be decreased or whether a pipeline needs to be replaced. While no specific results are documented, the researchers emphasised the potential of fully digital systems for substantially reducing monitoring costs and identified the development of such systems in transportation, electric transmission, and other corridor applications. Merchant and Tudhope (1994), cited by King (1995), document one such application.

Merchant and Tudhope (1994), cited by King (1995), applied 1280 by 1024 pixel DFCs at a very much larger scale for precisely mapping hydro towers and lines. They mounted two calibrated cameras in the wing tips of a small aircraft for stereo imaging and flew at an altitude of 61m to produce pixels of only 5cm. Precise positioning of the aircraft and imagery was achieved using differential GPS. Through standard photogrammetric bundle adjustment techniques, they were able to position various components of the hydro line system to within 10 to 15 cm, except for the main cables, for which the accuracy was only 40 to 60 cm. Merchant and Tudhope (1994), cited by King (1995), believed that a higher resolution camera, coupled with a larger base-to-height ratio for the imagery and more stability within the optical system, could allow digital camera imaging techniques to completely replace the expensive ground survey and photographic methods that were presently in use.

A final possible application of digital still cameras which has been researched by Mills and Newton (1996) is the verification and updating of existing large-scale digital maps. Mills and Newton

(1996) made use of the Kodak DCS200 digital camera to obtain imagery of a railway station. Such a site was considered to be suited to aerial survey due to the dangers inherent in land surveyor's venturing onto the railway lines in order to update mapping.

The three raster images that provided the required ground coverage of the station were imported into a PC-based Desktop Mapping System (DMS) and five well-distributed, natural GCPs for each image were identified and digitised. The coordinates of these GCPs were obtained from the digital vector map sheet that was to be updated using the imagery. Assuming that the area was flat the images were then rectified to fit the ground control, following which the images were mosaicked to create a single geographically referenced image. This allowed for continuous vector update without the need to switch between images. By overlaying the vector map sheet changes to the vector data could be easily detected and digitised. Mills and Newton (1996) found that the method worked well in this relatively flat area. The general fit of the vector data to the imagery was good, with only slight variations at the periphery of the images which can be attributed to lens and CCD chip distortions. They stressed, however, that in an area encompassing major changes in relief the imagery would have to be resampled using a DTM to produce a true orthophoto in order for the vector data and raster imagery to fit. They also recognised that some field work may still be required to verify features that may be masked by vegetation or shadow and for checking street names, house numbers and other spatial data that may be required in the GIS data set. In terms of the camera, Mills and Newton (1996) reiterated the problems that other researchers had regarding the format of the camera and the limitations on the download rate of imagery. Future digital camera developments would almost certainly overcome these problems (Mills and Newton, 1996).

The above review reflects the potential of using DFC's for remote sensing of natural and other resources. This potential, combined with the predicted improvement in resolution and stability of these sensors in the next decade and the advantages of DFC's previously discussed, is likely to make DFC's an equivalent to small and medium format aerial photography for remote sensing applications. While there widespread use is likely to depend on whether memory storage technology can improve to meet the improved resolution, it was decided to make use of a DFC for this project. Prior to developing the in-flight image acquisition system using a DFC though,



the pre-flight planning system had to be improved. The following chapter discusses the pre-flight planning system developed.

## 4. PRE-FLIGHT PLANNING IMPROVEMENTS

Based on the limitations of the pre-flight planning routine described in Chapter 2, a single program that could perform all the necessary calculations and output the required information with a minimum of user effort was developed. This program was written using Borland Delphi 3 object-oriented programming software. The required program inputs and outputs and the algorithms implemented are described below. Figure 5 shows the graphical user interface.

The screenshot shows a graphical user interface for pre-flight planning. The window title is "Pre-flight Planning: Video and digital camera". The interface includes a menu bar with "File", "View", "Options", and "Help". The main area is divided into several sections:

- Project Code and Name:** A text field containing "Test flight over FMB".
- Catchment Details:** Four input fields for "Max. Catchment Altitude (m ASL)" (1200), "Min. Catchment Altitude (m ASL)" (750), "Avg. Catchment Altitude (m ASL)" (1000), and "Max. Altitude Limit (m ASL)" (1200). An "O.K." button is located to the right of the last field.
- Camera:** Radio buttons for "Video", "Kodak DCS 460", and "Kodak DCS 420".
- Lenses:** Radio buttons for "Video" and "DCS Lenses".
- DCS Lenses:** Radio buttons for "Lens 1" and "Lens 2", and a "Focal Length (mm)" dropdown menu set to "20".
- Overlap %:** Two sets of dropdown menus. The "Side" set has "Desired" (35) and "Minimum" (20). The "Forward" set has "Desired" (30) and "Minimum" (20).
- Ground Pixel Size (m):** A dropdown menu set to "1.0".
- Aircraft Parameters:** Input fields for "Avg. Flying Heights: AGL: (m)", "ASL: (m)", "ASL: (feet)", and "Flight Strip Spacing: (m)".
- Image Parameters:** Input fields for "Avg. Swath Width (m)", "Avg. Area Covered/Image (km2)", "Avg. Ground Distance (m)", "Avg. % Overlap", "Min. % Overlap", and "Max. % Overlap".

Figure 5: The pre-flight planning graphical user interface

### 4.1 Program Inputs

Figure 5 displays a selection of the inputs which are required before the outputs of flight strip spacing, percentage overlap, flying heights and other parameters can be calculated. These include camera and lens parameters, ground pixel size, and overlap requirements. Further inputs not displayed in Figure 5 are a generate file of the catchment boundary and an optional DEM coverage of the area.

#### 4.1.1 Camera and lens parameters

The user is provided with the option of choosing the Kodak DCS 460 digital camera, the Kodak DCS420 digital camera, or the Panasonic video camera described previously. Based on this choice, the appropriate program constants relating to the camera CCD chip size and number of pixels in the CCD chip are initialised. The user is also prompted to choose a suitable lens based on his/her choice of camera. The choice of lens determines the focal length to be used in the calculation of the flying height and flight strip spacing.

#### 4.1.2 Ground pixel size

The choice of a suitable ground pixel size by the user is based on the intended use of the imagery. For land use mapping using the video camera as an example, a ground pixel size of 2 metres is typically chosen, while for alien vegetation studies higher resolution imagery is required in order to distinguish the alien vegetation from the indigenous vegetation and a ground pixel size of 1.2 to 1.4 metres is used.

#### 4.1.3 Catchment generate file

A generate file of the catchment boundary can be created from a shape file in ArcView 3.0a and contains the x and y coordinates of all the points that can be joined by lines to define the area's boundary. For the program, the coordinates for the generate file must be in the Gauss Conform projection, in other words in metres North or South of the equator, and metres East or West of a central meridian. It was decided to use this projection as having the coordinates in metres would make the calculation of, for example, flight strip spacings and photograph spacings far easier than if the generate file was in geographic coordinates. On opening the generate file the user is also required to enter the central meridian for the file.

#### 4.1.4 Digital elevation model

If a digital elevation model of the area of interest is available, the user has the option to open the DEM and make use of the information it contains. This DEM must be in ASCII text format and

in the geographic coordinate system. The geographic coordinate system was chosen as it avoids the need to know the central meridian for the DEM and ensures that the DEM can be used regardless of the central meridian of the generate file.

When the DEM is opened the appropriate altitude values of the DEM that are within the target boundary are read. A flow chart depicting the algorithm used in reading the DEM is shown in Figure 6 below.

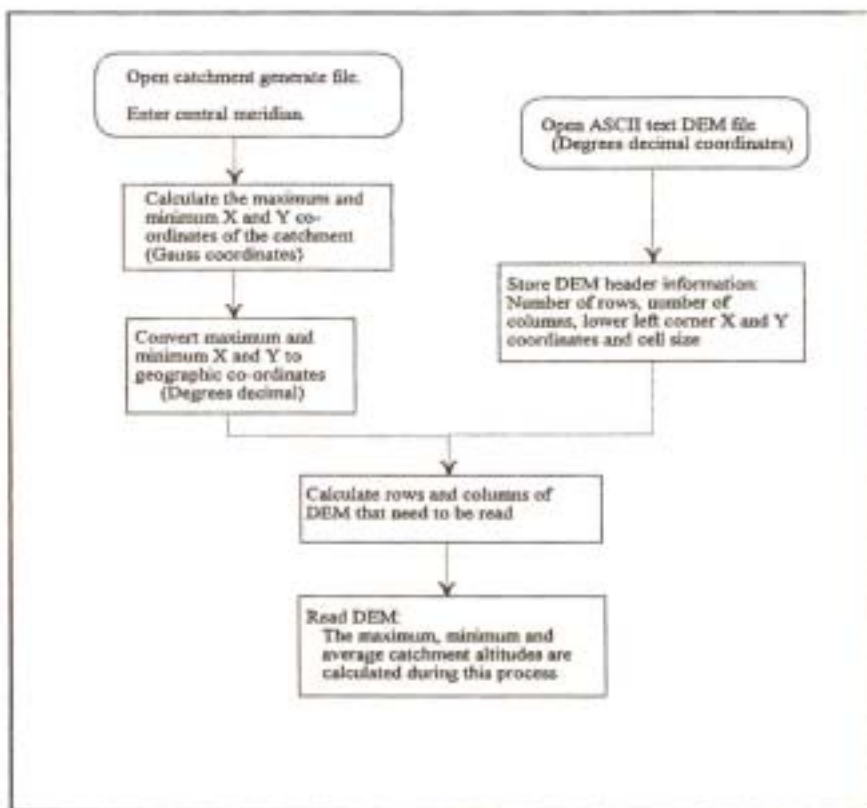


Figure 6: Flowchart depicting procedure for reading a DEM

Alternatively, if a DEM is not available, the user can manually input the maximum, minimum and average catchment altitudes. This information can be easily determined from a topographical map.

#### 4.1.5 Overlap requirements

The desired percentage overlap and a minimum overlap percentage between flight strips and between photographs is also required. 'Side Overlap' refers to the image overlap between flight strips and 'Forward Overlap' to the percentage overlap between consecutive images. The reason for including these options will become more apparent during the description of the program outputs which follows.

#### 4.2 Program Outputs

Using the inputs as described above, several program outputs are obtained. While the calculation of each output could be discussed separately, the determination of the flying height, average swath width, and minimum, maximum and average percentage overlaps, as shown in Figure 5 previously, are related to the calculation of the flight line spacing. For this reason, the calculation of these outputs will be outlined during the discussion of the calculation of the flight line spacing in the section below.

##### 4.2.1 Flight line spacing

An initial average swath width is calculated using the following equation:

$$SW_{\text{initial}}(\text{avg}) = CCDX_{\text{pixels}} \times \text{PixelSize} \dots\dots\dots(1)$$

Where;

$SW_{\text{initial}}(\text{avg})$  = initial estimate of average width of coverage on the ground at right angles to the direction of flight (m)

$CCDX_{\text{pixels}}$  = number of pixels in the camera's CCD at right angles to the direction of flight and

$\text{PixelSize}$  = ground pixel size chosen (m).

Based on this estimate of the average swath width, an initial flight line spacing is calculated using equation 4 below. This initial flight line spacing is then input into the algorithm depicted in the flowchart in Figure 7. This algorithm ensures that the percentage overlap at the highest point in the catchment is not less than the minimum overlap stipulated by the user and was included to avoid the situation where, in catchments with a large range of altitudes, a flight strip spacing based on the average catchment altitude may result in the overlap in the higher parts of the catchment becoming too small or nil. Such a situation is undesirable as a reasonable percentage of overlap is required to avoid loss of information due to aircraft tip and roll.

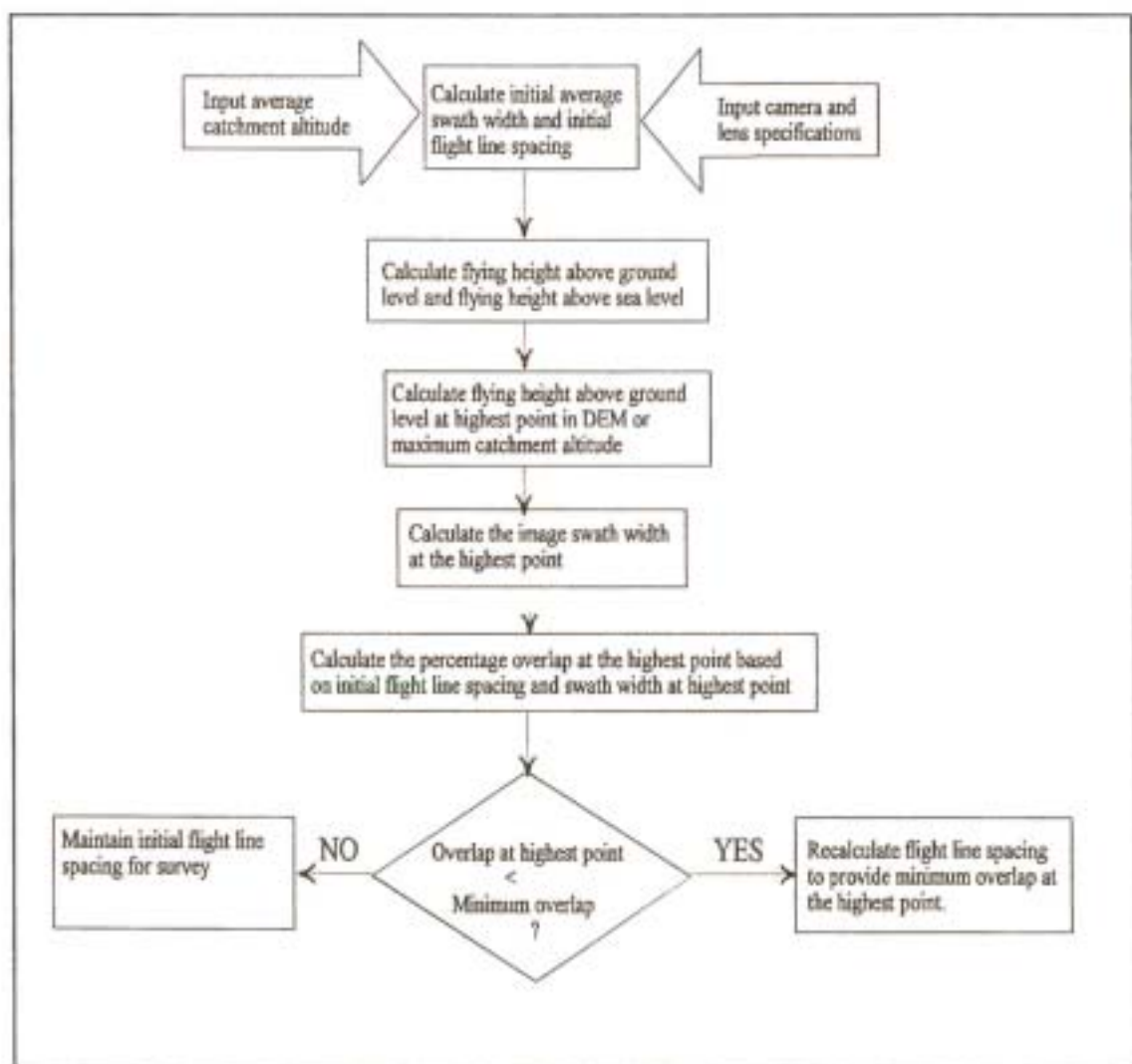


Figure 7: Flowchart of algorithm for calculating the flight strip spacing

The equations that are used in calculating the parameters shown in Figure 7 are as follows:

$$\text{FlyHeightAGL} = \frac{\text{SW} \times \text{flength}}{\text{CCDXdim}} \dots\dots\dots(2)$$

Where;

FlyHeightAGL = flying height above ground level (m) at the highest, lowest or average catchment altitude, respectively

SW = swath width at the highest, lowest or average catchment altitude (m), respectively

flength = focal length of the camera lens (mm) and

CCDXdim = dimension of the camera's CCD at right angles to the flight direction (mm).

$$\text{FlyHeightASL} = (\text{FlyHeightAGL} + \text{GroundHt}) \times 3.281 \dots\dots\dots(3)$$

Where;

FlyHeightASL = flying height above sea level (feet) and

GroundHt = height of the terrain above sea level (m).

The flying height above sea level is calculated in feet and not metres since the aviation community and aircraft instrumentation still operate in feet.

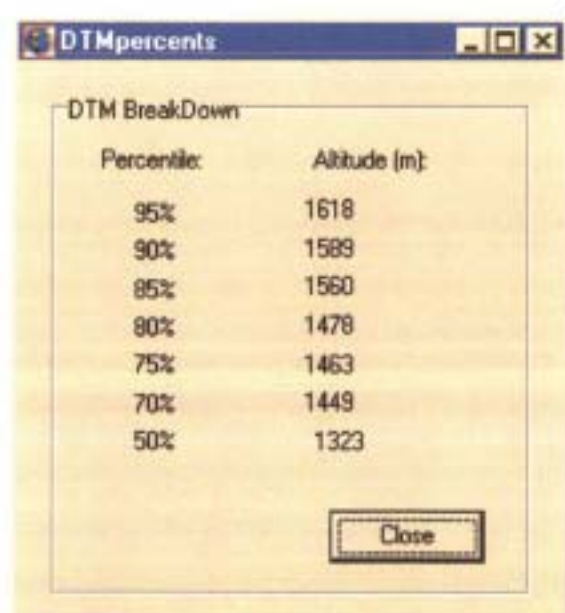
$$\text{FlsSpace} = \text{SW} \times \left( 1 - \frac{\% \text{Overlap}}{100} \right) \dots\dots\dots(4)$$

Where;

FIsSpace = flight line spacing (m) and

%Overlap = percentage overlap at the highest, lowest or average catchment altitude, respectively.

Furthermore, for the situation where a single mountainous section within a survey area has an overriding effect on the flight strip spacing calculated using the above algorithm, the user may decide that it is unnecessary to have image overlap in this section by entering a value for 'Altitude limit'. To aid in determining by how much the user can reduce the 'Maximum catchment altitude', as shown in Figure 5, without severely affecting the coverage of the area, a Delphi unit was added which provided a breakdown of the altitudes above which a certain percentage of the catchment occurs. The form associated with this unit is shown in Figure 8 below.



The image shows a software dialog box titled "DTMpercents". Inside the dialog, there is a section titled "DTM BreakDown" containing a table with two columns: "Percentile" and "Altitude (m)". The table lists the following data points:

| Percentile | Altitude (m) |
|------------|--------------|
| 95%        | 1618         |
| 90%        | 1589         |
| 85%        | 1560         |
| 80%        | 1478         |
| 75%        | 1463         |
| 70%        | 1449         |
| 50%        | 1323         |

At the bottom right of the dialog box, there is a "Close" button.

Figure 8: The altitude percentiles form

The altitude percentiles are calculated by dividing the range of altitudes, as read from the DEM of the area, into 10 equally sized classes. The lower boundary of each class is then used as the basis for calculating a cumulative frequency distribution of the altitude values, in other words a cumulative total of the number of altitudes falling within each class. The altitude values



representing different percentiles can then be easily calculated by first determining in which group the percentile occurs and then interpolating between the upper and lower bounds of that class to calculate the altitude.

Once the flight line spacing has been calculated, it is input into an algorithm that calculates the flight strip way point coordinates or, in other words, the beginning and endpoint coordinates of each flight strip. The algorithm is described in the following section.

#### 4.2.2 Flight strip way point coordinates

Before the flight strip positions and way point coordinates can be calculated, the user is required to choose whether the survey is to be flown in a North-South or East-West direction. This choice is typically based on the difference in flying times between these two options.

When the flying direction has been decided upon, the position of the first flight strip is calculated using the following formula:

$$FL1 = \frac{1}{2} \left[ (NFL \times SW_{avg}) - Width \right] \dots\dots\dots(5)$$

Where;

FL1 = distance of first flight line from edge of project area

NFL = Number of flight lines = Width/FlsSpace

SW<sub>avg</sub> = swath width at the average catchment altitude (m) and

Width = project area width (m).

The initial way point coordinates for flight lines flown in a North-South direction are then calculated using the algorithm shown in Figure 9 below. A similar algorithm is employed for calculating East-West flight lines.

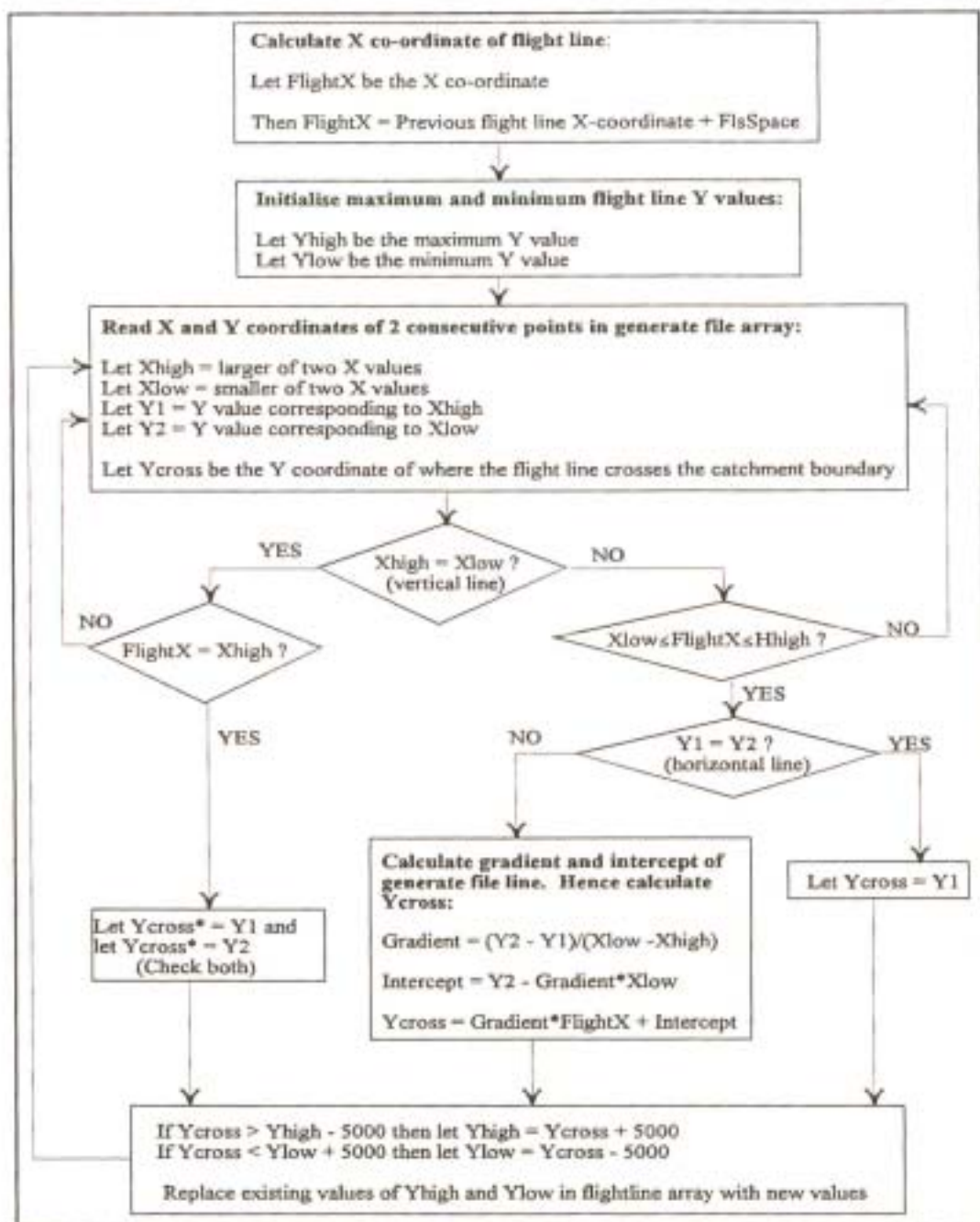
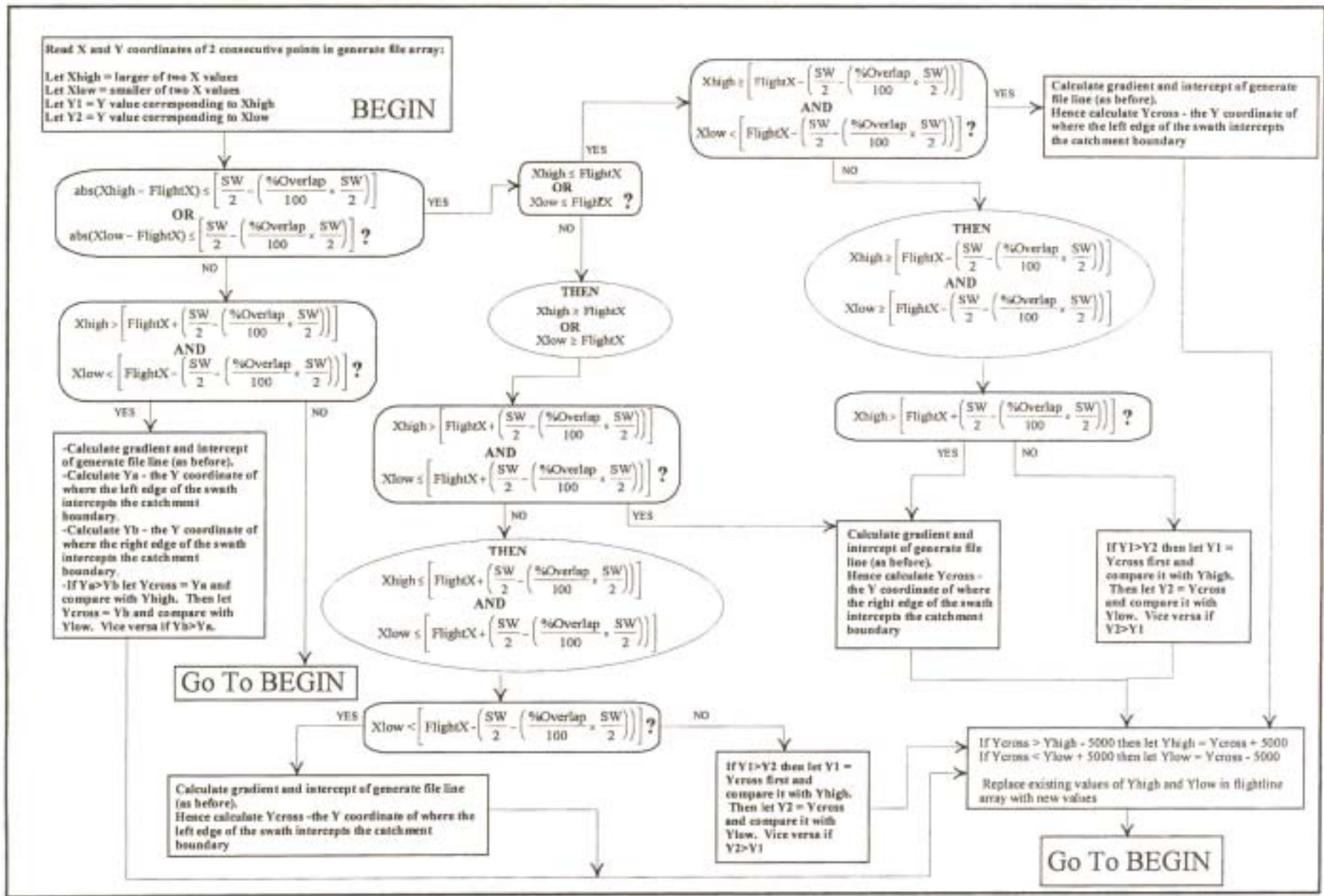


Figure 9: Flowchart of algorithm to determine initial flight line way point coordinates

A further algorithm is then employed to account for situations where there is the potential for information loss due to the flight strip beginning or ending at the incorrect position. Such situations were illustrated in Figures 1 and 2 in Chapter 2. A flowchart of the algorithm for North-South flight lines is shown in Figure 10. As before, a similar algorithm would be used to calculate the way point coordinates for East-West flight lines.

Figure 10: Flow diagram of algorithm to ensure no loss of data at the ends of flight strips



### 4.2.3 Flying time summary

To assist the user in deciding whether to fly the survey in a North-South or East-West direction, a summary of the flying time is provided. This summary is shown in Figure 11 below.

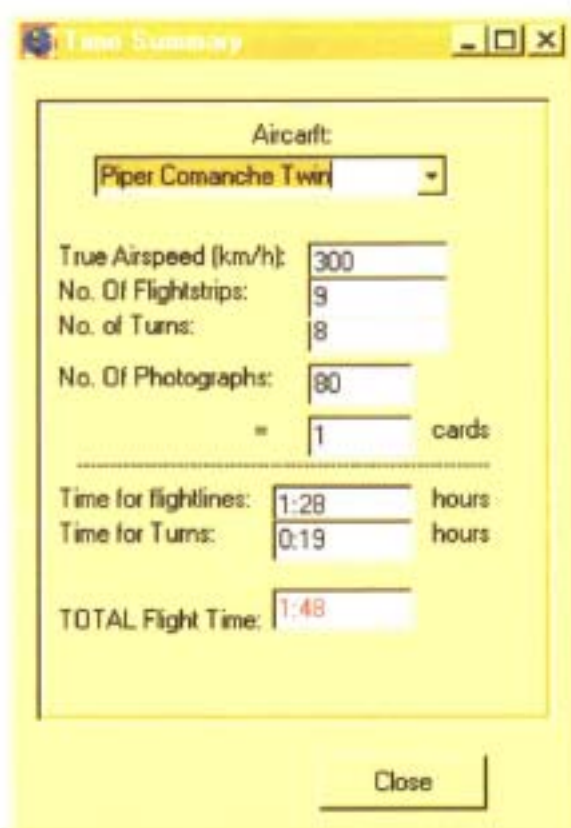


Figure 11: The program summary of flying times

The calculation of the various flying times shown is dependent on the user's choice of aircraft. The choice of aircraft determines the true airspeed displayed and used in the calculation of the times.

The time required to fly the flight lines is calculated by dividing the total length of all flight lines, including the 5km 'run-in' and 'run-out', by the true airspeed. The time to complete a turn is calculated using the following formula:

$$T = \frac{0.031022415 \times (3.281 \times R)}{\left(\frac{V}{1.853}\right)} \dots\dots\dots(6)$$

Where;

T = time in minutes to complete 180° turn

R = radius of turn (feet) and

V = velocity, true airspeed (knots).

The number of photographs to be taken, as shown in Figure 11, is determined during the calculation of the position of photographs along the flight lines. The algorithm for determining the photograph positions is described in the following section.

#### 4.2.4 Photograph/image positions

When considering how to calculate where each photograph or image should be taken, two alternatives were considered. Either the exact latitude and longitude of each photograph centre could be calculated and stored, or the position of the photograph centre could be represented as a distance from the end of the flight strip. In deciding which option to choose, the complexity of the processing required and the intended in-flight setup had to be considered.

The former option was discarded since, firstly, the amount of programming required to calculate the exact latitude and longitude coordinates of each photo centre was considered to be far greater than simply calculating a distance to the end way point of a flight line. Secondly, it was considered unnecessary to know the exact coordinates of a photograph's centre when it is very unlikely that a pilot is ever able to remain exactly on the planned flight line. Consequently, had this option been chosen, it would have meant that the current GPS position and the calculated photograph centre position would have had to be continuously compared, probably at one second intervals, to find the position where the distance between the GPS position and the calculated photograph position was a minimum. The camera would then be sent a signal to take a photograph. This would have required the writing of some efficient code to provide the necessary one second updates. Furthermore, the use of this type of algorithm would have meant that the exact position where the photograph should be taken would have to be passed before it could be confirmed using the GPS data that the aircraft had, in fact, passed that point. It would therefore be less likely that the required overlap could be consistently achieved using this algorithm.

However, the aircraft will always be at exactly the required distance from the end of the flight strip at some point. The in-flight processing would therefore entail the implementation of a simpler algorithm where the current GPS position is read and then the distance from this position to the known position of the end of the flight strip could be calculated. A procedure written in Fortran 77 was available for calculating the distance between two points whose geographic coordinates are known. If this calculated distance was equal to or less than the required distance, the camera would be fired. It was felt that this algorithm would be less complicated, more efficient and therefore more suitable for the application.

The algorithm used in calculating the photograph positions for a single flight line is depicted in the flowchart in Figure 12 on the following page. This algorithm is employed if a DEM coverage of the area has been previously opened. The algorithm to determine the maximum, minimum and average altitudes for each flight line is very similar to that described in section 4.1.4 for calculating the maximum, minimum and average catchment altitudes. The algorithm used to compute the required photograph spacing for each flight line is similar to the algorithm that is used to determine the flight line spacing. This algorithm was described in section 4.2.1.

For the situation where a DEM is not available, a photograph spacing based on the average catchment altitude is calculated and used to compute the distance of each photograph from the end of its respective flight strip. For this scenario it was decided not to check for sufficient forward overlap at the highest point in the catchment since this could result in the photograph spacing for the entire survey being based on a minimum overlap at the highest point in the survey area. This would significantly increase the number of photographs that had to be taken and thereby lead to possible image storage problems.

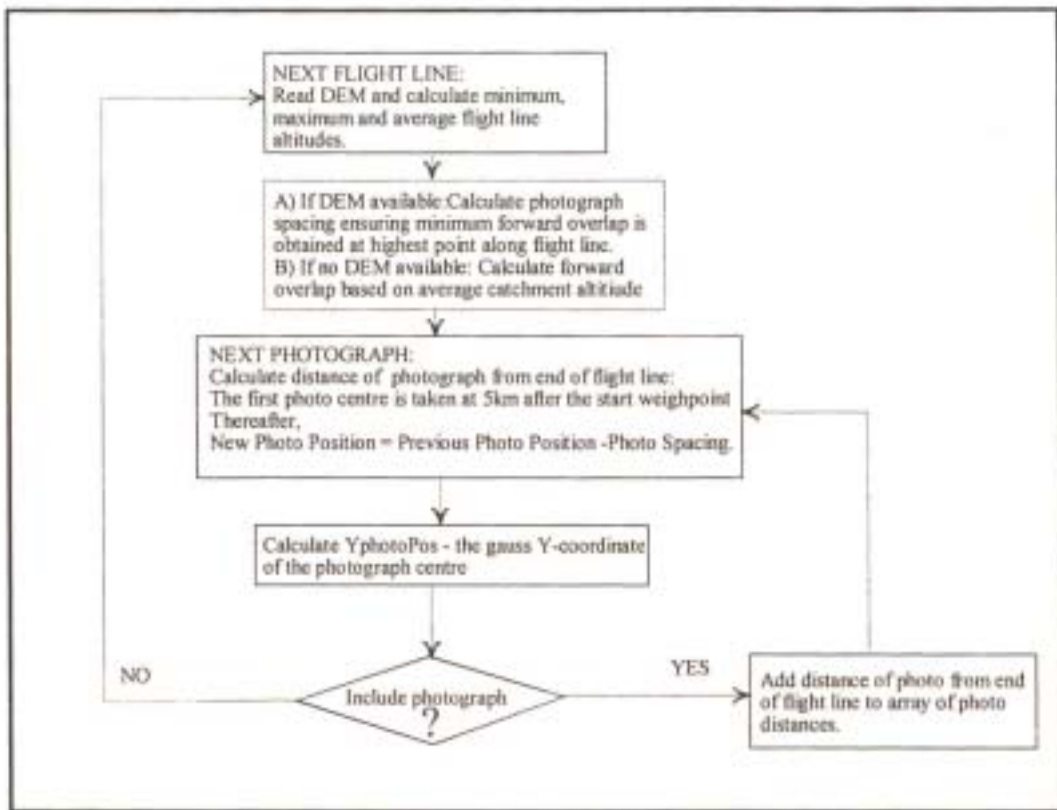


Figure 12: Flowchart of algorithm for calculating photograph positions

A photograph or image is included if it contains data of the survey area not present in a previous photograph or image. Examples of photographs or images that would be excluded and included are shown in Figures 13a and 13b on the following page, respectively. Referring to the Figures, if  $Y_{photoPos} + (0.5 \times SWY_{avg} - (Flap\% \times SWY_{avg} / 100)) > Y_{low} + 5000$  then the photograph or image is included. Recall that  $Y_{low}$  is the Y coordinate of a flight line's northern way point as described in section 4.2.2. A similar approach is employed for photographs or images at the southern end of the survey area and for flight lines flown from East to West and West to East.

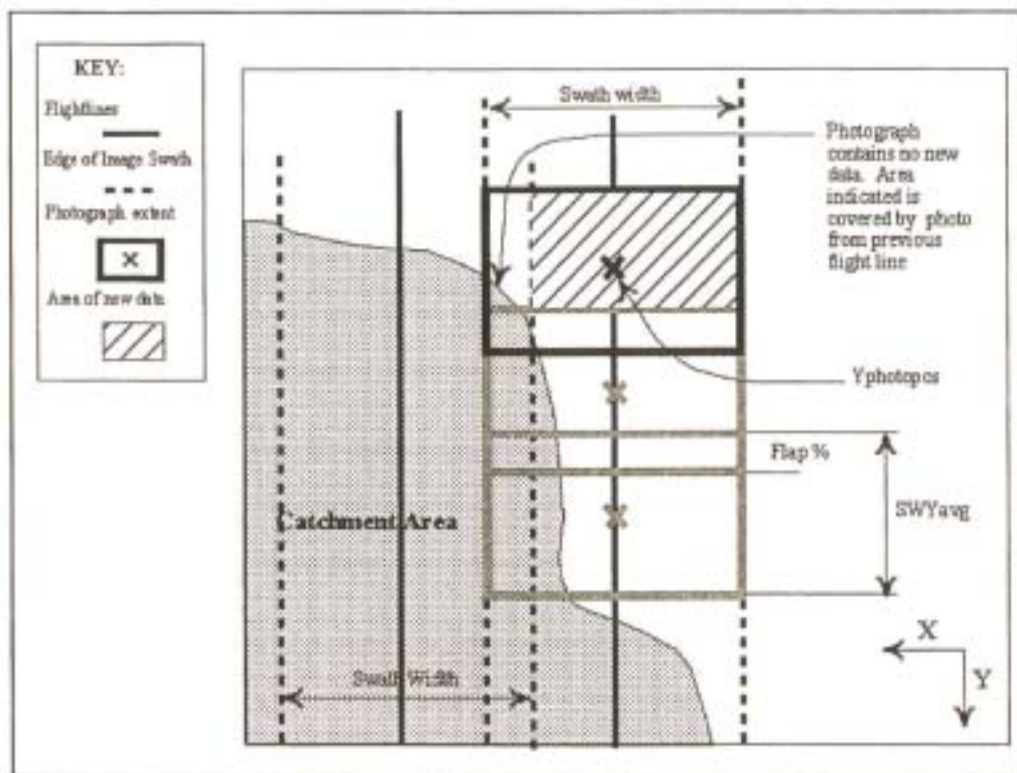


Figure 13a: Example of photograph or image that would be excluded

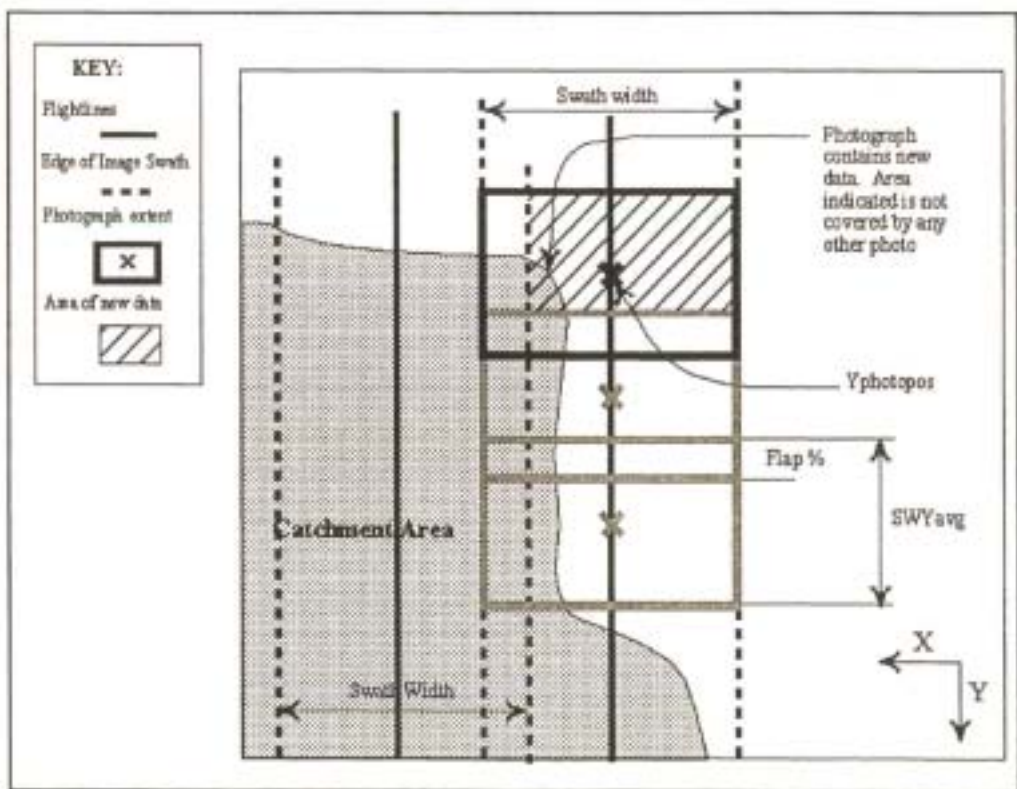


Figure 13b: Example of photograph or image that would be included



#### 4.2.5 GPS way point file

Since the pilot was accustomed to the existing Garmin GPS receiver used, it was decided to continue to make use of this GPS for navigational purposes. Unfortunately it was deemed to be impossible to automatically upload way point coordinates to this GPS and for this reason a GPS way point file had to be produced that would allow easy manual input of the coordinates into this GPS. To produce such a file, a routine was written that converts the gauss way point coordinates, calculated as described previously, into geographic coordinates and then outputs these coordinates to a file in a user friendly format. The format of the file is illustrated in Table 5 below.

Table 5: Garmin GPS way point coordinate file

| FLS Start | Lat     | Long    | FLS End | Lat     | Long    |
|-----------|---------|---------|---------|---------|---------|
| 1a        | 29.3943 | 31.3893 | 1b      | 29.4696 | 31.3898 |
| 2b        | 29.5067 | 31.4037 | 2a      | 29.3838 | 31.4029 |
| 3a        | 29.3773 | 31.4165 | 3b      | 29.5448 | 31.4177 |
| 4b        | 29.5510 | 31.4314 | 4a      | 29.3772 | 31.4302 |
| 5a        | 29.3607 | 31.4438 | 5b      | 29.5657 | 31.4453 |
| 6b        | 29.5598 | 31.4589 | 6a      | 29.3568 | 31.4574 |

Having developed the pre-flight planning program, the in-flight image acquisition system was developed. The development of this system is documented in the following chapter.

## 5. IMAGE ACQUISITION SYSTEM

Several improvements to the existing image acquisition system were investigated. The most important of these changes was the decision to move away from a video-based system to one based on a digital still camera. This change was based on the potential advantages and applications of a digital camera system as described in the literature review in Chapter 2. Other advantages of a digital system over the current video system and the implications of incorporating a digital still camera into an aerial survey system are described below.

### 5.1 The Sensor

Before deciding on which camera to use, a comprehensive survey of the digital camera market was performed to identify cameras which could possibly be used. A summary of the cameras identified and their respective characteristics is shown in Table 6.

Table 6: Summary of characteristics of available digital cameras

| Company  | Camera Model | Resolution (pixels)       | Maximum Memory              | Other Characteristics  |
|----------|--------------|---------------------------|-----------------------------|--|
| Kodak    | DCS 410      | 1.5 million (1500 x 1000) | 170 Mb (removable)          | -Full SLR functionality<br>-Voice annotation<br>-DLL for camera control available            |
|          | DCS 420      | 1.5 million (1500 x 1000) | 170 Mb (removable)          | -Full SLR functionality<br>-Voice annotation<br>-DLL for camera control available            |
|          | DCS 5        | 1.5 million (1500 x 1000) | 170 Mb (removable)          | -Full SLR functionality<br>-Voice annotation<br>-DLL for camera control available            |
|          | DCS 460      | 6 million (3000 x 2000)   | 170 Mb (removable)          | -Full SLR functionality<br>-Voice annotation<br>-DLL for camera control available            |
|          | EOS-DCS 1    | 6 million (3000 x 2000)   | 170 Mb (removable)          | -Full SLR functionality<br>-Voice annotation<br>-DLL for camera control available            |
| Minolta  | RD-175       | 1.75 million              | 130 Mb (removable)          | -auto focus<br>- SLR functionality<br>-compact<br>-3 CCD camera - excellent colour contrast. |
| Fuji     | DS-300       | 1.3 million               | removable                   | -auto/manual focus   |
| Polaroid | PDC2000-40   | 1.92 million              | 40 Mb (internal hard drive) | -auto or fixed focus   |
| Nikon    | E2N          | 1.28 million              | 15 Mb (removable)           | -SLR functionality<br>-compact   |

To choose between these different cameras, a Kepner-Tregoe (K.T.) decision analysis (Fogler and LeBlanc, 1995) was performed. This approach involves dividing the objectives of a decision into two categories: musts and wants. The musts are those objectives which are mandatory to achieving a successful solution. The wants are desirable, but not mandatory. Each alternative is first evaluated against each must. If it does not satisfy any one of the musts, it is not considered further. After eliminating some alternatives, a list of the wants is made and each want is assigned a weight (1-10) according to how important that particular want/objective is. An extremely

important want is given a weighting of 9 or 10, as an example. Each alternative is then evaluated against these wants and given a rating (1-10) according to how well it satisfies the want. If the alternative fulfills all aspects of a want it receives a rating of 10, while if it only partially fulfills the want it receives a rating of 4 or 5. The weight of the want is then multiplied by this rating to arrive at a score for that alternative. The scores for each alternative are summed and the alternative with the highest total score is the tentative first choice. Table 7 shows the decision analysis performed.

Table 7: Kepner-Tregoe decision analysis for digital cameras (after Fogler and LeBlanc, 1995)

|   |    | CAMERA |            |        |            |                  |                |          |              |
|---|----|--------|------------|--------|------------|------------------|----------------|----------|--------------|
| MUSTS                                     |    | DCS420 |            | DCS460 |            | Minolta<br>RD175 | Fuji<br>DS 300 | Polaroid | Nikon<br>E2N |
| High Resolution                           |    | Yes    |            | Yes    |            | Yes              | Yes            | Yes      | Yes          |
| Automated Camera Control                  |    | Yes    |            | Yes    |            | No               | No             | No       | No           |
| WANTS                                     | Wt | Rating | Score      | Rating | Score      |                  |                |          |              |
| Low Cost                                  | 7  | 5      | 35         | 2      | 14         | -                | -              | -        | -            |
| High storage capacity                     | 8  | 8      | 64         | 8      | 64         | -                | -              | -        | -            |
| Different lenses, focus/aperture settings | 5  | 9      | 45         | 9      | 45         | -                | -              | -        | -            |
| Large area mapping                        | 8  | 2      | 16         | 6      | 48         | -                | -              | -        | -            |
| Compact                                   | 3  | 5      | 15         | 5      | 15         | -                | -              | -        | -            |
| <b>TOTAL</b>                              |    |        | <b>175</b> |        | <b>186</b> | -                | -              | -        | -            |

Since the Kodak DCS410, DCS420 and DCS5 were cameras with very similar specifications and characteristics, only the Kodak DCS420 was considered in the analysis. Similarly, the Kodak DCS460 and EOS-DCS1 cameras were considered as equivalent cameras and only the DCS460 was analysed. The decision to only analyse the Kodak DCS420 and DCS460 was also based on

personal communication with Positive Systems (1998). They identified these two cameras as the most popular and frequently used of the Kodak range of cameras. Help in integrating either of these cameras would therefore be more easily obtainable.

Examining Table 7 it can be seen that high resolution and the possibility of automated camera control were identified as necessities or musts for the system. High resolution was considered in a relative sense by comparison with the existing airborne videography system. All cameras were thus considered to be of sufficiently high resolution to warrant further investigation.

However, when considering the necessity of having automated camera control via a PC or laptop, only the Kodak range of cameras were suitable. As alluded to in Table 6, Eastman Kodak have developed a Visual C++ Dynamic Link Library (DLL) for developers to integrate into their applications. This DLL, which is a component of Kodak's professional digital camera Software Developer's Kit or SDK (Kodak, 1998), is a library of camera, image acquisition, image storage and image processing functions which allows the user to incorporate a Kodak DCS420, Kodak DCS460, as well as other professional quality Kodak digital cameras into their application. The functionality of this DLL was seen as ideal for the purposes of this project. On the other hand, Minolta, Fuji, Polaroid and Nikon did not offer such a SDK or DLL and integrating any of the cameras listed would have required the development of some new code and functions to control and trigger the camera through the camera's serial port, or the development of an electronic unit to depress the camera's trigger button at the desired moment. It was thus decided that only the Kodak DCS420 and DCS460 cameras were suited to timely integration into an automated aerial survey system. The Kodak DCS420 is shown in Figure 14 below. The Kodak DCS460 looks identical.



Figure 14: The Kodak DCS420 digital camera

The comparative specifications of the two cameras are tabulated in Table 8 on the following page.

Table 8: Kodak DCS420 and DCS460 digital camera specifications

|   | Kodak DCS420  | Kodak DCS460  |
|---|---|---|
| Key Functions and Benefits                            | - 1.5 MP image size<br>- Traditional SLR operation<br>Nikon N90 Body accepts all F-mount lenses | - 6 MP image size<br>- Traditional SLR operation<br>Nikon N90 Body accepts all F-mount lenses |
| Resolution  | 1.5 MP image size (1524 x 1012 pixels)  | 6 MP image size (3060 x 2036 pixels)  |
| Image storage   | Removable hard drive or RAM card (PCMCIA-ATA): 104 images per 170 Mb card                       | Removable hard drive or RAM card (PCMCIA-ATA): 26 images per 170 Mb card                      |
| Dynamic range   | - 12 bits/colour<br>- ISO to 400 equivalent (colour)  | - 12 bits/colour<br>- ISO equivalent rating of 80   |
| Imager dimensions                                     | - 14mm x 9.3mm<br>- 2.5 x focal length  | - 27.6mm x 18.4mm<br>- 1.3 x focal length   |
| Host interface  | SCSI only   | SCSI only   |
| Flash   | Hot shoe or other external  | Hot shoe or other external  |
| Continuous frame capture rate (All rates approximate) | Burst capability:<br>- 2 images/s for 5 frames<br>- 1 frame every 3 s after burst               | Burst capability:<br>- 2 images in 2 seconds<br>- 8 s pause to store each image               |
| Battery capacity                                      | 500 images per charge   | 200 images per charge   |
| Voice recording                                       | 3 min = 1.5Mb   | 3 min = 1.5Mb   |
| Acquire rate  | High resolution, 24-bit image file: approx 38s  |   |
| AC adapter/charger power requirement                  | 110, 120, 220, 240V AC, 50 or 60Hz  | 110, 120, 220, 240V AC, 50 or 60Hz  |
| Approximate dimensions                                | 170mm W x 114mm D x 208mm H   | 170mm W x 114mm D x 208mm H   |

Having limited the choice to these two cameras the wants identified for the cameras, in order of priority, were the capacity to store a large number of images, the potential for large area mapping, low capital cost, the ability to utilise different lenses and focus settings, and a compact unit. Low capital cost could have been included as a must, but it was envisaged that lower flying and

processing costs for the higher resolution camera systems would offset the associated greater capital cost of the higher resolution cameras. Thus, including low cost as a must would have unfairly eliminated the higher resolution cameras as options. The cost-benefit analysis documented in the following section substantiates this decision. For the initial analysis neither the Kodak DCS420 or DCS460 were considered to be low cost and they were therefore given ratings of 5 and 2, respectively.

Storage of the imagery was considered to be a very important issue, particularly if the camera was to be used for applications other than for site-specific mapping. With a single image containing upwards of 1 Mb of information, it was imperative that the camera chosen was able to store a reasonable number of images per single removable storage card, or on its own internal hard-drive. As an example, if a hypothetical square area of 300km<sup>2</sup> was to be surveyed with the Nikon E2N at a ground pixel resolution of 1m with side overlap of 25% and forward overlap of 30%, this would require the capturing of approximately 475 images. If each image is 1.3 Mb (1 colour band stored per pixel) this would require in excess of 40 15Mb storage cards. This would mean that these storage cards would have had to have been changed almost continuously. This would be impractical and time-consuming, particularly in the confined area of an aircraft cockpit. Looking at the Kodak DCS420 and DCS460 cameras, the DCS420 and DCS460 can store approximately 110 and 28 images per 170Mb PCMCIA card<sup>3</sup>, respectively. For the same hypothetical area of 300km<sup>2</sup> the DCS420 would therefore require 4 PCMCIA cards to capture the 400 images of the area. The DCS460 would also require 4 cards to store the approximately 100 images required to cover the area. Consequently, the DCS420 and DCS460 were both given a rating of 8.

The potential of using the aerial survey system for large area mapping was considered to be an equally important want. MBB hoped to be able to use the system for more than site-specific surveys of, for example, single farms, factories or residential areas. Surveys of quaternary catchments of greater than 300 km<sup>2</sup> in size for land use mapping and other resource management applications had to be included as possible applications of the system. As described in the literature review, the small sensor size and poor spatial resolution when compared with photography of most digital cameras limits their use in such large-scale mapping. Consequently, only the Kodak

---

<sup>3</sup> Larger capacity cards of over 500 Mb have also become available (Kodak, 1998)



DCS460 and Kodak EOS-DCS1 could really be considered appropriate for MBB's purposes. These cameras offer the world's largest single-shot colour imager (Kodak, 1998) and have a chip size comparable to the format of a 35mm camera (Mason, 1997). The DCS460 was thus given a rating of 6 and the DCS420 a rating of 2.

The ability to make use of different lenses and aperture and focus settings was also identified as a want. Both the DCS460 and DCS420 had full single lens reflex (SLR) functionality. This functionality would allow the system to be versatile for a variety of aerial applications. The user would not be limited to a single focal length lens and could, for example, utilise a narrow angle lens when photographing mountainous terrain to limit the geometric distortions due to changes in terrain altitude. F-stops, shutter speeds and autofocus could also all be easily set in the same manner as with a traditional SLR camera. Both cameras could therefore perform reliably and predictably under a variety of lighting conditions and image blur could be limited or eliminated even when flying at high speeds and low altitudes above the scene of interest.

A final less important want was that the camera should be compact. This was to ensure that the camera could be easily mounted in an aircraft and that the system was portable. Both the cameras had dimensions of 170mm W x 114mm D x 208mm H. This was considered to be large in comparison with other digital cameras on the market and the video camera currently used, but compact in comparison with large format photographic cameras. An average rating of 5 was therefore assigned for both cameras.

From Table 7, it can be seen that the DCS460 camera achieved the highest overall score. However, this can only be considered as a tentative first choice since the risk associated with each alternative still needs to be investigated (Fogler and LeBlanc, 1995). In the traditional approach, as documented by Fogler and LeBlanc (1995), the risk associated with the top-scoring alternatives is investigated by looking at adverse consequences that could result from choosing that alternative. A probability (1-10) of occurrence and seriousness (1-10) is associated with each adverse consequence and the product of these two numbers is a measure of the risk associated with each alternative. For this project, a less subjective approach of performing a cost-benefit analysis was chosen to establish the relative risk of the two top-scoring alternatives. This analysis would also

provide an opportunity to compare the costs of running a digital camera system versus a video or traditional photographic system

### 5.1.1 Cost-benefit analysis

The cost-benefit analysis was performed by comparing the fixed and variable costs of flying a survey and producing geographically referenced digital imagery of the resource of interest using a Kodak DCS460, a Kodak DCS420, the existing video camera, a medium format (6cm by 6cm) Hasselblad photographic camera and a large format (9" or 22.86cm by 22.86cm) photographic camera.

A spreadsheet was created that calculated the fixed costs, variable costs and flying and processing times for operating an aerial survey system with each of these camera systems. Functionality was included to allow the number of surveys per year, average survey area and ground pixel size to be adjusted. These three variables were considered to be the variables that would have the greatest influence on the feasibility and profit of an air survey system.

The fixed costs for the three systems were interest on investment, depreciation and insurance. Interest on investment was determined as a constant annual interest charge (IC) using the following formula:

$$IC = \left( \frac{P + S}{2} \right) \times i \dots\dots\dots(7)$$

Where;

P = purchase price (rands)

S = salvage or selling price (rands) and

I = interest rate.

The purchase prices<sup>4</sup> for in-flight systems based on video, DCS420, DCS460 and Hasselblad cameras were taken as R90 000, R170 000, R270 000 and R80 000, respectively. These prices were for an automated in-flight image acquisition system. Such a system would include a laptop computer, camera or system control software, and a real-time differential GPS. The GPS would provide sub-metre accurate positional information for triggering the DCS420, DCS460 and Hasselblad cameras at pre-determined photograph positions. Furthermore, each photo or image captured could be tagged with positional information which would assist in post-flight image rectification. For the video system the GPS positions would be stored with each frame to facilitate automated framegrabbing of selected frames after the flight. The purchase price for the 9" photography system was estimated as R1 500 000. This price would be for a complete system, including functionality to automatically trigger the camera and store photograph centre coordinates.

The price for the photogrammetric software and computer workstation required for post-processing of the imagery was estimated at R75 000. This cost was added to the cost of the in-flight system to determine the final purchase price for each system. The salvage price was taken conservatively as 20% of the purchase price and the interest rate used was 24%.

Depreciation was calculated using the straight-line method. The constant annual depreciation charge  $D$  is given by:

$$D = \frac{P - S}{L} \dots\dots\dots(8)$$

Where;

$P$  = purchase price (rands)

$S$  = salvage value (rands) and

$L$  = life or time between buying or selling.

---

4

The base year for all purchase prices and operating costs used in the cost-benefit analysis was 1998. The base year is the year for which the rates tabulated are valid. To calculate the equivalent rate for a future year, multiply the base year rate by  $(1 + i)^y$  where  $i$  is the interest rate and  $y$  is the number of years since the base year

For the analysis, the life of the video, DCS420, DCS460 and Hasselblad systems was taken as 3 years since it was likely that in 3 years time these camera systems would be technologically outdated and a new image sensor would have to be purchased to remain competitive. For the 9" camera system the life of the system was 5 years. Development of improved large format systems was considered to be slower and technological advances are generally less pronounced, thereby substantiating the choice of a longer life for the 9" photography system. Insurance costs were taken as 5% of the purchase price.

The variable costs were the flying and image processing costs of producing geographically referenced digital imagery. Estimates of these costs and associated times were supplied by Brodie (1998), Wooding (1998), and Craigie (1999). For the analysis, the use of semi-automated photogrammetric software to stereoscopically rectify the imagery was chosen. This methodology and its strengths and weaknesses are described in section 6.3.2. Table 9 shows the time and costs assumed for the various processing steps.

Table 9: Costs and times used in the cost-benefit analysis

|  | SYSTEM |        |        |            |                |
|--|--------|--------|--------|------------|----------------|
|  | Video  | DCS420 | DCS460 | Hasselblad | 9" photography |
| <b>COSTS<sup>5</sup>:</b>                                  |        |        |        |            |                |
| Flying (R/h)   | 1200   | 1200   | 1200   | 1200       | 1200           |
| Production of digital image (R/image)                      | 2      | 4      | 4      | 30         | 150            |
| Obtaining image GCPs through ground-based survey (R/point) | 800    | 800    | 800    | 800        | 800            |
| Rectify imagery using photogrammetric software (R/h)       | 125    | 125    | 125    | 125        | 125            |
| <b>TIMES:</b>  |        |        |        |            |                |
| Production of digital image (min/image)                    | 1      | 2      | 3      | 15         | 20             |
| Rectify imagery using photogrammetric software (min/image) | 30     | 33     | 36     | 37         | 70             |

In establishing the cost and time to produce a digital image using the video system, it was assumed that the framegrabbing of video frames was completely automated. This framegrabbing process would make use of the differential GPS coordinates stored with each video frame during the flight. For the Hasselblad and 9" photo systems the production of a digital image would involve the development of the photograph negatives and the scanning of these negatives at 1200 dots per inch (dpi). A scanning resolution of 1200 dpi was chosen as this is the standard used by most photogrammetry laboratories (Brodie, 1999; Craigie, 1999) and provides a good balance between resolution, memory requirements and cost. Times to stereoscopically rectify a video, DCS420, DCS460 or Hasselblad image were estimates based on the time to rectify a 9" photograph scanned at 1200 dpi. They were derived after considering the relative sizes in Mb of the images to be

<sup>5</sup> Base year: 1998

processed and the steps involved in stereoscopically rectifying an image. The time required to obtain GCPs through a ground-based survey was not included in the analysis as it could vary considerably. It would depend largely on the accessibility of the GCPs and the distance between GCPs.

The algorithm used in the spreadsheet to determine flying time per survey and the total number of images to be captured is shown in Figure 15 below.

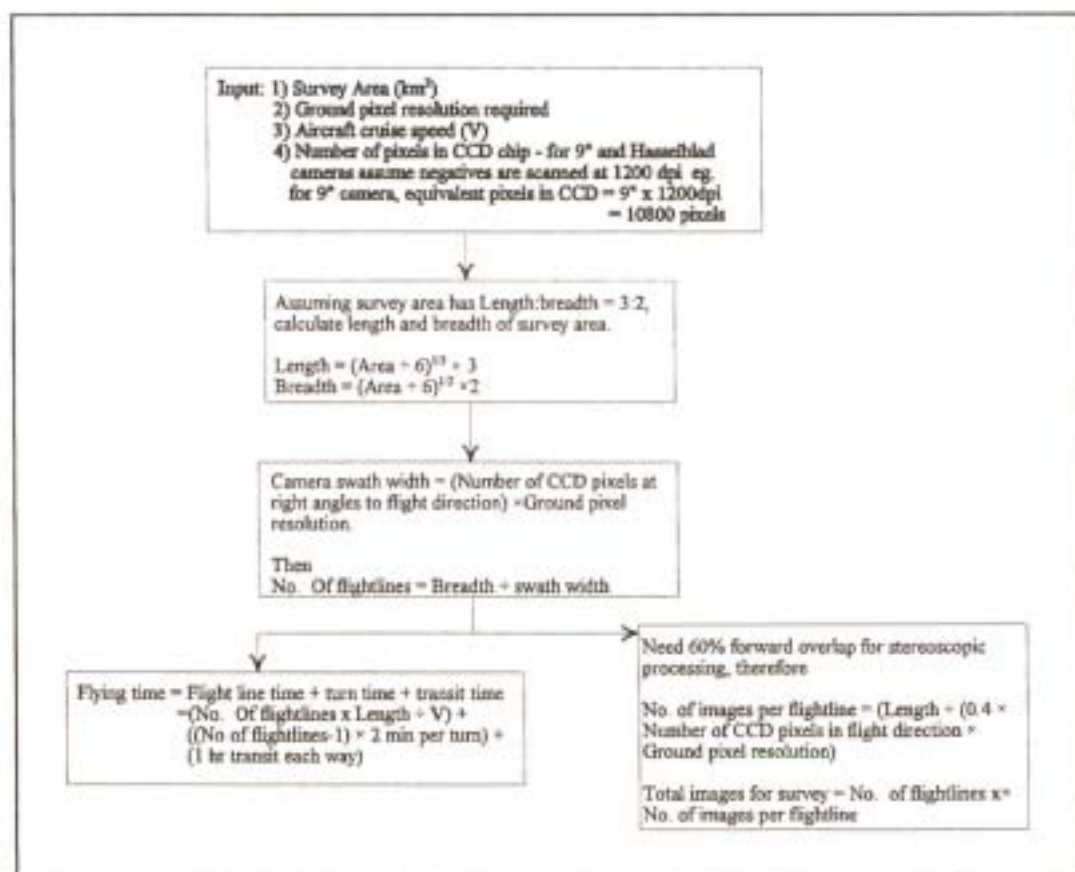


Figure 15: Algorithm used in cost-benefit analysis spreadsheet to calculate flying time and total number of photographs/images to be captured.

Using this algorithm and the costs outlined in Table 9, several scenarios were investigated and the results are displayed in Figures 16 through 20. Firstly, the cost of running the five systems for varying sized survey areas was investigated. A pixel size of 1m by 1m and a total of 30 surveys per year were chosen for this scenario. 1m by 1m pixels were selected since higher resolution imagery will not necessarily achieve improved results with a semi-automated photogrammetric

package, while coarser resolution imagery of 1.5 to 2m pixel resolution may not achieve acceptable results (Wooding, 1998). It was decided that 30 surveys per year would be the most number of surveys that could be expected to be flown and processed per year. Figure 16 shows a graph of the results.

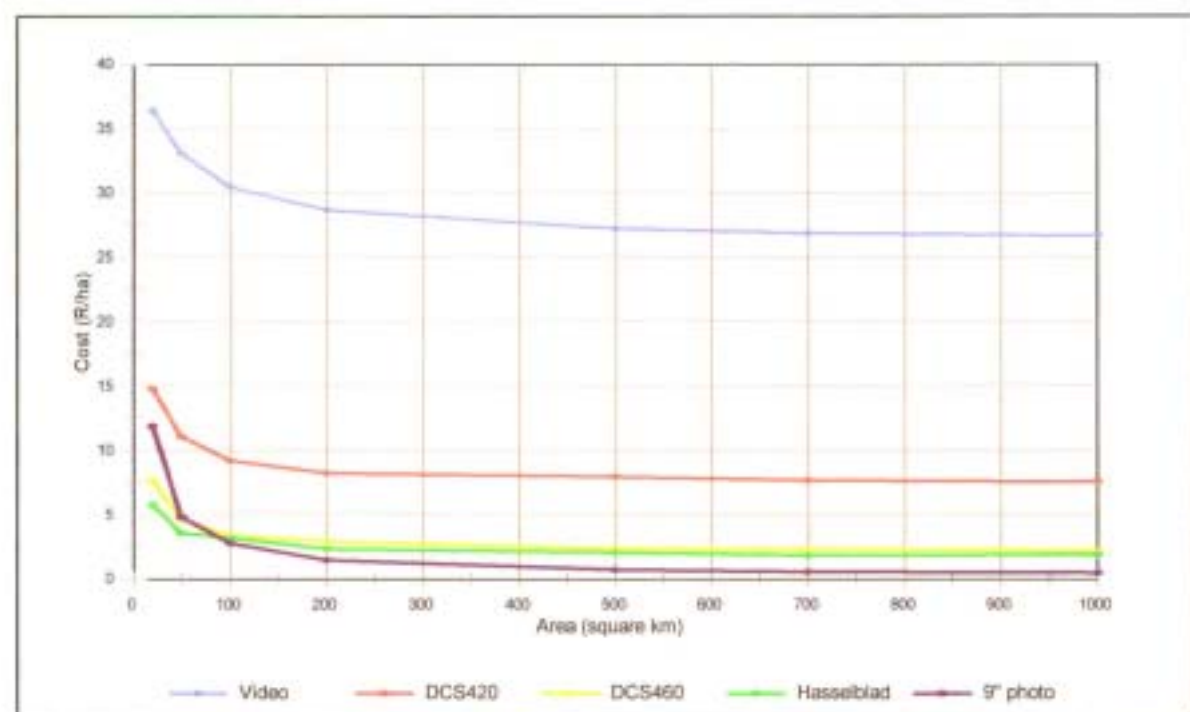


Figure 16: Cost (R/ha) vs survey area (km<sup>2</sup>) for different systems at 1m ground pixel resolution.

As can be seen from Figure 16, the 9" photography system is the most cost-effective option for all areas greater than approximately 80km<sup>2</sup>. The lower R/ha cost for this system for larger areas is as a result of the substantially larger format of 9" photography when compared with the other formats. This larger format means that for the same ground pixel resolution, far fewer 9" photographs need to be taken to cover an area. While the processing time to produce a geographically referenced digital image from a single 9" photograph is greater, resulting in a higher cost in rands per image, this is offset by the fact that fewer images have to be processed. As an example, to obtain imagery of a 500 km<sup>2</sup> area with 1m ground pixel resolution, in excess of 4500 video images and more than 300 DCS460 images would have to be captured and processed. Only 19 or 20 photographs with 9" format would be required.

As is evident in Figure 16, and as will become evident for all scenarios discussed below, the video system has a very high R/ha cost relative to the other systems. The high R/ha cost of video is due to video's very small image format which means that many more images have to be framegrabbed and processed to cover the same area. This substantiates MBB's decision to map directly from the raw video data rather than framegrabbing and rectifying the video images and importing these into a GIS. This approach was both lower cost and more timely, costing only approximately R2/ha to produce a detailed land use map with acceptable spatial accuracy (Brodie, 1998).

The DCS460 and Hasselblad systems could be used cost-effectively as alternatives to the 9" system for areas of less than 50km<sup>2</sup> and 80km<sup>2</sup>, respectively. The reason that the 9" photography system is more expensive for smaller survey areas is that the higher capital cost or purchase price of the 9" system contributes more in R/ha terms to the overall cost for smaller areas. The similar R/ha costs for the DCS460 and Hasselblad systems is due to their very similar sized formats in terms of pixels. When a Hasselblad negative is scanned at 1200 dpi the equivalent pixel resolution obtained is 2835 by 2835 pixels, compared with the DCS460 format of 3000 by 2000 pixels. These similar formats result in a similar number of flight lines needing to be flown and a similar numbers of photographs or images being taken.

Comparing the DCS420 and DCS460 camera systems, it can be seen that the DCS460 system offers a significantly reduced R/ha cost over the DCS420 system for all sized survey areas. For all areas the difference in cost is at least R5/ha. This is a significant difference, particularly if converted into absolute rand terms. For an area of 300km<sup>2</sup> for example, the DCS420 system would cost a minimum of R150 000 more than the DCS460 system.

For 0.5m ground pixel resolution imagery the differences in R/ha costs for the different systems is more pronounced and the 9" photography option is most cost-effective for all sized areas. This can be seen in Figure 17 below.



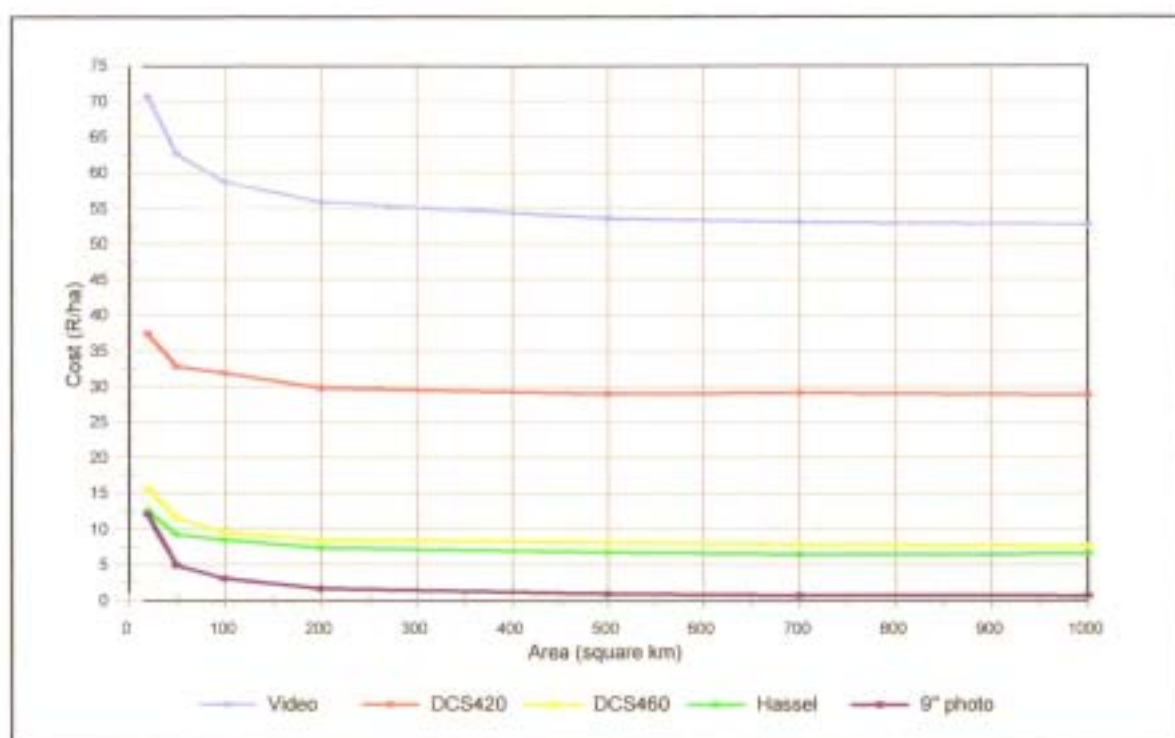


Figure 17: Cost (R/ha) vs survey area (km<sup>2</sup>) for different systems at 0.5m ground pixel resolution.

As for the 1m pixel resolution imagery, the 9" photography is most cost-effective at 0.5m pixel resolution due to its larger format. Looking specifically at the DCS420 and DCS460 systems, the difference in R/ha costs is more marked at 0.5m pixel resolution. For all areas over 200km<sup>2</sup> in size the DCS460 system costs approximately R8/ha compared with R21/ha for the DCS420 system. This is a substantial difference which would indicate that the DCS420 is unsuitable for capturing higher resolution (sub-metre) imagery for any sized area. Considering that MBB were hoping to use the system to acquire sub-metre resolution imagery for applications such as alien vegetation identification and mapping, this finding was considered to be sufficient evidence to indicate that the DCS460 camera was the camera to use. However, to establish when the DCS460 camera could be used as an alternative to 9" photography, further scenarios were analysed. Figure 18 shows the R/ha costs of the various systems for imagery captured at 2m pixel resolution.

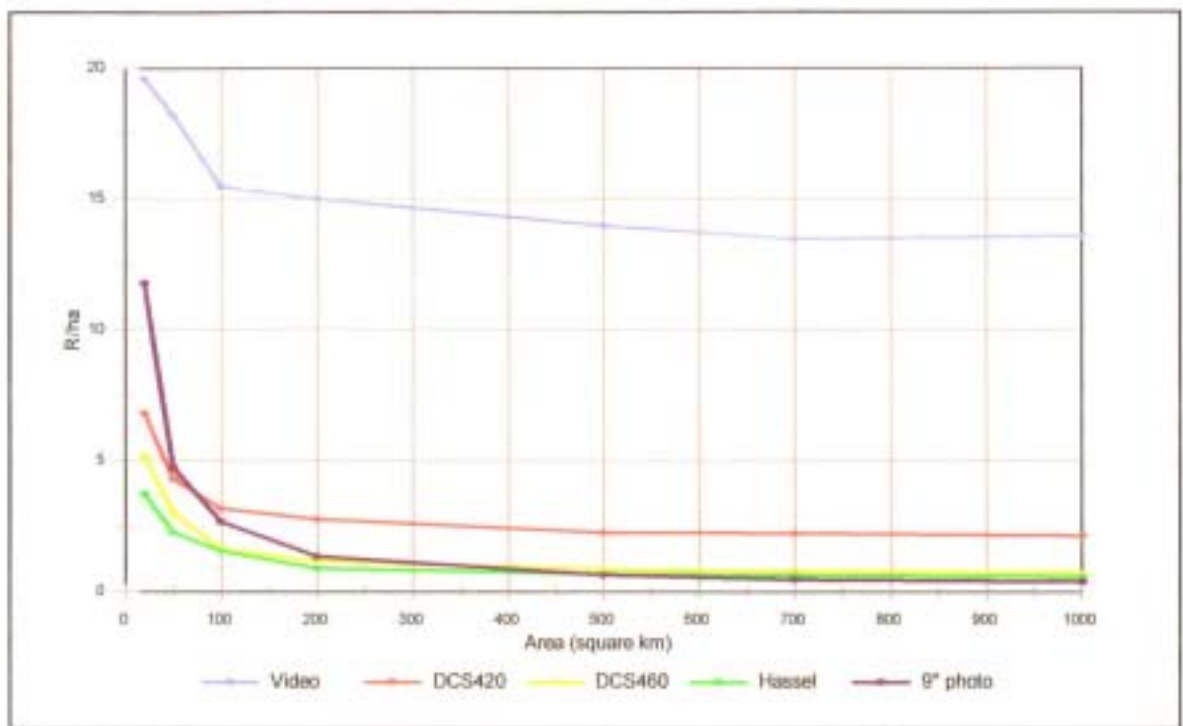


Figure 18: Cost (R/ha) vs survey area (km<sup>2</sup>) for different systems at 2m ground pixel resolution.

At 2m ground pixel resolution, which would be suitable for detailed land use mapping, the DCS460 and Hasselblad systems become alternatives to 9" photography for larger areas than at 0.5m or 1m pixel resolutions. The DCS460 could achieve lower R/ha costs for areas up to approximately 350 km<sup>2</sup>. The Hasselblad system would be a cost-effective alternative for areas up to 450km<sup>2</sup>. However, for areas of greater than approximately 500 km<sup>2</sup> the 9" system would still have to be considered as the best alternative, despite the apparently small R/ha cost difference between the three systems for areas from 500 to 1000km<sup>2</sup> in size. For a survey of an area of 700km<sup>2</sup> for example, the DCS460 system will cost R0.80/ha, the Hasselblad system R0.64/ha and the 9" photograph system R0.47/ha. These equate to a cost saving in rand terms of R23100 and R11 900 when opting for the 9" photography option versus the DCS460 and Hasselblad systems, respectively. Such savings were considered to be significant, particularly considering that the total rand costs for the DCS460 and Hasselblad options for this sized area would be R56 000 and R44 800, respectively.

In addition to the lower cost of 9" photography, it could also offer reduced turn-around times between acquiring the imagery and providing geographically referenced image data for input into a GIS. The times to produce geographically referenced imagery at 1m ground pixel resolution for varying sized areas are shown in Figure 19 below. For this analysis a 10 hour working day was assumed.

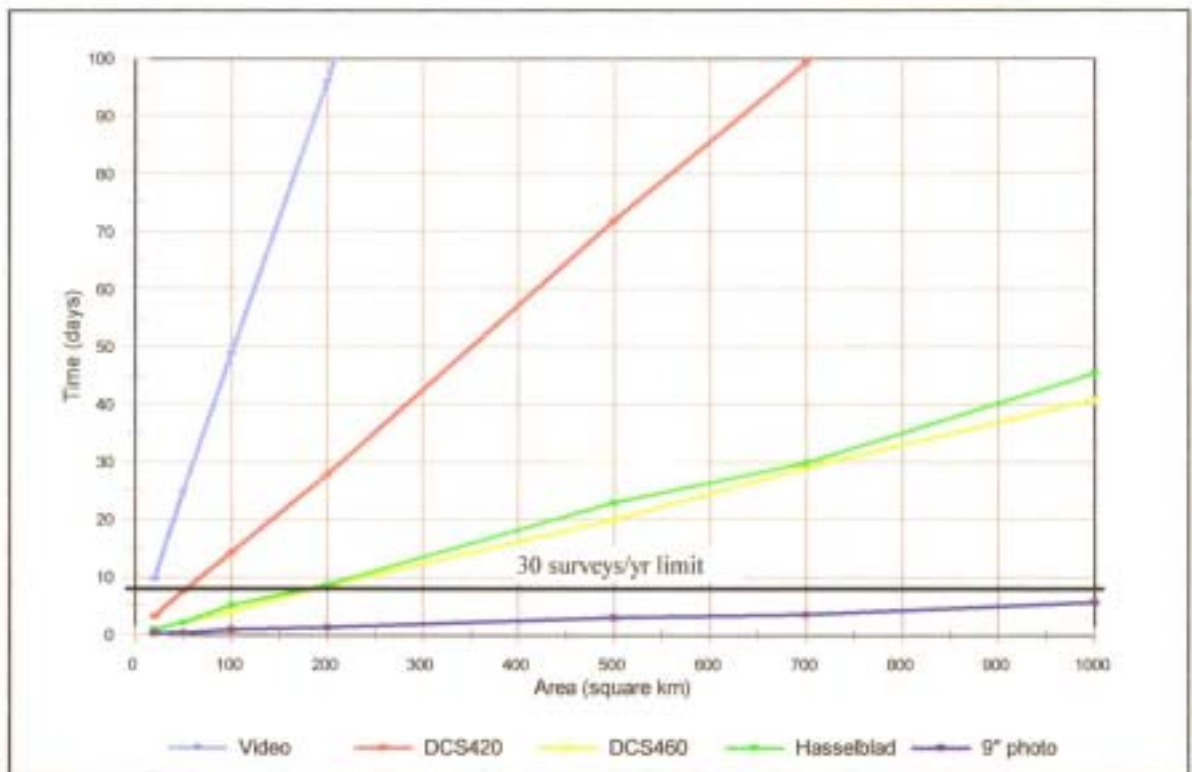


Figure 19: Total processing time per survey (days) vs survey area (km<sup>2</sup>).

Considering the digital camera systems, it can be seen from Figure 19 that even for relatively small survey areas of around 100km<sup>2</sup>, the DCS460 system will produce imagery which can be used in a GIS in significantly less time than the DCS420 system. The DCS460 system will produce photogrammetrically rectified imagery of a 100km<sup>2</sup> area in approximately 5 days. The DCS420 system would only provide imagery of the same area in approximately 10 days. This increased time is due to the greater number of images that have to be processed when using a DCS420 camera. A delay of 5 days could be significant for applications such as crop monitoring and disease detection for which a delay of such magnitude may result in a problem area being identified too late for corrective measures to be implemented. Perhaps more importantly though, Figure 19

indicates that using the video, DCS420, DCS460 or Hasselblad systems will restrict the number of large area surveys that could be performed per year.

If 30 surveys are to be flown and processed per year at 1m ground pixel resolution, and assuming there are 240 ten-hour working days available per year, then an average of 8 days is available per survey. Therefore, the DCS420 system could only perform and process 30 surveys per year if the areas surveyed were an average of approximately 50km<sup>2</sup>. Similarly, the DCS460 and Hasselblad systems could only perform 30 surveys per year for an average area of 200km<sup>2</sup> per survey. On the other hand, the 9" photography option could manage 30 surveys of 1000km<sup>2</sup> each per year. Since larger area surveys produce proportionally larger profits in rand terms, the fact that more large area surveys could be accommodated with the 9" photography system further endorses the view of many researchers that the resolution of currently available digital cameras limit their use for surveys of more than localised areas. However, if deciding between the DCS420 and DCS460 cameras, the DCS460 would be the camera of choice.

Although not illustrated, it is of interest to note that for a ground pixel resolution of 2m, the average area for which 30 surveys could be processed per year increases to approximately 170km<sup>2</sup> and 500km<sup>2</sup> for the DCS420 and DCS460 systems, respectively. At this resolution, which would be suitable for detailed land use mapping, the DCS460 system could be considered suitable for large area surveys. The DCS420 camera is still limited by its small image format.

If fewer than 30 surveys were performed and processed, then the DCS460 could be cost effective for larger areas. Figure 20 compares the R/ha cost for the DCS460 and 9" photography systems for 10, 20 and 30 surveys per year. The ground pixel resolution used was 1m by 1m.

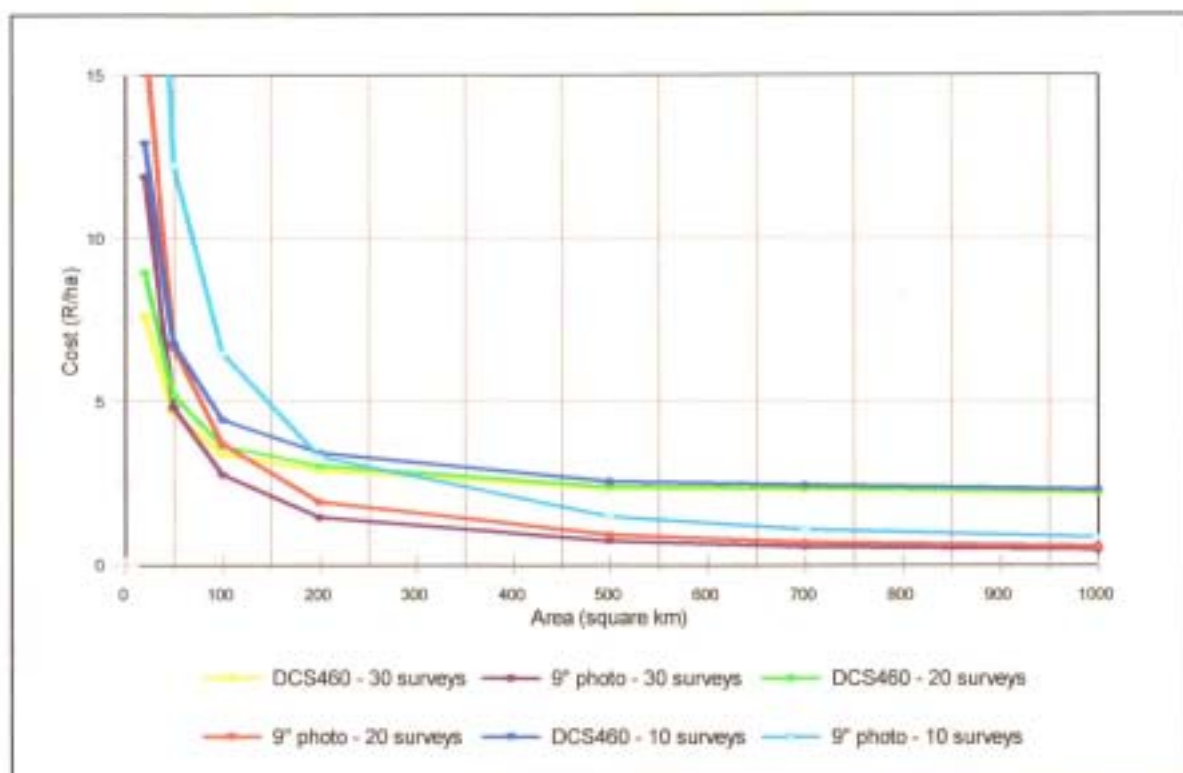


Figure 20: Cost (R/ha) vs survey area (km<sup>2</sup>) for varying numbers of surveys per year.

The higher R/ha cost associated with fewer surveys of small areas is as a result of the higher fixed cost contribution to the overall cost. While the variable costs in rands are directly dependent on the number and area of surveys, the fixed costs in rands remain unchanged. Consequently, in R/ha terms, the fixed costs per survey increase if fewer surveys are performed.

For 20 surveys per year, the DCS460 system has a lower R/ha cost than the 9" photography system for areas up to 100km<sup>2</sup>. If only 10 surveys are performed and processed per year then the DCS460 could be a cost effective alternative for areas up to 200km<sup>2</sup> in size. While these are improvements over the situation for 30 surveys per year it would not make economic sense to limit the number of surveys to be flown per year to 10 or 20 merely to make the DCS460 system more profitable than the 9" photography option for areas as small as 200km<sup>2</sup>.

In the above discussion, the possibility of even higher resolution digital cameras becoming available on the market has not been discussed or evaluated. As previously mentioned in Chapter 2, cameras with resolutions of greater than 20 million pixels have already been developed, but as

yet they are not commercially available. It is extremely difficult to determine whether the reductions in processing time and operational costs offered by the Kodak DCS460 over the DCS420 and video camera systems could be extrapolated to such high resolution cameras. The capital cost of higher resolution digital cameras could not be predicted and the times for downloading the imagery and estimating the time required to rectify such higher resolution imagery from an orthophoto or stereoscopically would have been mere speculation. Thus, including such a camera in the analysis was not possible at the time. However, when digital cameras with higher resolutions than the Kodak DCS460 camera become available then the same cost-benefit analysis procedure outlined above could be applied to these cameras to assess their viability relative to 9" photography. In anticipation of these higher resolution digital cameras it is important to highlight some of the potential limiting factors or disadvantages of a 12 million or 20 million pixel resolution camera. These factors or disadvantages have been mentioned in Chapter 3, but it is worth reiterating them here.

First, it is important to re-emphasise that even 20 million pixel resolution is modest in comparison with the equivalent resolution of in excess of 20k by 20k of high quality 9" format aerial cameras. Consequently, such cameras could still not replace large format aerial photography although they would compete with and/or replace medium format photographic cameras. Secondly, the rate at which data can be transferred and stored will become an increasingly important issue. As previously mentioned, a Kodak DCS460 image consists of over 4 Mb of information (Kodak, 1998) and requires a storage time of 8 seconds per image (Maas and Kersten, 1997; Kodak, 1998). Higher resolution cameras will require more storage capacity and more time for storing imagery on a PCMCIA card or computer hard drive. This will severely limit the use of such cameras for capturing overlapping imagery and, in particular, stereoscopic imagery. As discussed, this problem of image overlap could be overcome by flying each strip a number of times (Mason *et al.*, 1997). However, this solution would increase the complexity of both the flight planning and execution of the survey and would consequently increase the operational cost of the system.

In conclusion, although the times and costings used in the above analysis were estimates and could not be verified in an actual study, it is evident that 9" photography will continue to be the format of choice for providing geographically referenced high resolution imagery within a short period of time. This is due to the reduced number of 9" photographs or images that have to be processed

to cover an area at a particular resolution in comparison with the other remote sensing alternatives considered. However, the potential of using the Kodak DCS460 in conjunction with semi-automated photogrammetric software to perform low cost, rapid turn-around mapping of more than just localised areas can be seen from the analysis. Unfortunately, the high capital cost of the Kodak DCS460 camera meant that one could not be purchased for this project and, furthermore, no individual or organisation with such a camera was willing to lend or rent the camera out. However, it was possible to borrow a Kodak DCS420 camera which could be controlled using the same protocol and DLL as required for the DCS460 camera. Thus, despite the poorer spatial resolution and reduced area coverage of the DCS420 camera in comparison with the DCS460, the DCS420 represented an ideal substitute until MBB were able to purchase a DCS460 camera. To provide a secure and stable platform for acquisition of good quality imagery using this camera, a custom-built camera mount was designed.

## 5.2 Camera Mount

An identical metal sheet to the one used for the video camera mount was used as the basis for the digital camera mount since this sheet was manufactured to fit and be secured in the place of a floorboard between the pilot and passenger seats in the Piper Twin Comanche aircraft. However, due to the unusual shape and additional weight of the Kodak DCS420 digital camera in comparison with the video camera, a more substantial mount than the video mount was manufactured. The camera would be mounted on wooden blocks covered with sorbothane. Sorbothane was used since it has excellent dampening properties and would prevent any unwanted vibration of the camera that could result in the acquisition of poor imagery. To keep the camera firmly in position even in turbulent conditions, a 5mm thick steel plate was bent into an L-section and bolted to the base steel sheet to provide a platform to which the camera could be bolted by utilising the camera's supplied tripod screw hole.

To ensure that the camera mount had been properly manufactured, the mount and camera were placed in the aircraft and some test images were taken. It was confirmed from viewing the test images that a clear, unobstructed view of the ground below was obtained when using the mount.

Having borrowed a camera and designed and built a mount, a means of readily and cost-effectively obtaining accurate positional data for in-flight camera control and to assist in post-flight image processing was required. GPS was identified as being able to fulfill the requirements of high precision, universal availability, reliability, ease of operation and low cost (Becker and Barriere, 1993).

### 5.3 Global Positioning System (GPS)

The GPS chosen for use with the camera was to serve two purposes. First, it would provide one second updates of the aircraft's latitude and longitude so that the distance to the end of a particular flight strip could be calculated. As previously described the distance to the end of the flight line would be used to determine whether or not the camera should be triggered. Secondly, the GPS position at the time of image capture would be stored in a file to assist in post-flight positioning and geographical referencing of the imagery. Before a GPS unit could be chosen it was necessary to examine the limitations of standard GPS and how these limitations could be overcome in order for GPS to be sufficiently accurate and reliable for aerial survey applications. In addition, the problems and errors relating specifically to the application of GPS in aerial surveys had to be examined. How GPS works is not included in this document and readers who are unfamiliar with the science and methodology behind GPS are referred to Hurn (1989).

#### 5.3.1 Standard GPS errors

The accuracy of the basic, autonomous GPS system of a single earth-based GPS receiver receiving signals at different frequencies from four or more satellites in order to calculate its position is determined by the sum of several sources of error. These errors, which are documented by Hurn (1989), and a summary of their contribution to the overall error are tabulated in Table 10 below.



Table 10: Summary of GPS error sources (after Hurn, 1993)

| Error Type                  | Description   | Std. GPS error (m) | DGPS error (m) |
|-----------------------------|---|--------------------|----------------|
| Satellite clocks            | Slight inaccuracies in timekeeping  | 1.5                | 0.0            |
| Satellite orbits            | Slight drifts of satellites from predicted orbits   | 2.5                | 0.0            |
| Atmospheric                 | Delay of GPS signal through the atmosphere  | 5.5                | 0.6            |
| Receiver Noise              | Inaccuracy of receiver clocks, internal electrical noise  | 0.3                | 0.3            |
| Multipath                   | Reflection of GPS signal off local obstructions before reaching receiver                                | 0.6                | 0.6            |
| Selective Availability (SA) | "Intentional" error or noise introduced by the U.S. Department of Defence into the GPS satellite clocks | 30                 | 0              |

The errors tabulated above combine to give a basic GPS system a typical positional accuracy of 50 m horizontally and 78 m vertically (Hurn, 1993). This can be considered to be sufficiently accurate for navigation using GPS, but for accurately determining the position of the camera for purposes of triggering the camera, a better estimate of position is required. Differential GPS (DGPS) provides the means to eliminate all but the multipath and receiver noise errors and can be used to achieve sub-metre positional accuracy even when SA is activated (Trimble, 1997). Its use in aerial surveying is well documented.

### 5.3.2 Differential GPS

DGPS requires two GPS receivers. One receiver, located at a known position such as a survey control point, serves as a base station to compute satellite range corrections that account for satellite, receiver clock, and atmospheric errors. Selective availability is also accounted for. These corrections are calculated by subtracting the measured range from the true range for each of the satellites within the base station's view (Bobbe, 1992). Then, provided that the second GPS

receiver in the aircraft, often referred to as the rover station, locks onto at least three of the same satellites as the base station receiver, these corrections can be used by the rover station to compute a more accurate latitude and longitude positional solution. If four of the same satellites are locked then a three-dimensional position including altitude can be calculated. This differential correction can be computed and applied in either a real-time or a post-processing mode. Bobbe (1992) and Curry and Schuckman (1993) provide reviews of these two methodologies.

Post-processing uses the GPS data recorded simultaneously by the base and rover stations. The GPS data are loaded into a computer with software that determines the differentially corrected positions and then the processed data can be formatted for hard-copy display or input into a GIS. Real-time DGPS, on the other hand, involves the transmission of the correction message from the base station to the rover station during flight. This Real Time Correction Message (RTCM) can be sent via radio link from the base station to the aircraft, although the more popular alternative is to receive the RTCM via a geo-stationary satellite (Smith, 1998). By receiving this RTCM the GPS unit is able to differentially correct the positions it logs in real time and this higher positional accuracy data can be stored along with the image or photograph. Post-processing of the GPS data does not permit this and consequently processing of the image data would be more difficult and time-consuming. Real-time DGPS does, however, require more expensive GPS receivers with advanced processing capabilities that can perform the required corrections within milliseconds. A very high degree of co-ordination with the base station is also required (Linden *et al.*, 1996). A further restriction is that the base station should be within 300 km of the survey area to ensure that both receivers have the same satellites in view (Curry and Schuckman, 1993). To combat this restriction Omnistar (1998) have developed what is known as Virtual Base Station (VBS) technology. VBS technology uses correction data from a number of base stations to provide consistent accuracy over larger areas. Data from several distant base stations are weighted and then combined to achieve sub-metre accuracy regardless of the user's location relative to any base station.

The effects of multipath and receiver noise errors can be reduced by the GPS receiver itself. Modern receivers use smoothing techniques to smooth the range measurements thereby reducing errors due to receiver noise (Bobbe, 1992). They also employ complex algorithms to identify and

reduce multipath errors (Trimble, 1997) which, according to Colombo and Peters (1992), may not average out as well as in static surveys.

### 5.3.3 Carrier-phase GPS

If the sub-metre accuracy of DGPS is not sufficient then carrier phase GPS technology can be used. This methodology has been widely used in land surveying, but has only recently been introduced into aerial surveying as GPS receivers improved in terms of performance and portability.

Carrier phase GPS makes use of measurements based on the GPS carrier signal which has a much higher frequency than the standard Coarse/Acquisition or civilian code (Hurn, 1993). This sinusoidal carrier signal arrives at different locations with different phases (Colombo and Peters, 1992) and these phase shifts can be measured and used to obtain an exact lock on the pseudo random code which standard GPS uses to calculate position (Hurn, 1993). Consequently, carrier-phase measurements are much more accurate than standard GPS measurements and accuracies to decimeters for position when post-processing methods are used have been reported (Colombo and Peters, 1992).

Carrier phase GPS does, however, require more sophisticated and expensive receivers. The inherent cycle ambiguity of the carrier phase signal also needs to be resolved. This involves finding the total number of integer cycles the signal has travelled through from the satellite to the receiver/s. This can be done in ten minutes or less by starting from a known GPS-determined base line (Ackermann and Schade, 1993). Once this is done, the GPS receiver/s stay locked onto the carrier waves and the kinematic positioning can continuously track the flight trajectory of the moving GPS antenna until a cycle slip, which involves the measured carrier phase skipping whole multiples of  $2\pi$  radians (Colombo and Peters, 1992), or loss of signal occurs. Cycle slip detection and repair is difficult and requires automation when the operator is processing large amounts of kinematic GPS data. Colombo and Peters (1992) and Ackermann and Schade (1993) described techniques to repair cycle slips.

#### 5.3.4 Further considerations

Loss of lock on the GPS signal is a problem common to differential and carrier phase GPS. Loss of signal due to cycle slips or constellation changes can be detected and corrected during data processing. Loss of signal due to obstruction by wings or fuselage of an aircraft flying in a steep turn can, however, last for tens of seconds. In such cases it is practically impossible to precisely reconnect the interrupted trajectory by new ambiguity solutions (Ackermann and Schade, 1993). For differential pseudo-range positioning which does not utilise the carrier signal, data is only lost until at least four satellites are re-acquired (Curry and Schuckman, 1993). Nevertheless, some compensation for this problem is required.

To avoid losses of lock each GPS antenna needs to be mounted on the aircraft where it is free to receive the GPS signals with a minimum of obstruction. Recommended locations include on the fuselage directly over the camera, in order to minimise the position difference between the camera and GPS antenna, or on the tip of the vertical stabiliser on the aircraft's tail (Curry and Schuckman, 1993). The fuselage position may be subject to increased multipath off other parts of the aircraft and to shadowing of the antenna by the aircraft's wings during turns. Major signal interruptions can also be avoided by slipping the aircraft through the turns with low banking angles (Ackermann and Schade, 1993). Curry and Schuckman (1993) recommended that the banking angles be restricted to 20 or 25 degrees during turns, depending on the satellite elevations. Unfortunately, such wide, flat turns would take considerably longer and use up valuable flying time.

A further problem is introduced due to tip and roll of the aircraft. Maintaining a horizontal film plane is an assumption made regularly with regard to photogrammetric applications (Wunneberger, 1992). Slight turbulence and resultant tip and roll of the aircraft causes the image's principal point (PP) or centre point to move away from the image nadir or intended image swath centerline. Consequently, the accuracy of absolute orientation is adversely affected (Wunneberger, 1992; Evans, 1992). This reduction in accuracy occurs because the GPS determines and records the aircraft position rather than the position of the swath centre line on the ground, making geo-location more difficult (Evans, 1992). The error involved is confirmed by Bobbe (1992) who found that for one degree of tip at 305 m (1000 feet) above the ground an error of 5.3 m was

introduced. This suggests that correcting for or accounting for tip and roll is very important if an accurate geo-referenced image is to be obtained.

Regardless of these requirements and problems, differential and carrier phase GPS offer the most reliable means of obtaining high accuracy positional information in real-time for locating images in space. Based on the characteristics of differential and carrier GPS described above, a real-time differential GPS (DGPS) was chosen for this project.

The sub-metre accuracy of DGPS was deemed to be more than sufficient for the purposes set out in section 5.2 and would be less expensive than a carrier phase GPS. The real-time differential correction capability was required to provide accurate positional data during image capture for calculating the distance to the end of a flight strip and for storing an accurate position with an image at the time of exposure. No time-consuming post-flight differential correction of the stored coordinates of each photograph exposure would then be necessary. On the other hand, the extremely high accuracy of carrier phase GPS was considered to be unnecessary. Coupled with the high cost of carrier phase GPS units, the problems of resolving cycle ambiguities, and the difficulty in detecting and repairing cycle slips, carrier phase GPS was unsuitable for use in the low cost, simple system being developed. The Trimble Pro-XRS GPS (Trimble, 1998) was thus chosen to provide the real-time differentially corrected positional data required.

### 5.3.5 The Trimble Pro-XRS GPS

The Trimble Pro-XRS GPS (Trimble, 1998) system consists of a Trimble Pro XRS antenna unit, a 12 channel GPS receiver and a Trimble TDC1 data logger unit. Instead of requiring a base station at a known position and relaying the differential correction message from this base station to the aircraft in real-time using a radio link, this system provides real-time differentially corrected positional data by utilising two antenna housed in a single compact unit. The one antenna receives the normal pseudo random code from the GPS satellites while the second antenna receives a Real Time Correction Message (RTCM) that is sent via a geo-stationary satellite. This RTCM is calculated using data from well-established base stations situated throughout South Africa. The satellite used to obtain the RTCM can be specified using the TDC1 data logger unit.

In order for a PC to be able to read the GPS positional data in real-time, the Trimble Pro-XRS GPS continuously outputs comma-delimited ASCII text strings using the National Marine Electronics Association (NMEA) 0183 protocol. NMEA 0183 is a marine standard protocol for interfacing with marine electronic devices and defines electrical signal requirements, data transmission protocol, timing and specific sentence formats. Each specific format of the NMEA text strings contains different information relating to the GPS, including GPS position, velocity, satellite status, speed over ground, number of satellites in view, elevation of satellites in degrees and signal to noise ratio. The two formats of particular interest for this project were the GGA and VTG formats. The GGA strings contain positional information as well as information relating to the number of satellites in view of the GPS. Its format is as follows:

```
$GPGGA, UTC of position, latitude, N, longitude, E, GPS quality indicator, No.
of satellites in use, HDOP, Antenna altitude, M, Geoidal separation, M, Age in
seconds since last update from differential station, Differential reference station
no., *Checksum
```

An example of a GGA string is as follows:

```
$GPGGA,140311.90,2940.04,S,03024.46,E,1,04,1.9,882,M,28.8,M,8,220,*4F
```

The VTG format provides velocity information and has the following format:

```
$GPVTG, Track made good, T,,,Speed over ground in knots,N,Speed over ground
in km/h,K*Checksum
```

An example of a VTG string is as follows:

```
$GPVTG,358,T,,,1.31,N,2.42,K*4E
```

In the \$GPGGA string format, the N and E refer to North and East, respectively while the M indicates that the antenna altitude and geoidal separation are in metres. HDOP is the Horizontal Dilution Of Precision which is a measure of how accurately the latitude and longitude are being

calculated. A smaller HDOP value indicates that the latitude and longitude being output are more accurate. In the \$GPVTG string, the T, N and K indicate that the track made good is relative to True north, the first speed over ground value is in knots, and the second speed over ground value is in km/h, respectively. The \$GPXXX string is the string header and is always sent regardless of whether the GPS can provide the positional and velocity or not. Similarly, the '\*' and checksum are always sent.

The NMEA strings can be sent at user-defined fixed intervals from the GPS via a data cable to the communications port of a PC. In order to read these strings at the PC's com port and then extract the relevant information, a GPS interface had to be developed. The development of this interface is detailed in the following section.

#### 5.4 GPS Interface

The GPS interface was developed using third party Delphi software called AsyncPro (Turbopower, 1998). This software provides all the necessary tools and components to integrate and control a variety of peripherals via the com port of a PC and was thus well-suited for the purposes of reading incoming NMEA 0183 strings from the GPS.

The software provided several methods of identifying the presence of data at the com port and then reading the data strings. The method chosen for this project was the use of a 'data trigger'. This method attempts to match a user-defined string with a string in the received data stream. When a matching string is found in the input buffer an OnTriggerData event is generated for the match. What occurs when the event is generated is defined by the programmer.

In this case, the 'data trigger' used was the text string 'K\*' which is always present towards the end of the VTG string. The OnTriggerData event algorithm which was initiated each time this 'data trigger' was received was responsible for reading the latitude, longitude, velocity and UTC from the GGA and VTG strings and performing the necessary calculations to determine whether a photograph was to be taken. A flowchart of the algorithm for this OnTriggerData event is shown in Figure 21 below.

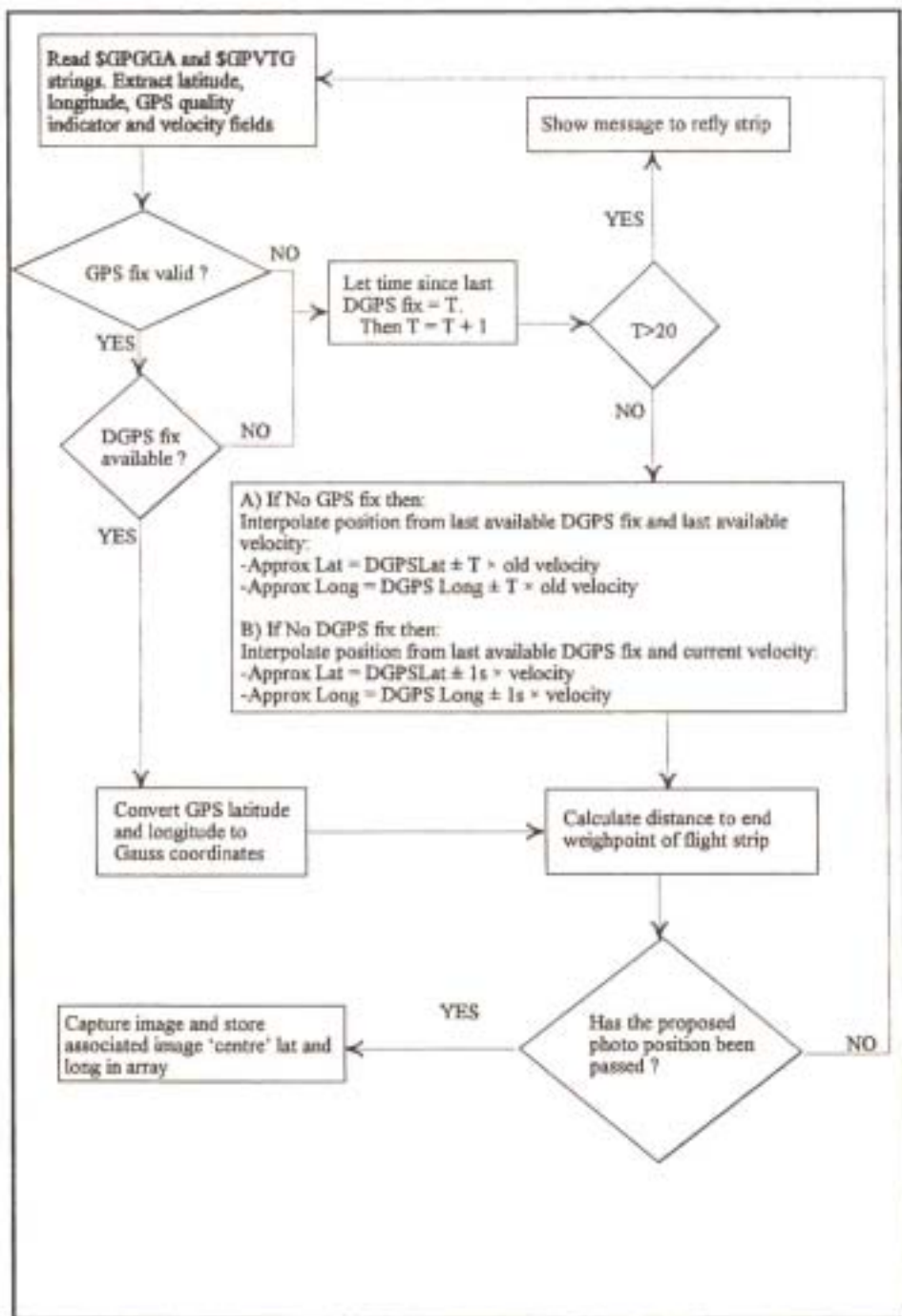


Figure 21: Flowchart of OnTriggerData event for reading the GPS NMEA strings and triggering the camera

To determine whether DGPS is enabled, the 'GPS quality indicator' field of the \$GPGGA string is read. This field has a value of 0 if the position fix is not valid, a value of 1 if a GPS fix is available, and a value of 2 if a DGPS fix is available. If the quality indicator is 1 then the latitude



and longitude read are ignored and the approximate latitude and longitude are interpolated as described in Figure 21. The velocity read from the \$GPVTG string is used in the interpolation since GPS velocity is unaffected by a lack of a differential signal.

If not enough satellites are in view of the GPS then most of the \$GPGGA and \$GPVTG fields, including the latitude, longitude, velocity and GPS quality indicator fields, become null and the strings are reduced to mostly commas. To identify and account for this situation, code was included to check for a comma character in the latitude or longitude being read. If one is found then it is assumed that no GPS fix is available and the position is interpolated as shown in the flow diagram in Figure 21 above. The last available velocity reading (old velocity) is used to interpolate the aircraft's position since the aircraft's velocity is unlikely to vary by more than 10 km/h over the maximum 20s period for which interpolation is required.

To insure that the system could still be used if a Trimble Pro-XRS DGPS was not available, the algorithm described above was subsequently improved to allow for the use of a lower cost 12 channel Omnistar 3000L DGPS system. This system operates on the same principle as the Trimble Pro-XRS system, but the two antennae are not housed in a single unit. Instead, two separate antennae are utilised. One antenna receives the standard GPS signal and the second antenna receives the RTCM. Also, although the NMEA-0183 protocol is supposedly a standard protocol, this GPS unit's output format was slightly different to that of the Trimble unit and had to be accounted for. However, the basic algorithm remained the same.

To communicate with the camera and capture an image based on the GPS position, a camera control interface was developed independently of the GPS interface. This interface was developed to communicate with and control the camera via a SCSI host adapter installed on a host computer or laptop. In this project, a New Media Bus Toaster PCMCIA SCSI host adapter card was utilised in order for a laptop to be used in the confined space of an aircraft cockpit. The development of the camera control interface is described below.

## 5.5 Camera Control Interface

The basis of the camera control interface was Kodak's Professional Digital Camera Software Developer's Kit (PDC-SDK) which was available for downloading off the Kodak website (Kodak, 1998). This SDK is a software interface specification which provides the developer with a single method for controlling any Kodak DCS digital camera and retrieving digital images from these cameras. The SDK relieves the developer of any need to know specific information about the camera, since details of image storage, camera control commands, image compression, image processing, and hardware interface commands are all encapsulated in the SDK. It is provided to the developer as a Dynamic Link Library (DLL) which the developer must link to at build time, along with Visual C++ code for the developer to adapt and convert into the programming language of their choice.

The Visual C++ code, in the form of C++ header files, defined the variables, structures and functions required to link to and make use of the DLL. Structures, or records as they are known in Delphi, are a useful way of storing a group of related information and unlike an array, the items in a record do not have to be of the same type. The header files were converted into Delphi code and compiled into a Delphi unit which other units could then access and make use of the functions defined therein.

To use the SDK to set up the camera before acquiring images, the following calling sequence was required:

- 1) Call `DCOpenDriver` to initialise and check version compatibility between the SDK and the application. After verification of the version number, the SDK initialises an internal structure that allows it to communicate properly with the camera and provide high quality image processing.
- 2) Call `DCFindFirstCamera` to search the available communications channels on the host computer for the first Kodak DCS camera. This call opens and then closes a communications channel with the device and returns a `DCSourceStruct` record with information regarding the DCS digital camera found and supported. The `DCSourceStruct` record contains information on the camera type, model, name and firmware version, as

well as the SCSI adapter number, device number and Windows driver name. The adapter number field specifies which SCSI host adapter number to use while the SCSI device number field is associated with the camera and is configurable at the camera.

- 3) If no camera or the wrong device is found with a call to `DCFindFirstCamera`, call `DCFindNextCamera` repeatedly until the correct camera is found.
- 4) Call `DCOpenSource` to initialise and open the communications channel or source specified by `DCSourceStruct`.

On successful completion of these calls the camera was ready to capture images by calling `DCCaptureImage`. Calls to `DCCaptureImage` were to be based on the GPS position as described in the previous section.

The GPS and camera control interfaces were then combined into a single in-flight program with a common graphical user interface (GUI). This GUI and the additional algorithms developed for the final program are described below.

## 5.6 In-flight Graphical User Interface and Program

The GUI of the in-flight program is shown in Figure 22 below. The GUI provided all the functionality to open the required files for a survey, setup the camera to capture imagery, configure the com port connected to the GPS, and control and track the progress of a survey.

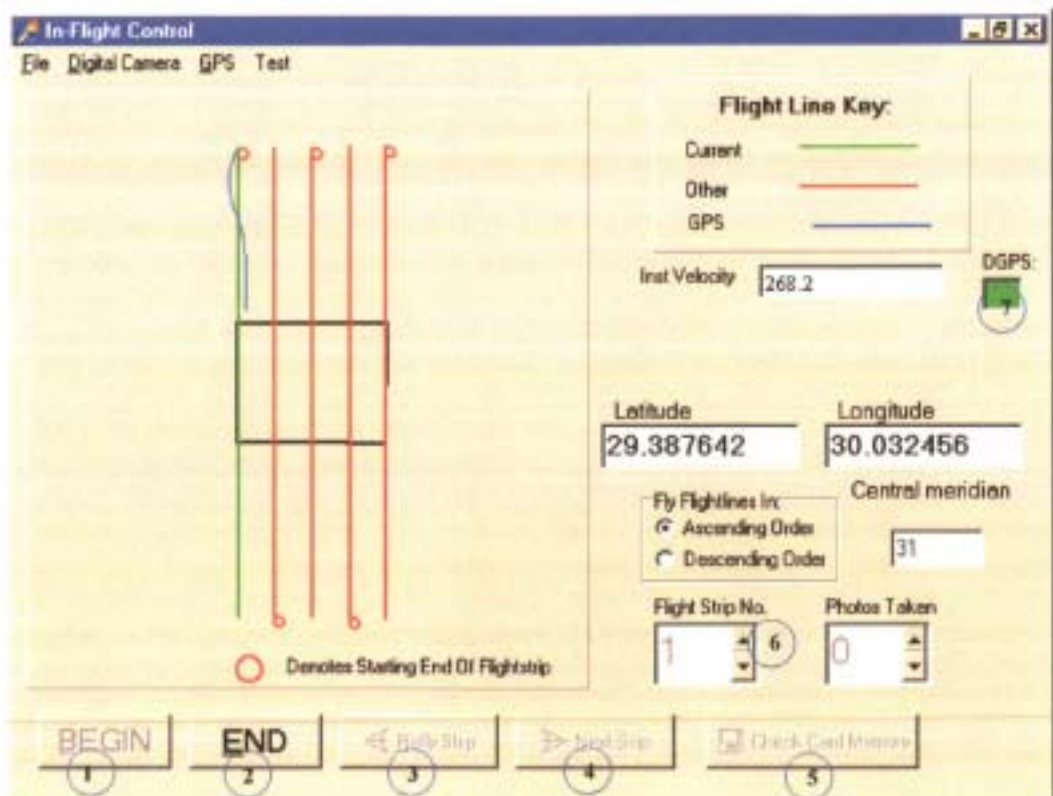


Figure 22: The in-flight GUI

Required inputs to the program prior to a survey are those created in the pre-flight planning program. These include the gaussian coordinates way point file, the geographic coordinates way point file, and the photograph distances file. The geographic way point coordinates and photograph distances are stored in arrays. The catchment boundary generate file used in the pre-flight planning program is also required. Furthermore, the user has to configure the com port in order for the program to properly read the incoming GPS NMEA strings. The make of GPS to be used and the com port baud rate, data bits and stop bits must all be set.

During a survey, the program displays a graphic of the catchment boundary, the planned flight lines and the actual flight path of the aircraft. Having a display of the actual flight path is very useful for establishing whether the aircraft has deviated too far from the proposed flight line and whether the flight line should be reflown due to insufficient side overlap and a consequent potential loss of data. In such a case the decision to re-fly a strip would be subjective. The user has control over the program through use of the buttons numbered 1 to 5 in Figure 22. These buttons all have hot keys associated with them to avoid the need to use a mouse in the aircraft. For

example, Alt-B would enable the 'BEGIN' button and Alt-E the 'END' button.

When button 1 is enabled the input buffers used by both the Windows device driver and the Async Professional internal dispatcher are cleared to remove any characters left in the buffers. The 'K\*' data trigger is also initialised. When button 2 is enabled, the data trigger is removed. If a flight line needs to be reflighted, due to a system malfunction or because the aircraft has deviated too far from the proposed flight line then enabling button 3 will reset the photograph distances and geographic way point coordinates arrays, and the GPS tracking graphic for the particular flight line will be deleted. If the flight line is successfully completed then enabling button 4 will advance the flight line number by 1 and reset the photograph number to 0. The flight line way point coordinate and photograph position arrays are also advanced. Alternatively, the user can choose the next flight line to be flown by accessing the spinedit component labelled as 6 in Figure 22.

Prior to flying a flight line, the user is required to enable button 5 to check whether there is sufficient remaining memory on the camera's PCMCIA memory card to store the proposed images for the flight line. A running total of the number of images captured is kept and this is checked against the number of images which the card can store. If there is sufficient memory then the user is prompted to continue with the current card and button 1 is made active. If there is insufficient memory then the user is prompted to replace the current card with an empty PCMCIA card before continuing with the next flight line.

During the flying of a flight line the box labelled 7 indicates the status of the DGPS signal. If a DGPS fix is available then the box is green, if no DGPS fix is available then the box is red. After 20 seconds without a DGPS fix an error window is shown warning the user that the flight line should be reflighted.

At the end of the survey the stored coordinates of the image centres' latitudes and longitudes can be saved as a text file. These coordinates will assist with post-flight positioning and rectifying of the images.

## 6. SYSTEM VERIFICATION

Prior to the in-flight system being tested in an aircraft, it had to be ensured that the system was working as required. Initial testing was therefore performed using a passenger vehicle and based on the results of this testing, some refinements were made to the in-flight program. The initial testing performed and the refinements made are described in the following section.

### 6.1 Initial Qualitative Testing and Refinement

In order to test the pre-flight planning and in-flight system, a 700m straight section of road was located in the Oribi suburb of Pietermaritzburg, South Africa. This section of road was relatively free of traffic and was oriented in a true North-South direction.

The Trimble Pro-XRS GPS was used in DGPS mode to accurately determine the metre coordinates of the 'boundary' of this section of road for input as the catchment boundary into the pre-flight planning program. The pre-flight program was then run and the ground pixel size was adjusted to provide photograph centres at 80m intervals along the road section. The required in-flight program input files were then created and saved to disk, and the photograph positions file was printed out so that the photograph positions could be marked out on the roadside.

The Trimble Pro-XRS was once again used in DGPS mode to place wooden markers on the roadside at the pre-planned photograph positions or distances. The positions of the markers were checked using a distance measuring wheel and the sub-metre accuracy of the Trimble Pro-XRS in DGPS mode was confirmed.

For the test runs, the whole system was placed in a passenger vehicle. The road section was traversed at 60 km/h (16.7 m/s) and a visual evaluation of where the camera was triggering relative to the wooden markers was performed. It was observed that the camera consistently triggered after the marker had been passed. Although the delay was variable it was estimated that the camera was triggering approximately 0.5 to 1s too late. In an aircraft, travelling at 300 km/h this would equate to the camera firing 40 to 80 m too late. This was considered to be a significant delay.

After analysing these results, it was decided that there were two factors which could be contributing to this delay. First, the GPS could only provide a position fix every 1s. Consequently, unless the GPS NMEA output happened to coincide exactly with reaching a marker, the marker would be passed before it could be calculated that the camera should be triggered using the algorithm described previously. Secondly, there could be a delay between the calling of `DCCaptureImage` and the camera actually capturing an image.

To remove the delay due to the GPS only outputting positional strings every second, it was necessary to modify the original `OnTriggerData` algorithm described in section 5.4. to project the aircraft/vehicle's current position forward by 1s and then determine whether the planned photograph position would be passed within that second. If a photograph position was to be passed then the time to reach this position at the current velocity was calculated and a timer was initialised that calls the `DCCaptureImage` function when this calculated time had elapsed. The flowchart for this revised `OnTriggerData` event is shown in Figure 23 on the following page.

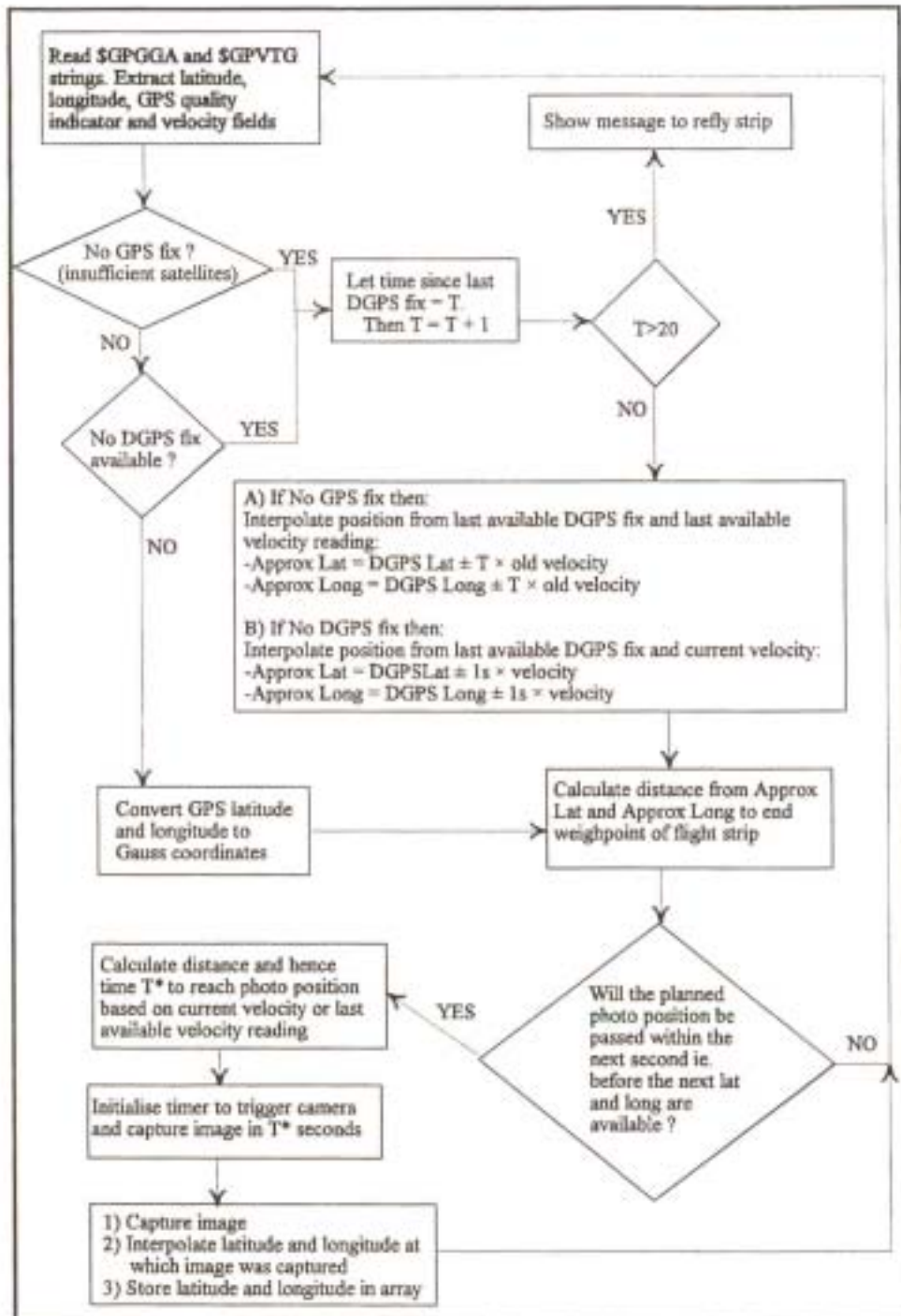


Figure 23: Revised algorithm for OnTrigger event

The delay between the calling of DCCaptureImage and the camera capturing an image could not be precisely determined. It was not possible to time this delay as there was no method available for establishing exactly when the camera's shutter opens to capture an image. Research on the



internet and personal communication with Kodak (1999) did not yield any results regarding the magnitude of the delay for the Kodak DCS420. Wood (1999), who had made extensive use of the DCS420 camera for capturing aerial imagery for precision farming applications, could not provide an estimate of the delay. Similarly, King (1999) and Benkelman (1999) had both used the DCS420 camera for airborne remote sensing, but had never done experiments to establish the delay. Benkelman (1999) had done some shutter timing tests with four Kodak DCS200 cameras and had found that when the four cameras were sent a simultaneous trigger, there was approximately 2 ms of random variation between which camera triggered first and last. There was no consistency in which camera triggered earliest or latest. Unfortunately, the delay between the trigger command being sent and the first shutter opening was not measured. For the Kodak DCS260, Anon (1999a) stated that the delay between the camera's shutter release button being pressed and the shutter opening also varied, and estimated the delay as between 100 and 200 ms.

While the DCS260 is not a Kodak professional digital camera it was likely that the delay of 100 to 200 ms was of similar magnitude for the DCS420. This was considered to be a significant delay, but since the delay for the DCS420 was likely to also be variable it was not possible to include code to consistently account for the delay. While this was not ideal it would mean that when flying at 300 km/h all photographs would be taken at a maximum of 16.7 m beyond the desired point. In the worst case, one photograph will be taken with a delay of 100 milliseconds and the next with a delay of 200 milliseconds. Assuming that this is the only delay involved, this will result in the overlap between consecutive images being approximately 8.3 m too little. For images captured at a ground pixel resolution of 0.5m this equates to a reduction in the desired percentage overlap of 1.6%. This reduction in overlap was considered to be acceptable and it was decided to ignore the delay. If data regarding the camera delay became available at a later stage then the in-flight program would be adjusted accordingly to account for the delay.

The system was once again tested at 60 km/h using the improved algorithm and it was visually confirmed that the camera was consistently firing within 3 metres of the wooden markers for all photographs. Assuming for now that there is a linear relationship between the triggering error and ground speed, this equates to the camera triggering within a maximum of 15 metres of the pre-planned photograph distance when operating at 300km/h in a light aircraft. Considering that a

pilot is unlikely to be able to fly to within 50 metres of the proposed flight line, this accuracy was considered to be acceptable.

On testing the system at 70 km/h (19.4 m/s) and then 80 km/h (22.2 m/s) a further problem was encountered. It was found that at 80 km/h the camera did not trigger at every wooden marker. After analysing this problem and reviewing the camera's specifications it was established that the camera's continuous frame capture rate, specified as approximately 3 s, was being exceeded when travelling at 80 km/h. As a result the camera was unable to capture images at all the pre-planned positions.

To confirm that the continuous capture rate was the limiting factor, the photograph position file was edited so that only every second photograph would be taken. The route was driven again at 80 km/h and as expected the camera fired at every second marker without fail. This confirmed that at 80 km/h (22.2 m/s) or faster, a photograph spacing of 80 m would not be possible due to the limitation of the rate at which the camera can continuously capture images. In simpler terms, for any survey the camera will not be able to continuously capture imagery if the photographs have to be captured at less than 4 s intervals. This could limit the applicability of the Kodak DCS420 camera and the Kodak DCS460 for low altitude, high resolution or stereoscopic image capture. It was considered to be important that the pre-flight planning program be updated at a later stage to warn the user of situations when the camera's continuous capture rate may be exceeded.

## 6.2 Quantitative Testing

The in-flight system was subsequently re-tested using a similar methodology to that outlined above to provide a quantitative measure of the triggering accuracy of the system. Unfortunately, the Kodak DCS420 could not be obtained for this test, but since the delay relating to the camera was to be ignored, the test was performed without the camera.

Prior to the test being performed, the accuracy of the Trimble Pro-XRS GPS was established using a technique based on research by Wilson (1999). Differential GPS measurements were taken with the Trimble Pro-XRS GPS at 3 survey beacons. First, 120 GPS readings were logged and averaged to determine the each beacon's position accurately. This was repeated 10 times for each

beacon. For each averaged position the error was calculated by comparison with the survey beacon's position as supplied by the Pietermaritzburg City Engineers Department. The average error and standard deviation of the error was hence calculated. The Root-Mean-Squared (RMS) error was then calculated using the following equation:

$$\text{RMS\_Error} = \sqrt{\mu^2 + \sigma^2} \dots\dots\dots(9)$$

Where;

- μ = average error (m) and
- σ = standard deviation of error (m).

Secondly, GPS positions were logged at 1 second intervals for a period of ten minutes at each survey beacon. The average error and standard deviation of the error for these instantaneous measurements were then calculated for each survey beacon. The RMS error was similarly calculated using equation 9. The results of these tests for each survey beacon are shown in Table 11.

Table 11: RMS errors for averaged GPS positions and instantaneous GPS positions

| Survey Beacon No. | RMS Error (Averaged position) | RMS Error (instantaneous) |
|-------------------|-------------------------------|---------------------------|
| 250               | 0.209m                        | 0.396m                    |
| 265               | 0.348m                        | 0.611m                    |
| 232               | 0.351m                        | 0.333m                    |

The lower RMS error for the instantaneous positions versus the averaged positions at survey beacon 232 was as a result of the very low PDOP that was associated with the capturing of the instantaneous positions at this beacon. During the ten minute period when the instantaneous positions were logged, the GPS unit was tracking 7 satellites continuously and the PDOP was 1.9 on average. A PDOP of 1 is perfect. On the other hand, during the logging of GPS positions for averaging, the PDOP went as high as 4.4 and only 5 satellites were being tracked. This resulted

in poorer position fixes for some of the averaged points. In general, however, if the PDOP is the same for all GPS measurements then averaging 120 readings will produce improved accuracy. Results for the other two beacons support this fact. Looking at the overall results, the sub-metre accuracy of the Trimble Pro-XRS was confirmed.

Displaying the GPS's accuracy in terms of a RMS error does not indicate the maximum error that can be expected. Since the maximum error was to be of interest in estimating the maximum triggering error of the system, the maximum error for a single averaged and instantaneous position at each survey beacon was also determined. These are shown in Table 12.

Table 12: Maximum errors for averaged GPS positions and instantaneous GPS positions.

| Survey Beacon No. | Max. Error (Average) | Max. Error (1s) |
|-------------------|----------------------|-----------------|
| 250               | 0.377m               | 1.242m          |
| 265               | 0.611m               | 1.913m          |
| 232               | 0.655m               | 1.077m          |

For the quantitative test in a light motor vehicle the in-flight program was adapted to include a second timer. The OnTimer event for this second timer was set up to increment an integer variable called 'Time' by one at 1/100s intervals. Each time a latitude and longitude were received via the com port the corresponding value of 'Time' was read and stored along with the latitude and longitude. Similarly when DCCaptureImage was called the corresponding value of 'Time' was recorded. By recording these times the precise latitude and longitude at which DCCaptureImage was called could be subsequently interpolated.

White paint was used to demarcate the position of photographs at approximately 100 m intervals along the 700 m section of Oribi Road used previously. The latitude and longitude of these points were then accurately captured using the Trimble Pro-XRS in differential mode. A minimum of 120 differential GPS positions were averaged per point to obtain coordinates of the planned photograph centres to an accuracy of better than 0.5m. Mock pre-flight planning files were created to correspond with these points.

The road was traversed in a light motor vehicle at average speeds of 40,60 and 70 km/h while running the adapted program incorporating the second timer. The coordinates at which DCCaptureImage was called were interpolated and compared with the latitude and longitude of the 7 trigger/photograph points obtained using the Pro-XRS GPS. The results are tabulated in Table 13 below.

It is important to note that the error introduced by the vehicle/GPS antenna not passing directly over the designated trigger point is included in the results tabulated. This error was estimated to be a maximum of 0.5m. The maximum instantaneous (C) and averaged (B) GPS errors shown in Table 13 were taken from the GPS accuracy test results described previously.

Table 13: Maximum triggering errors of in-flight system.

| Average speed (km/h) | (A) Maximum triggering error (excl. GPS inaccuracy) | (B) Maximum GPS error (averaged point) | (C) Maximum GPS error (instantaneous) | (A)+(B)+(C) Maximum triggering error (incl. GPS inaccuracy) |
|----------------------|---|--|---------------------------------------|---|
| 40                   | 0.883m  | 0.655m                                 | 1.913m                                | 3.451m  |
| 60                   | 1.212m  | 0.655m                                 | 1.913m                                | 3.780m  |
| 60                   | 1.140m  | 0.655m                                 | 1.913m                                | 3.708m  |
| 70                   | 1.465m  | 0.655m                                 | 1.913m                                | 4.033m  |

The maximum triggering error, including the GPS inaccuracy, was calculated by assuming that the maximum error due to averaging of 120 GPS positions to establish the coordinates of the photograph trigger points was in the opposite direction to the maximum instantaneous GPS error occurring when the road was traversed in a light motor vehicle. This is unlikely to ever be the case in reality and so the maximum triggering error shown in Table 13 could be considered the upper limit for the system triggering error at the speeds indicated. To determine whether these errors could be extrapolated to aircraft operating speeds of 250 to 300km/h would require extensive repetitive testing at the same and other speeds. The relationship between the triggering error and ground speed could then be established conclusively. Unfortunately, the availability of resources

did not permit more testing and consequently only very tentative conclusions can be drawn regarding the maximum triggering error at higher speeds. Looking at Table 13 the relationship between the maximum triggering error and ground speed would appear to be approximately linear. If the relationship is linear then at 300km/h the maximum triggering error would be approximately 8.3 metres. Adding to this the maximum error due to the camera delay of 8.3 metres, the final triggering error would be approximately 16.6 metres. For images captured at 0.5m ground pixel resolution with the Kodak DCS420 this equates to a maximum reduction in the percentage forward overlap of 3.4%. This was considered acceptable and could be allowed for in the pre-flight planning program by increasing the planned percentage forward overlap.

Having established that the in-flight system was operating within acceptable accuracy limits, the system was ready for a test flight in a light aircraft.

### 6.3 Test Flight

A test flight was flown in a Jabiru light aircraft under clear weather conditions over the city of Pietermaritzburg, South Africa. The camera was mounted flush with the floor of the Jabiru aircraft using the custom-built camera mount designed for the Piper Twin Comanche aircraft. The mount was held in place using adhesive packing tape. An urban test area was chosen to provide numerous easily identifiable and accessible Ground Control Points (GCPs) such as street corners, sidewalks and land survey markers for subsequent image rectification and registration.

The flight was flown at an average altitude of 8300 ft (2530 m) above ground level with a Nikon 28mm lens to produce an average ground pixel resolution of 0.6 metres. This resolution was deemed suitable for post-flight identification of GCPs as described above. In total five flight lines were flown at a prescribed flight line spacing of 640m. A total of 80 images with a planned 60% forward overlap and 30% sidelap were acquired. No problems were encountered during the acquisition of the images and the system performed as expected. Unfortunately, due to a programming error the latitude and longitude of the photograph centres could not be saved to disk when the flight was complete. While having the image centre coordinates would have assisted in the automated post-flight image orientation and geographical referencing it was not imperative and

since a re-fly would have been too costly it was decided to continue without these coordinates. The programming error was rectified to avoid this problem occurring again.

Having obtained imagery of the area it was necessary to quantitatively determine the potential spatial accuracy of the imagery. The following section discusses the options considered for achieving this and the results obtained. No comparison was made with the spatial accuracy of the videographic system since the same techniques could be applied to framegrabbed video imagery and at the same image resolution similar accuracies would be obtained. However, it is important to remember the advantages of immediate availability of digital imagery and the reduction in flying and processing time and cost for the digital camera system.

#### 6.4 Image Spatial Accuracy Assessment

In order to quantitatively assess the spatial accuracy that could be achieved using imagery captured with the digital survey system, two techniques were considered. The two techniques investigated were the use of orthophotos to provide the GCPs required to "rubbersheet" and then mosaic the individual digital images, and the use of photogrammetric software to orientate and rectify the images.

##### 6.4.1 Rubbersheeting and mosaicing

To locate an image in real world coordinates so that each pixel in an image has discrete longitude and latitude coordinates requires the identification of ground control points (GCP's) in the image. These GCP's, which are identifiable features in the image at which the coordinates are precisely known, are then used in a mathematical polynomial transformation to "rubber sheet" or warp the image to fit these GCP's (Bobbe *et al.*, 1993; Mason, 1997). This process, which is known as geometric correction (Thomas, 1996b), has its inherent problems. According to Cosandier *et al.* (1993), rubbersheeting requires two spatial transformations of the image which may reduce radiometric as well as spatial accuracy. The rubbersheeting algorithms may also be unable to compensate properly for navigation data errors, since the method tries to solve a spatial problem from what is essentially two-dimensional information (Schwarz *et al.*, 1993).

Traditionally the methods of obtaining these GCP's have included deriving them from maps and orthophotos, or through precise ground survey. According to Thomas (1996b), citing Thomas (1996a), a dependence on maps in georeferencing in remote regions is a potential limitation where maps are out-of-date, inaccurate, at inappropriate scales, or simply unavailable. Nevertheless, several researchers including Myhre *et al.* (1990) and Topolniski and Roussell (1994) have used base maps to register images in geographic space. Orthophoto images are also suitable sources of GCP's for this purpose (Bobbe *et al.*, 1993). The alternative of locating GCP's on the ground through ground surveys also has its limitations. There is the potential for site inaccessibility and difficulties in GPS surveying in wooded areas due to signal interference (Thomas, 1996b, citing Thomas, 1996a). A common problem is that a minimum of three GCP's is required per image for proper geometric correction, making both these methods time-consuming and costly. This is particularly true for the labour intensive ground survey option. Also, as Johnston *et al.* (1997a) stated, ecologists generally work in terrain that lacks the anthropogenically-derived features such as road intersections and field corners that are needed for rubbersheeting.

Despite these disadvantages, simple rubbersheeting using GCP's is a non-rigorous technique that is available in most desktop image processing packages and recent desktop GIS imaging extensions and it can produce reasonable spatial accuracy, particularly in flat terrain. The accuracy depends on the number and distribution of GCP's, the area covered by the image, the image scale, the order of polynomial used in warping the image, the surface terrain and image distortions, but Mason(1997) states that accuracies of 5m are commonly achieved. Brodie (1998) believed that the spatial accuracy of rubbersheeted images for five GCPs per image was more in the range of 10 to 15m, except in mountainous regions where the spatial accuracy would be approximately 25m.

Having positioned the images in geographic space and geometrically corrected the images, they can be mosaicked together to form a single image. Mosaicing involves the combining or merging of pixels common to two or more images in order to form a single continuous image. Pixels may be merged by, for example, averaging the brightness, contrast and colour values of the common pixels or by taking the value of the pixel from one of the images.



#### 6.4.2 Aerotriangulation and bundle adjustment

Aerotriangulation (AT), which is an essential task in photogrammetry, involves the computation of the unknown photograph orientations and the unknown ground coordinates of image tie points, based on measured photograph coordinates and a few control points (Anon, 1999b). AT is a well-established technique which has been successfully used in conjunction with block adjustment programs and analytical plotters for the last two decades, and it is receiving increased interest since the advent of digital photogrammetry and softcopy workstations (Toth and Krupnik, 1996). Digital photogrammetry and softcopy workstations have led to a revolutionary change in photogrammetric production as many of the time-consuming, labour intensive photogrammetric procedures such as interior and relative orientation, digital terrain or surface modelling, orthoimage generation, can now be automated (Tang *et al.*, 1997). These fully automated procedures combined with the powerful editing and visualisation techniques of modern digital systems have the potential to substantially improve the price/performance ratio as well as the reliability of photogrammetric procedures (Tang *et al.* 1997; Krzystek *et al.*, 1999). Krzystek *et al.* (1999) believe that once AT has reached an automatic level in a digital production environment, project costs will be significantly reduced.

AT is usually realised by a block adjustment using tie points determined in the neighbouring overlapping images (Tang *et al.*, 1997). A "block" is defined by Erdas (1999) as all of the information associated with a photogrammetric mapping project, including:

- 1) Projection, spheroid, and datum information,
- 2) Imagery used within a project,
- 3) Camera or sensor model information associated with the imagery
- 4) Ground control points (GCPs) and their measured image positions, and
- 5) Geometric relationships between the imagery in a project and the ground

Of the adjustment techniques used, bundle block adjustment is the most rigorous and flexible method of block adjustment. It leads to the most accurate results of any type of block adjustment and also allows an adjustment with a smaller number of ground control points. Requiring fewer ground control points is not only more convenient, but it is also more cost effective. Although

different approaches to AT exist, mainly with respect to the strategy of point matching, the basis of an automated AT system is the same. Figure 24 and the discussion which follows summarises the steps of a typical digital AT procedure.

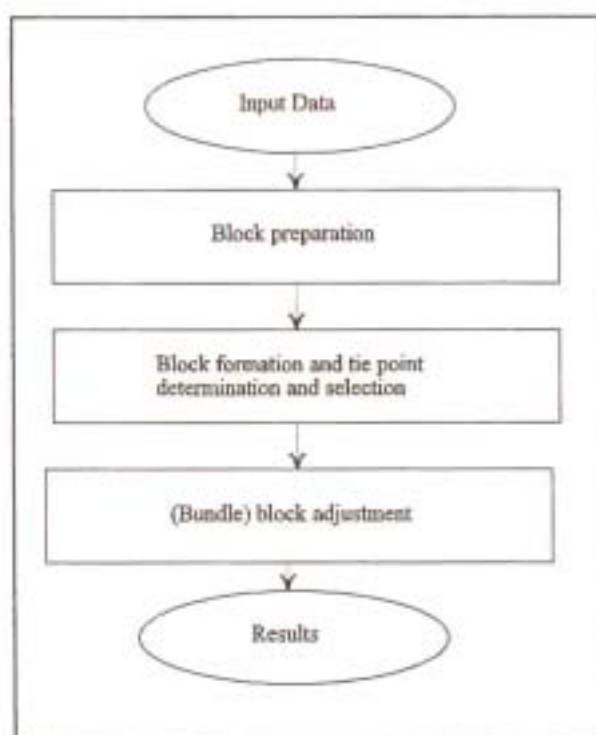


Figure 24: Flow chart of aerotriangulation process (Adapted from Tang *et al.*,1997)

Inputs to a typical AT procedure are the images comprising the photograph block, the interior orientation of the camera used, a list with the sequence of images per flight strip and block, and the GCPs to be used in the block adjustment (Toth and Krupnik, 1996). Precise airborne GPS antenna positions can also be introduced as additional control information to reduce the number of ground control points required. The interior orientation of the camera is determined by performing a camera calibration. Camera parameters that can be input include the lens focal length, lens radial and decentering distortion parameters and position of the principal point of the camera. The principal point is where the optical axis of the lens intersects the imaging plane.

Preparation of the block involves ordering the images according to the flight plan and collecting the camera and ground control information. This stage requires human interaction and knowledge

to position the images and identify GCPs which can often vary considerably in terms of type and shape (Tang *et al.*, 1997). It is the only part of the AT process that cannot be fully automated (Krzystek *et al.*, 1999). Toth and Krupnik (1996) and Tang *et al.* (1997) do, however, identify the possibility of using GPS positional data of photograph centres to assist in preparing the block. Furthermore, semi-automatic matching tools could be applied to find established GCPs in other images.

The purpose of the block formation is to generate a reference system for all images in a block. This reference system is then used in the following steps to automatically select tie points (Toth and Krupnik, 1996). Toth and Krupnik (1996) identify the steps involved in the formation of a block as being:

- 1) Matching neighbouring images, using a feature based approach,
- 2) Establishing the relative orientation parameters,
- 3) Strip formation when each photograph is scaled and translated into the strip coordinate system,
- 4) Dependent relative orientation of the photographs,
- 5) Scaling of the photographs using tie points between images of a strip, and
- 6) Connection of adjacent strips by identifying tie points and performing a dependent relative orientation.

The identification and selection of tie points, which largely determines the success of an aerotriangulation (Toth and Krupnik, 1996), can be fully automated since no specific features need to be identified (Tang *et al.*, 1997). Selection of points depends on a number of criteria, including image quality and the number of images in which the tie point appears. Importantly, unlike in traditional aerotriangulation where the cost increases proportionally with the number of points measured, the number of points that can be processed in an automated digital system is not restricted (Toth and Krupnik, 1996). This has further benefits in that better connectivity is achieved between images and strips thereby ensuring greater reliability and robustness of the final results. Also, a stronger interior geometric stability of the images is achievable and block distortions can be compensated optimally.

Having completed the above steps, a bundle block adjustment is performed using the image coordinates of tie points, image and object coordinates of GCPs and camera parameters as input. GPS data of photograph centres could also be input to reduce the number of GCPs required, as Krzystek *et al.* (1998) did. In fact, the integration of kinematic GPS data into the photogrammetric process appears to have been the focus of numerous researchers in recent years (Becker and Barriere, 1993; Colomina, 1993; Curry and Schuckman, 1993; Gruen *et al.*, 1993). Unfortunately, all these researchers employed the higher accuracy of carrier phase GPS for their research. As previously discussed, the higher cost and inherent problems of carrier phase GPS made it impractical to use such a GPS for this project.

The process of block triangulation or aerial triangulation simultaneously estimates the following (Erdas, 1999):

- 1) The position (X, Y, Z) and orientation (omega, phi, kappa) of each image in a block as they existed at the time of image capture.
- 2) The X, Y, and Z coordinates of tie points collected manually or automatically throughout the block of images. Once the X, Y, and Z coordinates of tie points are computed they can be converted to GCPs.
- 3) The interior orientation parameters associated with a camera or sensor model.
- 4) Additional parameters (AP) characterizing systematic error within the block of images and observations, such as lens distortion.

The results of the bundle adjustment are the exterior orientation parameters of the images and the object coordinates of the tie and ground control points.

While the accuracy of the imagery produced is dependant on, amongst others, the scale of the imagery used, the number of GCPs used, the position and accuracy of the GCPs, the availability or lack of accurate photograph centre coordinates and the overlap between consecutive images and between flight strips, accuracies of 1 to 5m are achieved when using 1:30 000 scale 9" metric camera imagery with a minimum number of GCPs and 10m source contours for the DEM (Craigie, 1999). If 20m source contours are used then the accuracy degrades to 5 to 10m. The accuracy obtainable for non-metric cameras should be similar.

Based on the strengths and weaknesses of the two techniques described above, the photogrammetric option was chosen. This decision was based mainly on the potential for automation. By automating many of the steps involved in this procedure, the possibility of human error is greatly reduced and the time required to produce geographically referenced imagery can be reduced. Other reasons for choosing this technique were the higher spatial accuracy that could be achieved, particularly in mountainous terrain, and the need for fewer GCPs per image in comparison with rubbersheeting.

As indicated in the above section, one of the inputs to a bundle adjustment procedure is the interior orientation parameters of the camera used. These parameters include the lens focal length, lens radial distortion coefficient and the position of the principal point. To establish these parameters a camera calibration was done using the Tsai Camera Calibration Software (Tsai, 1998).

#### 6.4.3 Camera calibration

The Tsai camera calibration software package (Tsai, 1998) contains routines for calibrating Roger Tsai's perspective projection camera model which is based on a pin-hole camera model of 3D-2D perspective projection with 1st order radial lens distortion. An explanation of the basic algorithms and descriptions of the variables is documented by Tsai (1987). Although the software was designed for calibrating video camera/framegrabber combinations it was possible to adapt the program to calibrate the Kodak DCS420 digital camera (Will, 1999).

The Tsai model uses given 3D ( $x,y,z$ ) world coordinates of a point to predict the 2D pixel coordinates of the point in the image. The model has 11 parameters: five internal or intrinsic parameters relating to the camera and lens, and six external or exterior parameters which describe the relationship between the world and camera coordinate systems. The interior parameters are:

- 1)  $f$  - effective focal length of the pin hole camera,
- 2)  $kappa_1$  - 1st order radial lens distortion coefficient,
- 3)  $C_x, C_y$  - coordinates of centre of radial lens distortion and the piercing point of the camera coordinate frame's  $Z$ -axis with the camera's sensor plane (principal point), and

- 4)  $s_x$  - scale factor to account for any uncertainty due to framegrabber horizontal scanline resampling.

The external or extrinsic parameters are:

- 1)  $R_x, R_y, R_z$  - rotation angles for the transform between the world and camera coordinate frames, and
- 2)  $T_x, T_y, T_z$  - translational components of the transform between the world and camera coordinate frames.

In addition to the 11 variable camera parameters, Tsai's camera model has six fixed intrinsic camera constants, namely:

- 1)  $N_{cx}$  - number of sensor elements (sels) in camera's x direction
- 2)  $N_{fx}$  - number of pixels in framegrabber's x direction
- 3)  $dx$  - x dimension of camera sensor element (mm/sel)
- 4)  $dy$  - y dimension of camera sensor element (mm/sel)
- 5)  $dpx$  - effective x dimension of pixel in framegrabber (mm/pixel)
- 6)  $dpy$  - effective y dimension of pixel in framegrabber (mm/pixel)

For calibration of the Kodak DCS420, Will (1999) suggested that  $N_{fx}$  be taken as equal to  $N_{cx}$  since there was no framegrabber in the system and the digital image produced by the DCS420 has the same number of pixels as the camera's CCD chip has sensor elements (sels). The constants  $dx$  and  $dy$  were calculated by dividing the CCD chip's x and y dimensions by the number of sels in the x and y directions, respectively.  $dpx$  and  $dpy$  were set equal to  $dx$  and  $dy$ , respectively, since there was no framegrabber in the system (Will, 1999). In summary, the fixed intrinsic camera parameters had the following values:

- 1)  $N_{cx} = N_{fx} = 1524$  sels or pixels
- 2)  $dx = dpx = 0.0092$  mm per sel or pixel
- 3)  $dy = dpy = 0.0092$  mm per sel or pixel

To capture the required image, a rectangular grid of circular calibration and test targets was set up in the foyer of the Rabie Saunders building, University of Natal, Pietermaritzburg, South Africa. Figure 25 shows the layout of the calibration grid. Black disks of 19mm diameter were used for the calibration points and smaller 13mm diameter black disks were used for the test points. Black targets were chosen to provide the best possible contrast between the targets and the foyer floor, while smaller disks were chosen for the test points so that they could be easily distinguished from the calibration points. It was ensured that the grid was broadly distributed across the field of view of the camera. This was necessary to ensure that the radial lens distortion and image centre parameters could be accurately estimated (Tsai, 1998).

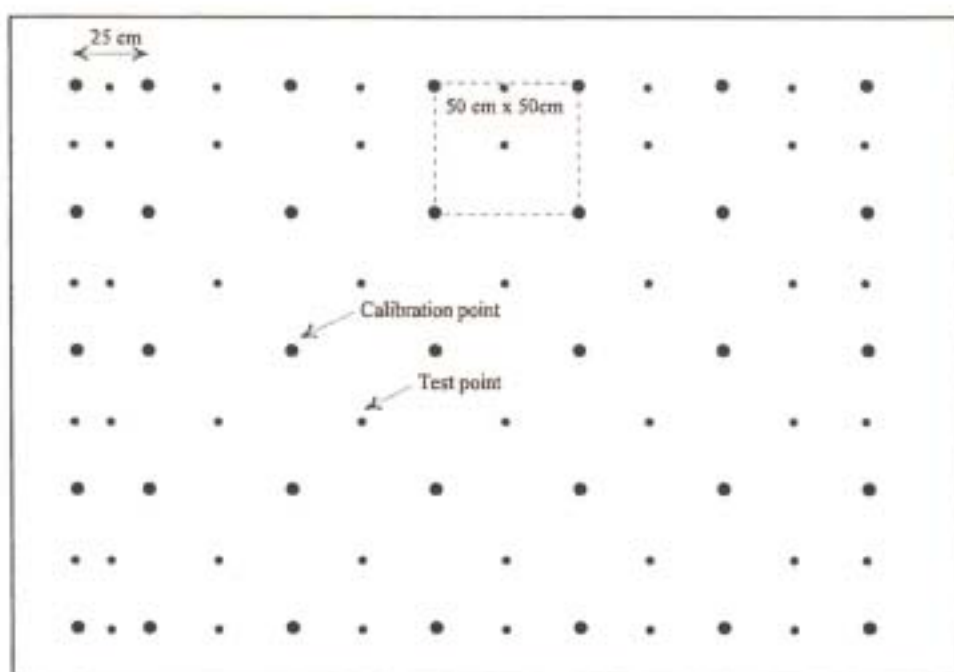


Figure 25: Camera calibration grid layout

The camera was placed on a camera tripod to provide a stable base for the calibration and was then positioned on a balcony approximately five metres above the calibration grid. To be able to separate the effects of  $f$  and  $T_z$  on the image it was a requirement that there was some perspective distortion or foreshortening effects in the calibration image. In the Frequently Asked Questions (FAQ) file included with the software a relative angle of 30 degrees between the camera's image plane and the calibration grid plane was suggested to produce the necessary perspective distortion.

The camera was setup on the tripod to provide a relative angle of approximately 30 degrees.

After capturing an image of the calibration grid the image was opened in the Scion Image software package (Scion, 1998). The package was used to threshold the image so that all pixels equal to or greater than a single threshold level were displayed in black, and all other pixels (the background) were displayed in white. In this case, the image was thresholded so that only the calibration and test targets were displayed as black. The individual targets were then analysed using the software's 'Particle Analysis' tools. Each target was clicked on and hence outlined and numbered. The software used image processing algorithms to automatically find the pixel coordinates of the centre of each target. The software also produced a summary table of the calibration points' centroid pixel coordinates. This table was saved as a text file and imported into Quattro Pro as a tab delimited text file. In Quattro Pro the corresponding real world x and y coordinates of the calibration points were added to the spreadsheet and the spreadsheet was then exported as a tab-delimited file to produce a file suitable for input into the Tsai camera calibration software.

The 'coplanar calibration with full optimisation' program of the Tsai camera calibration software was used to calculate the camera's extrinsic and intrinsic parameters. The full optimization program was chosen over the 'basic coplanar calibration' program since, although full optimisation is slower, it provides the most accurate calibration results (Tsai, 1998). The results of the calibration were as shown in Table 11.

Table 14: Camera calibration results

|                             |                                   |
|-----------------------------|-----------------------------------|
| Intrinsic camera parameters |                                   |
| f (mm)                      | 30.92                             |
| kappa1 (1/mm <sup>2</sup> ) | 1.361509e-04 [1/mm <sup>2</sup> ] |
| Cx, Cy (pixels)             | 739.2, 354.6                      |
| Extrinsic parameters        |                                   |
| Rx, Ry, Rz (degrees)        | -29.86, -0.12, -0.59 [deg]        |
| Tx, Ty, Tz (mm)             | -1379.4, -659.5, 6851.9           |



It is important to note that although the calibrated effective focal length was close to the focal length of 28mm specified on the lens it was unlikely to ever be the same. In the algorithms used in the Tsai software package the effective focal length is a parameter in a pin-hole camera, while the focal length printed on the lens is a parameter in a thick-lens camera model. While the two parameters have similar effects on the image they are actually different quantities (Tsai, 1998).

Along with the calibration results tabulated above, the program also outputs an ordered list of numbers which relate to the inputs to, and outputs from, the calibration program. This list of numbers was used as input into a program that converted the 2D image coordinates of the test points to 3D world coordinates. This program forms part of the Tsai camera calibration software package. The estimated 3D world coordinates output by this program were compared with the actual world coordinates of the test points in order to provide a measure of the accuracy of the calibration. The average absolute error in the estimated x and y world coordinates of the test points was 0.97mm and 1.32mm, respectively. With the average ground pixel size in the image being approximately 2mm these errors equated to an error of less than 1 pixel in the image. This was considered to be acceptable. The maximum absolute errors for the test points were 7.92mm and 7.11mm in the x and y coordinates, respectively. In both cases the corresponding x or y error of the test point was of similar magnitude, suggesting that the Scion Image software had estimated the centroid of these particular test points poorly.

A further input into a bundle adjustment procedure is Ground Control Points (GCPs). The following section is an outline of the procedure which was followed to obtain the required GCPs for input into the photogrammetric software.

#### 6.4.4 GCP survey

GCPs should be easily identifiable features such as small bushes and street corners which appear on two or preferably more photographs or images. GCPs which appear in the forward overlap between three consecutive images as well as in the side overlap between these images and a neighbouring flight line's image are most desirable (Craigie, 1999). Such points provide a high degree of connectivity within the block and consequently produce better aerial triangulation results with fewer GCPs. Figure 26 illustrates an example of such a GCP.

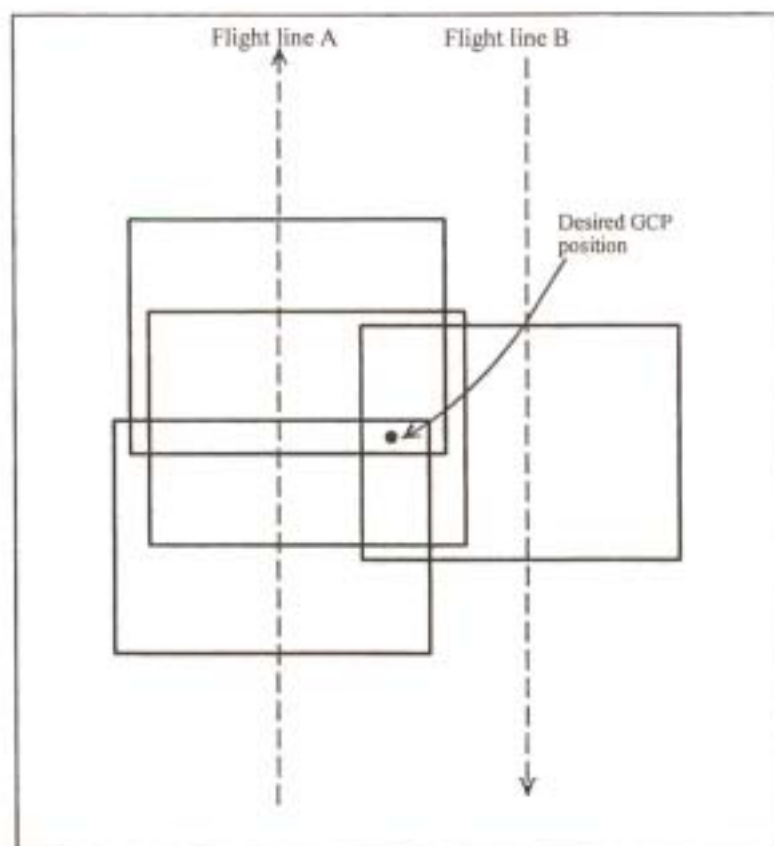


Figure 26: Example of desired GCP position

Prior to commencing the GCP survey, all the digital images that were to be processed were printed out at the same scale. In total, 27 images from 3 flight lines (9 images per flight line) were chosen for processing. The printed images from a flight line were layed out and overlapped to form a single strip of images. The 3 flight lines' images were then examined to identify areas where GCPs that were preferably positioned as shown in Figure 26 above could be captured. In total 40 GCP areas were identified.

Each GCP area was clipped out of the larger digital image and an A4 plot of each GCP area was printed. Figure 27 shows an example of a completed GCP locality plot.

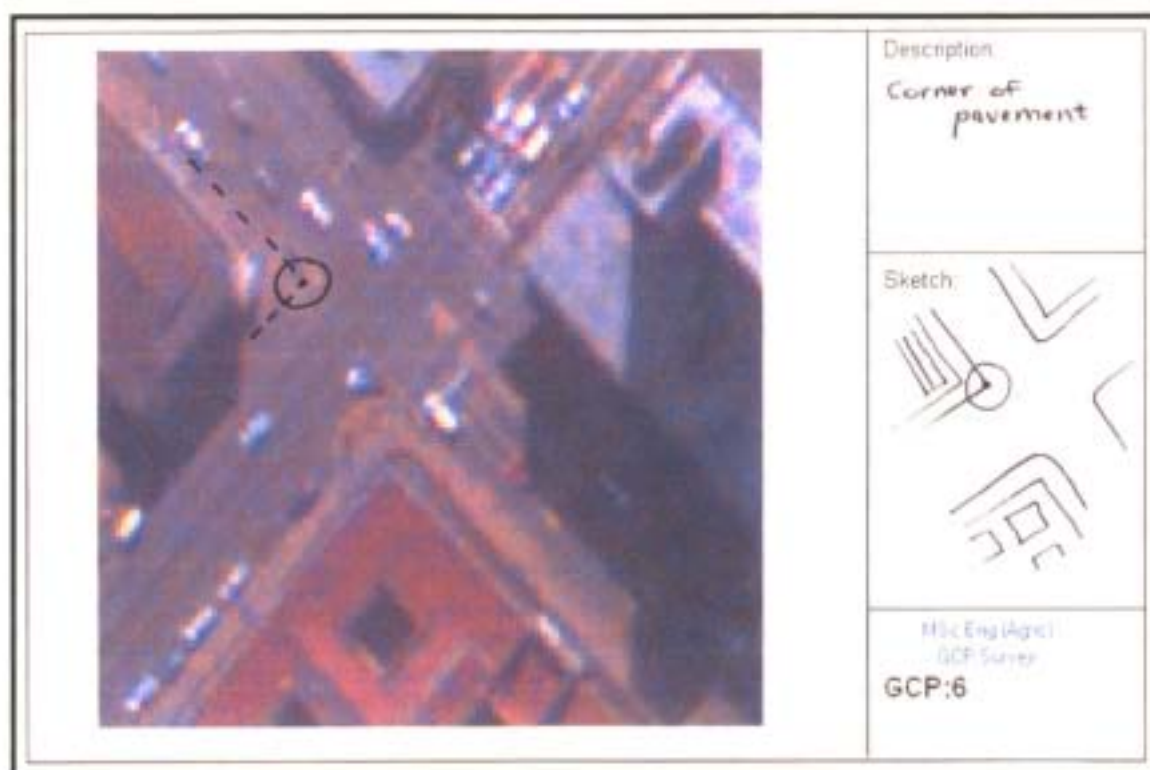


Figure 27: Example of completed GCP locality plot.

These GCP locality plots were used in the field to clearly identify, describe and sketch each GCP that was captured. These plots were made to aid the measurement of the GCPs in the office using the photogrammetric software.

The GCP field survey was performed using a Trimble Pro-XRS GPS system. The Pro-XRS was chosen for the survey since the GCP positions should be captured to a spatial accuracy of the order of 3 times the final pixel resolution of the imagery (Craigie, 2000). For the digital imagery captured this equated to a GCP accuracy of approximately 1.8m in the X-Y plane. Based on the accuracy tests performed previously, the Pro-XRS was suitable to achieve this accuracy.

Each GCP's position was captured by averaging two minutes of real-time differentially corrected GPS readings. GPS line data was also captured while travelling between the GCPs to serve as additional control if required and as a means of estimating the spatial accuracy of the rectified imagery. Due to the many tall buildings in the Pietermaritzburg city centre the signal from the GPS

satellites was frequently blocked and the capturing of sufficient continuous line data was thus not possible. However, as discussed later, cadastral data for the city centre was obtained in order to estimate the spatial accuracy of the processed imagery.

The GPS data from the GCP field survey was transferred to a PC using Trimble's Pathfinder Office software. Pathfinder Office was then used to export all the GCP points as an Arcview shapefile in Transverse Mercator projection, Clarke 1880 spheroid, with 31° East of Greenwich as the central meridian. The minimal GPS line data captured was also exported as an Arcview point shapefile in the same projection and spheroid. In Arcview, the X, Y and Z coordinates of each point were calculated and added to the database table.

The approximate coordinates of where each image was captured, hereafter referred to as the photo station coordinates, were also determined. The centre point of each image was first located using Paint Shop Pro and this point was then identified on scanned, geographically referenced orthophotos obtained from the City Engineers Department of the Pietermaritzburg City Council. Hence, on the assumption that all images were captured with zero tip, roll or yaw, the photo station coordinates were determined. It was believed that these approximate coordinates would be sufficiently accurate to assist in positioning the photos relative to one another in order to subsequently allow for automated tie point matching using the photogrammetric software.

The Kodak DCS420 digital camera images, the GCP shapefile, the photo station coordinates spreadsheet and the GCP locality plots were then sent to GIMS Photogrammetry lab in Midrand, South Africa. These data were used in conjunction with Orthobase photogrammetric software to produce orthophotographs of the urban test area. The following sections outline the procedure followed by the GIMS Photogrammetry' staff and the results obtained.

#### 6.4.5 Photogrammetric process

IMAGINE Orthobase was chosen to process the digital camera images of the urban test area since it provides the functionality to import non-metric camera photographs or images. Non-metric cameras are cameras which do not have fiducial marks. These fiducial marks, which are standard on 9" camera photographs, allow the software to automatically locate the centre pixel of each image, but are generally not present in smaller format camera photographs or in digital camera images. Many photogrammetric software packages are only able to process images which have fiducial marks, but IMAGINE Orthobase can utilise the corners of the image to automatically define the origin of the image/photo-coordinate system (Erdas, 1999).

Having chosen the software, the following procedure was initially followed:

- 1) The projection, datum and spheroid for the project was set.
- 2) The digital camera images were imported,
- 3) The camera model for the Kodak DCS420 was defined. This included inputting the lens focal length (mm), x and y pixel dimensions (mm), CCD chip size (mm), the camera's principal point and the radial lens distortion coefficient.
- 4) The Ground Control Points (GCPs) were identified (measured) and the coordinates as defined in the Arcview shapefile database table were input. In total 27 of the 40 GCPs captured during the field survey were used for the block. The GCPs captured on the corners of tall buildings were not used since the height of the building causes a perspective distortion between images and makes accurate measurement of GCPs captured at the base of the building both difficult and inaccurate. Figure 28 illustrates perspective distortion between two images from different flight strips. Figure 29 shows the GCP measurement window of Orthobase.

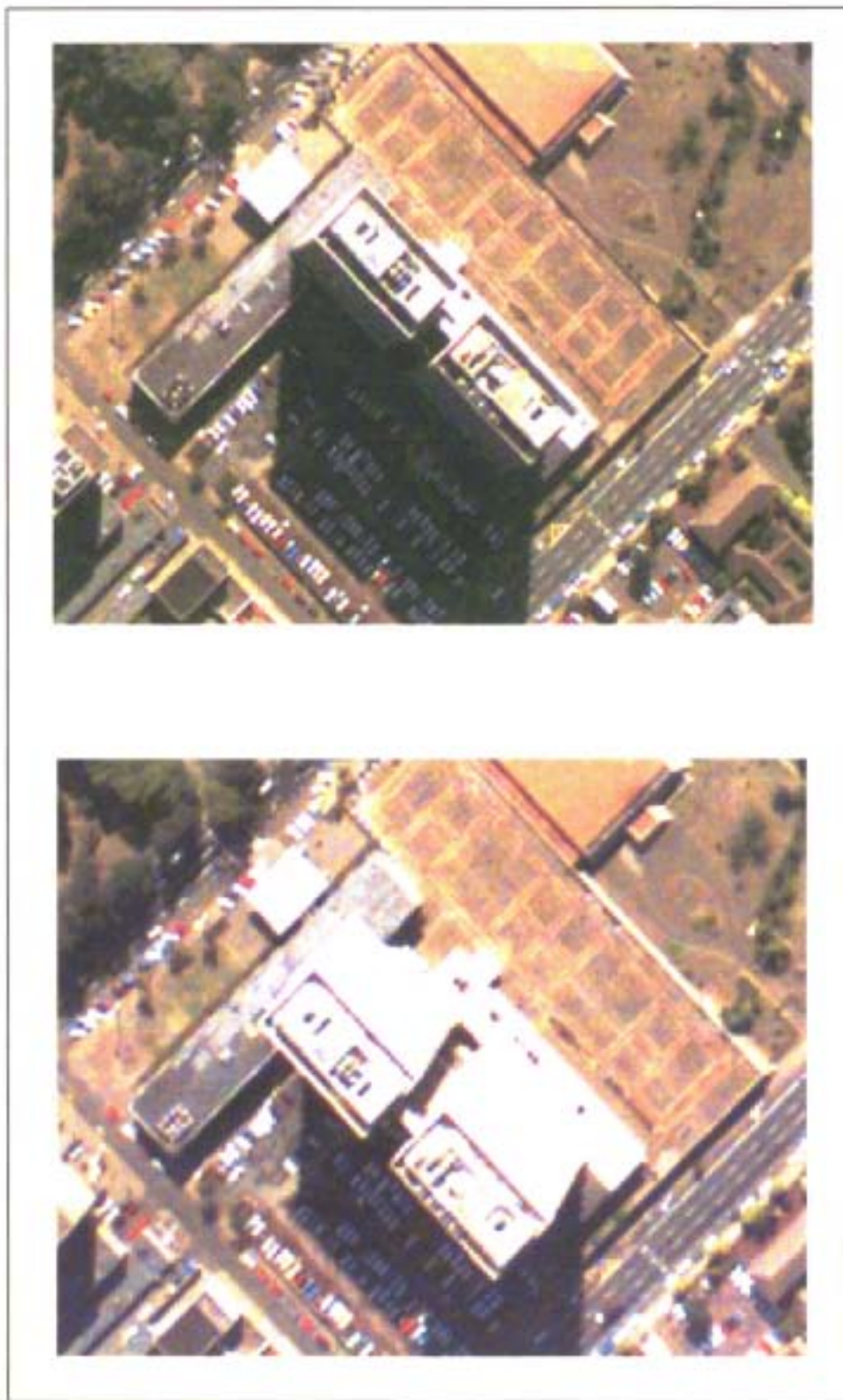


Figure 28: Example of perspective distortion between two images from different flight lines.



Figure 29: Orthobase GCP measurement window.

- Initial X and Y coordinates for the photo stations were input from the spreadsheet provided. The rotation angles for tip, roll and yaw were set as zero.
- The automated tie point matching utility of Orthobase was run. This utility uses image processing algorithms to find corresponding points in overlapping images.

It was found during step 6 that the software was unable to find tie points between the images automatically. This was due in part to the inaccuracy of the initial photo station coordinates provided. After analysis of the process by which the approximate photo stations were determined it was calculated that at the flying height of 2530m AGL and for a tip or roll of  $5^{\circ}$ , these coordinates would have been incorrect by more than 220m. The images only covered an average area of 1250m by 830m and an error of 220m was therefore significant and accounted for the software's inability to automatically find tie points. If it had been possible to save the photo station

coordinates that were output by the Trimble Pro-XRS unit during the test flight then Craigie (2000) believed that the auto-tie point functionality would have worked. Craigie (2000) has successfully processed scanned air photographs using GPS photo station coordinates without any problems which would indicate that the same would be possible if digital camera imagery was used. However, Craigie (2000) emphasised that the accuracy of the auto tie point matching would also depend on the variation of the pitch and roll angles between consecutive photographs being small. Orthobase uses the input data to calculate the approximate location of feature points on the overlapping areas of multiple images. Once an approximate location has been defined, Orthobase uses a pixel search window to search for the exact image position in neighbouring images. The size of the search window can be defined by the user and is 21 x 21 pixels by default. This would equate to an approximate search window size of 13m x 13m on the ground for the digital camera imagery captured in the test flight. If there are large changes in the tip and roll angles from one image to the next then the location of feature points in neighbouring images will be poorly approximated and tie points may not be found. A much larger search window could be defined to allow for large tip and roll angles, but this would dramatically increase the computer processing power and time required to achieve a solution.

Furthermore, the heading (yaw) of the aircraft should be known and should vary by less than 2 degrees from frame to frame (Craigie, 2000). The yaw was not measured or accounted for during the flight and an analysis of the results of the bundle block adjustment subsequently performed and documented in section 6.4.6 indicated that the variation in the yaw was in excess of 2 degrees between some of the photos. This would account in part for the software's inability to perform the auto tie point matching routine. Furthermore, the difference in the tip and roll angles between certain consecutive images was in excess of 7 and 10 degrees, respectively. These high pitch and roll angle variations, together with the unavailability of accurate photo station coordinates and yaw measurements, contributed to the failure of the auto tie point process. The need to measure or account for tip, roll and yaw of the aircraft was therefore identified as a future requirement in order to achieve optimal automation of the post-flight image rectification procedure. A sensor, such as an Inertial Navigation System (INS) or cheaper tip/roll sensor, would need to be incorporated into the in-flight system to measure the tip, roll and yaw in real time. As previously discussed, no suitable low cost sensor with sufficient sensitivity and accuracy was found during



the research phase of this project.

Due to the auto tie point process failing, the tie points were identified manually. This resulted in far fewer tie points being identified and used in the bundle block adjustment than if the tie point matching had been automated. Only 33 tie points were identified and used in the bundle block adjustment, whereas the number of tie points could have been increased to 500 points per image with very little increase in processing time if the process had been automated (Craigie, 2000). Having fewer tie points reduced the connectivity between the images in the block and was likely to reduce the quality of the triangulation solution, in other words, reduce the spatial accuracy of the orthophotos produced. The increase in accuracy with an increase in tie points can be attributed to the increase in data redundancy, thus allowing for the minimization and distribution of error throughout the photogrammetric network of observations (Erdas, 1999). Since GIMS had never worked with digital camera images before, the likely reduction in spatial accuracy due to having fewer tie points could not be estimated.

A possibility which was not explored in this project was to use the photo station coordinates and tip, roll and yaw angle results from the bundle block adjustment described above as initial estimates of the photo station coordinates and tip, roll and yaw angles of each image in a second bundle block adjustment using the auto tie point functionality of Orthobase. While repeating the bundle block adjustment procedure would require additional time and increase costs, these initial results would be sufficiently accurate to ensure that the auto tie point matching would work for a second block adjustment (Craigie, 2000). The GCPs measured in the initial run could be saved and used as input into the second run. The increase in the spatial accuracy of the results of the bundle block adjustment using auto tie point matching could also be sufficient to offset the extra cost and time of repeating the bundle block adjustment. If a low cost sensor to measure tip, roll and yaw in real time is not found then this approach would have to be investigated further. Obviously, the need to repeat the bundle block adjustment would depend on whether higher accuracy imagery than could be obtained from an initial bundle block adjustment with manually defined tie points was required for a particular application.

The results of the bundle block adjustment using the manually defined image tie points are presented and discussed in the following section.

#### 6.4.6 Bundle block adjustment results

Table 15 shows the exterior orientation parameters output by Orthobase. Xs, Ys and Zs are the x, y and z coordinates of the photo stations, respectively. Omega, Kappa and Phi are the angles relating to the tip, roll and yaw of the aircraft, respectively.

Table 15: Exterior orientation parameters.

| Flight line    | Image | Xs (m)    | Ys (m)      | Zs (m)  | OMEGA (tip) - degrees | PHI (roll) - degrees | KAPPA (yaw) - degrees | Absolute Values       |                      |                       |
|----------------|-------|-----------|-------------|---------|-----------------------|----------------------|-----------------------|-----------------------|----------------------|-----------------------|
|                |       |           |             |         |                       |                      |                       | OMEGA (tip) - degrees | PHI (roll) - degrees | KAPPA (yaw) - degrees |
| 4              | 5     | -60019.94 | -3276742.49 | 2427.16 | 13.76                 | -1.36                | -3.99                 | 13.76                 | 1.36                 | 3.99                  |
| 4              | 6     | -59987.68 | -3276489.23 | 2466.95 | 12.85                 | -3.29                | -4.85                 | 12.85                 | 3.29                 | 4.85                  |
| 4              | 7     | -59838.81 | -3276083.65 | 2501.89 | 6.78                  | 0.58                 | -4.23                 | 6.78                  | 0.58                 | 4.23                  |
| 4              | 8     | -59911.53 | -3275856.83 | 2475.08 | 6.00                  | -2.53                | -2.15                 | 6.00                  | 2.53                 | 2.15                  |
| 4              | 9     | -59987.87 | -3275862.49 | 2473.57 | 6.17                  | -4.21                | -1.13                 | 6.17                  | 4.21                 | 1.13                  |
| 4              | 10    | -59956.20 | -3275387.48 | 2473.58 | 4.94                  | -0.75                | -1.94                 | 4.94                  | 0.75                 | 1.94                  |
| 4              | 11    | -59970.77 | -3275206.01 | 2467.28 | 5.53                  | 0.12                 | -3.71                 | 5.53                  | 0.12                 | 3.71                  |
| 4              | 12    | -60031.04 | -3274997.26 | 2470.79 | 5.78                  | -3.90                | -6.05                 | 5.78                  | 3.90                 | 6.05                  |
| 4              | 13    | -59583.44 | -3275264.70 | 2314.37 | <b>21.72</b>          | <b>8.75</b>          | <b>-8.71</b>          | <b>21.72</b>          | <b>8.75</b>          | <b>8.71</b>           |
| 5              | 2     | -59267.41 | -3274472.58 | 2518.48 | -4.72                 | 3.32                 | 3.88                  | 4.72                  | 3.32                 | 3.88                  |
| 5              | 3     | -59277.26 | -3274477.83 | 2484.23 | -10.23                | 1.99                 | 4.26                  | 10.23                 | 1.99                 | 4.26                  |
| 5              | 4     | -59293.98 | -3274778.84 | 2506.05 | -8.14                 | 1.02                 | 4.74                  | 8.14                  | 1.02                 | 4.74                  |
| 5              | 5     | -59327.62 | -3274972.93 | 2507.28 | -9.16                 | -0.01                | 4.91                  | 9.16                  | 0.01                 | 4.91                  |
| 5              | 6     | -59328.16 | -3275190.88 | 2505.05 | -8.62                 | 1.14                 | 6.43                  | 8.62                  | 1.14                 | 6.43                  |
| 5              | 7     | -59545.94 | -3275451.06 | 2500.71 | -6.46                 | -9.15                | 5.25                  | 6.46                  | 9.15                 | 5.25                  |
| 5              | 8     | -59516.59 | -3275694.92 | 2497.78 | -5.51                 | -9.49                | 2.87                  | 5.51                  | 9.49                 | 2.87                  |
| 5              | 9     | -59270.36 | -3275681.10 | 2448.39 | -13.28                | -2.10                | 1.72                  | 13.28                 | 2.10                 | 1.72                  |
| 5              | 10    | -59292.82 | -3275932.92 | 2475.84 | -12.72                | 0.00                 | 2.51                  | 12.72                 | 0.00                 | 2.51                  |
| 6              | 5     | -58800.37 | -3276610.39 | 2454.62 | 11.01                 | 0.91                 | -1.74                 | 11.01                 | 0.91                 | 1.74                  |
| 6              | 6     | -58867.18 | -3276338.78 | 2475.30 | 9.17                  | 0.62                 | -3.75                 | 9.17                  | 0.62                 | 3.75                  |
| 6              | 7     | -58833.42 | -3276186.62 | 2465.74 | 11.59                 | -0.76                | -4.37                 | 11.59                 | 0.76                 | 4.37                  |
| 6              | 8     | -58846.11 | -3275868.65 | 2487.07 | 8.59                  | -1.58                | -3.89                 | 8.59                  | 1.58                 | 3.89                  |
| 6              | 9     | -58820.47 | -3275630.67 | 2489.49 | 7.08                  | -1.66                | -3.57                 | 7.08                  | 1.66                 | 3.57                  |
| 6              | 10    | -58787.23 | -3275404.03 | 2489.90 | 7.12                  | -0.21                | -3.30                 | 7.12                  | 0.21                 | 3.30                  |
| 6              | 11    | -58811.66 | -3275242.76 | 2472.37 | 8.59                  | 0.58                 | -3.75                 | 8.59                  | 0.58                 | 3.75                  |
| 6              | 12    | -58773.75 | -3275030.59 | 2471.15 | 9.39                  | -1.80                | -1.99                 | 9.39                  | 1.80                 | 1.99                  |
| 6              | 13    | -58778.38 | -3274810.39 | 2480.79 | 8.41                  | -1.13                | -0.70                 | 8.41                  | 1.13                 | 0.70                  |
| <b>Average</b> |       |           |             |         | <b>3.17</b>           | <b>-0.92</b>         | <b>-1.01</b>          | <b>9.01</b>           | <b>2.33</b>          | <b>3.72</b>           |

Looking at the results it can be seen that image 13 of flight line 4, hereafter referred to as image 4-13, had the highest absolute tip, roll and yaw angles. Tip, roll and yaw angles of these magnitudes were unexpected since the flight was flown on a wind still day and there was very little air turbulence. On analysis of this photograph it was established that GCP number 1 which appeared only on photo 4-13 had been incorrectly measured in Orthobase. It had been positioned

approximately 55m South East from the position where it had been captured in the field, as shown in Figure 30.



Figure 30: Incorrect measurement of GCP number 1.

By incorrectly measuring this point, Orthobase had calculated large tip, roll and yaw angles for the image in order for the GCP position measured in Orthobase to spatially match the coordinates of the actual point captured with the GPS in the field. Figure 31 shows image 4-13 and the position of GCP number 1. It is evident from the non-rectangular shape of the image that the software has had to stretch the North-West corner of the image to make the measured GCP position match the GPS coordinates of the actual point captured.

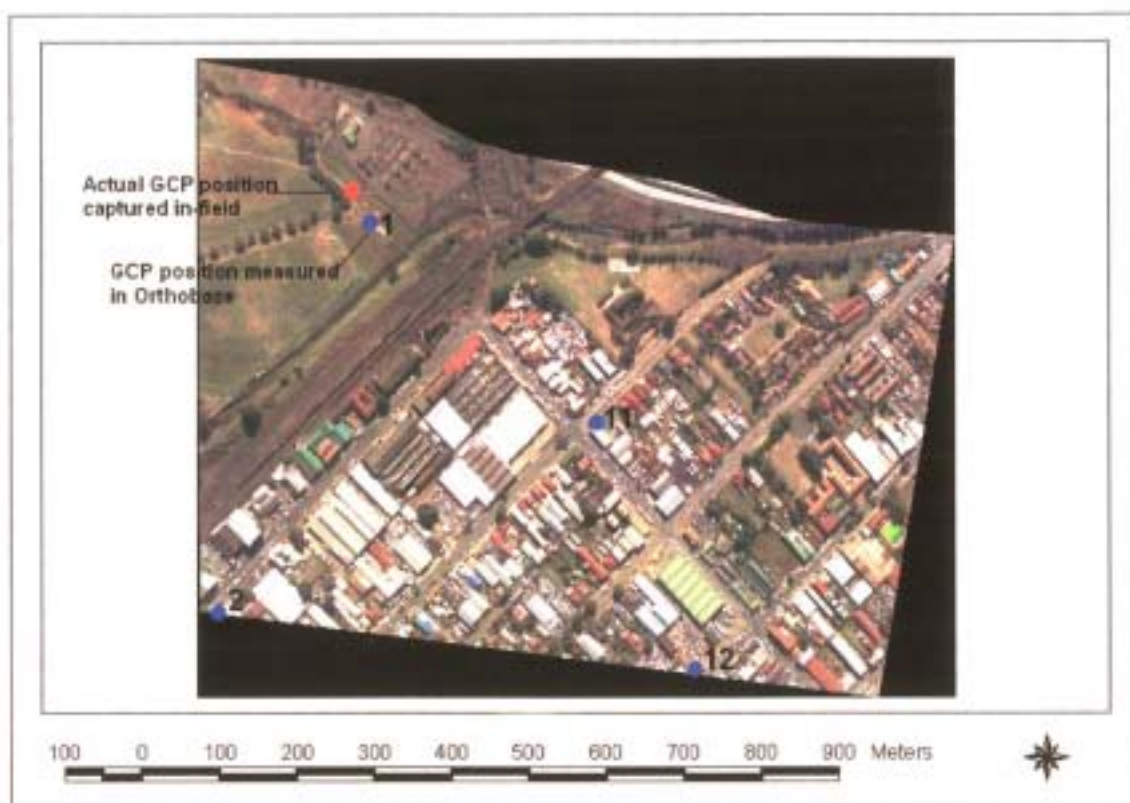


Figure 31: Image 4-13 showing the distortion due to the incorrect measurement of GCP 1.

It was confirmed with Craigie (2000) that the incorrect measurement of GCP number 1 would not have affected the calculation of the exterior orientation parameters for the remaining images or the overall results of the bundle block adjustment.

From Table 15 it is also evident that the tip angles are high for all images. Again, this was unexpected based on the good conditions under which the test flight was flown. However, the tip angles did not fluctuate dramatically from one photo to the next and were all positive or negative<sup>6</sup> for a particular flight line. This indicated that there was possibly a constant error in these results. On further analysis it was concluded that the error had been introduced by the manner in which the camera had been mounted in the aircraft. The camera had been mounted flush with floor of the

<sup>6</sup>

The positive or negative values of Omega, Phi and Kappa are as a result of the rotation coordinate system used. Omega is a positive rotation around the X-axis, phi is a positive rotation around the Y-axis, and kappa is a positive rotation around the Z-axis. X is the primary axis, indicating that the first rotation in forming the rotation matrix is around the X-axis. Rotation follows the right-hand rule, which says that when the thumb of the right hand points in the positive direction of an axis, the curled fingers point in the direction of positive rotation for that axis.

aircraft and as a result the camera CCD chip's x, y and z axes were not orthogonal to the x-y-z axes of the aircraft when in flight. Therefore, even if the aircraft had been flown so that its x and y axes were parallel to the x and y axes of the reference coordinate system for all the images, the camera's axes would be rotated relative to the reference coordinate system. If the aircraft was flown from South to North and its x and y axes were orthogonal to the reference coordinate system, then mounting the camera flush with the aircraft floor would have introduced a positive rotation about the X-axis, in other words, a positive tip angle. Furthermore, it was likely that the aircraft would fly with its nose pointing slightly upward, thereby introducing a further positive rotation about the X axis when a flight line was flown from South to North, as flight lines 4 and 6 were. A negative rotation about the X-axis would be introduced for flight lines flown from North to South, as flight line 5 was. The results tabulated in Table 15 substantiate this hypothesis. If the absolute average tip angle of 9.01 degrees was assumed to be the constant error introduced by mounting the camera in this manner, then rotation about the X-axis due to turbulence (excluding image 4-13) was less than 5 degrees for all images. This magnitude of tip was considered to be reasonable and would not significantly reduce the accuracy of the orthophotographs produced.

Excluding image 4-13, the roll and yaw angles were considered to be correct and acceptable, although the variation in the yaw was in excess of 2 degrees for four pairs of the images. The implications of a large variation in the yaw angle between consecutive images were discussed previously.

To establish the spatial accuracy of the imagery, the cadastral boundaries of Pietermaritzburg were obtained from the City Engineers Department of the Pietermaritzburg City Council. These cadastral boundaries were assumed to be 100% accurate and were overlaid on the digital orthophotographs produced as shown in Figures 32 through 35. The colour orthophotographs have been displayed as greyscale images in Figures 32 to 35 in order for the cadastral boundaries to be clearly visible. A visual estimation of the images' accuracies was hence made.

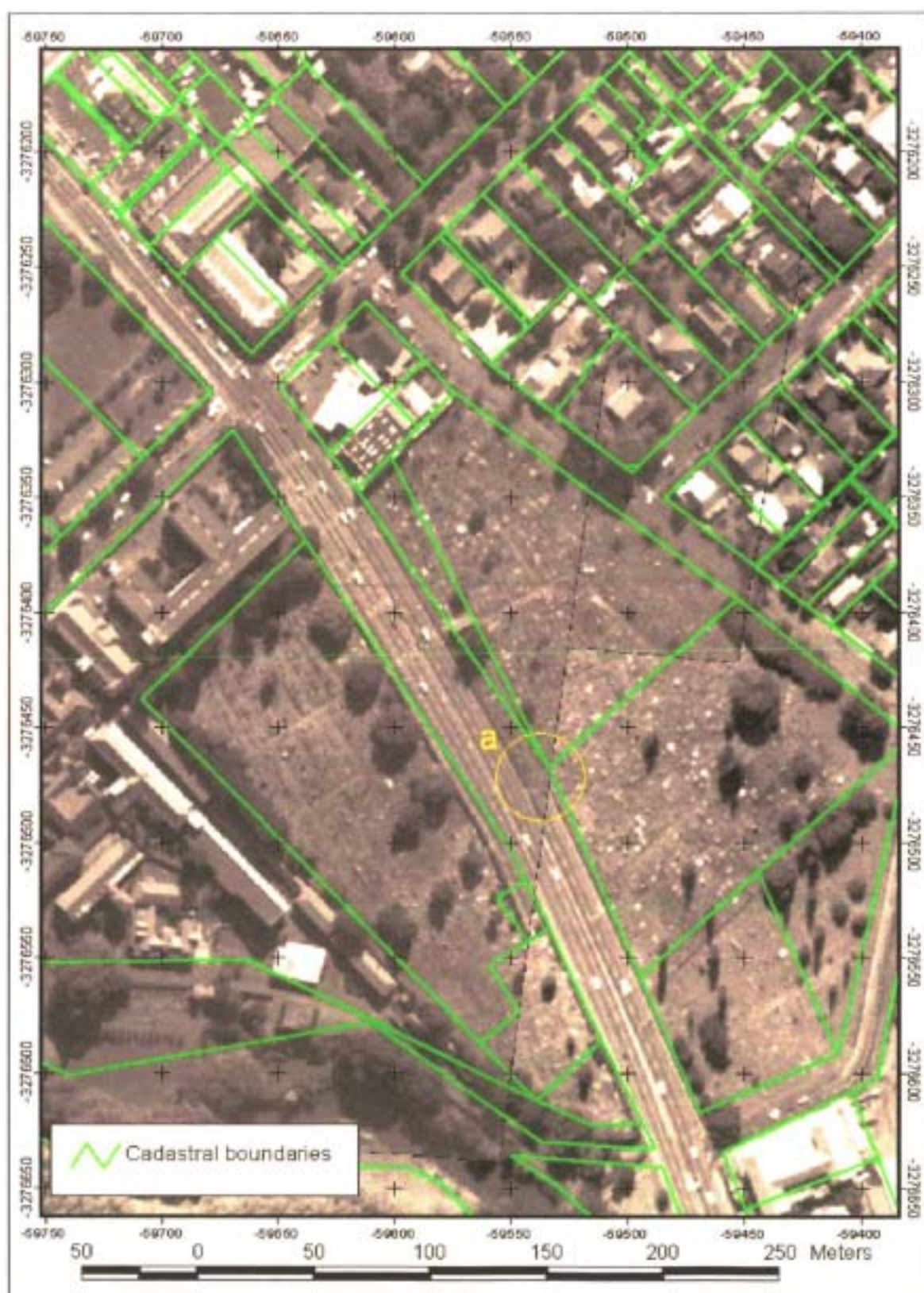


Figure 32: Example 1 of cadastral boundaries overlaid on digital camera orthophotographs.



Figure 33: Example 2 of cadastral boundaries overlaid on digital camera orthophotographs.

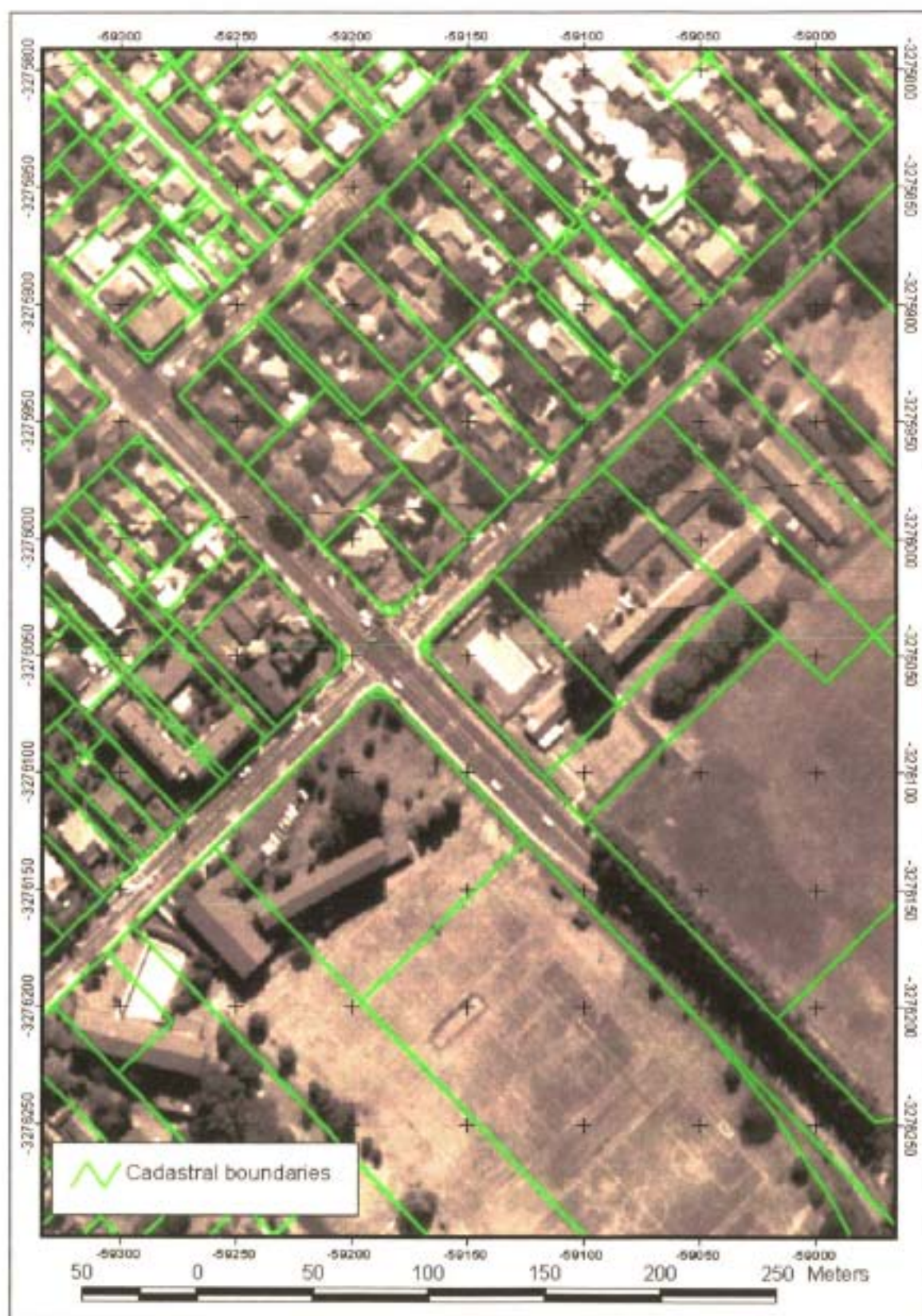


Figure 34: Example 3 of cadastral boundaries overlaid on digital camera orthophotographs.



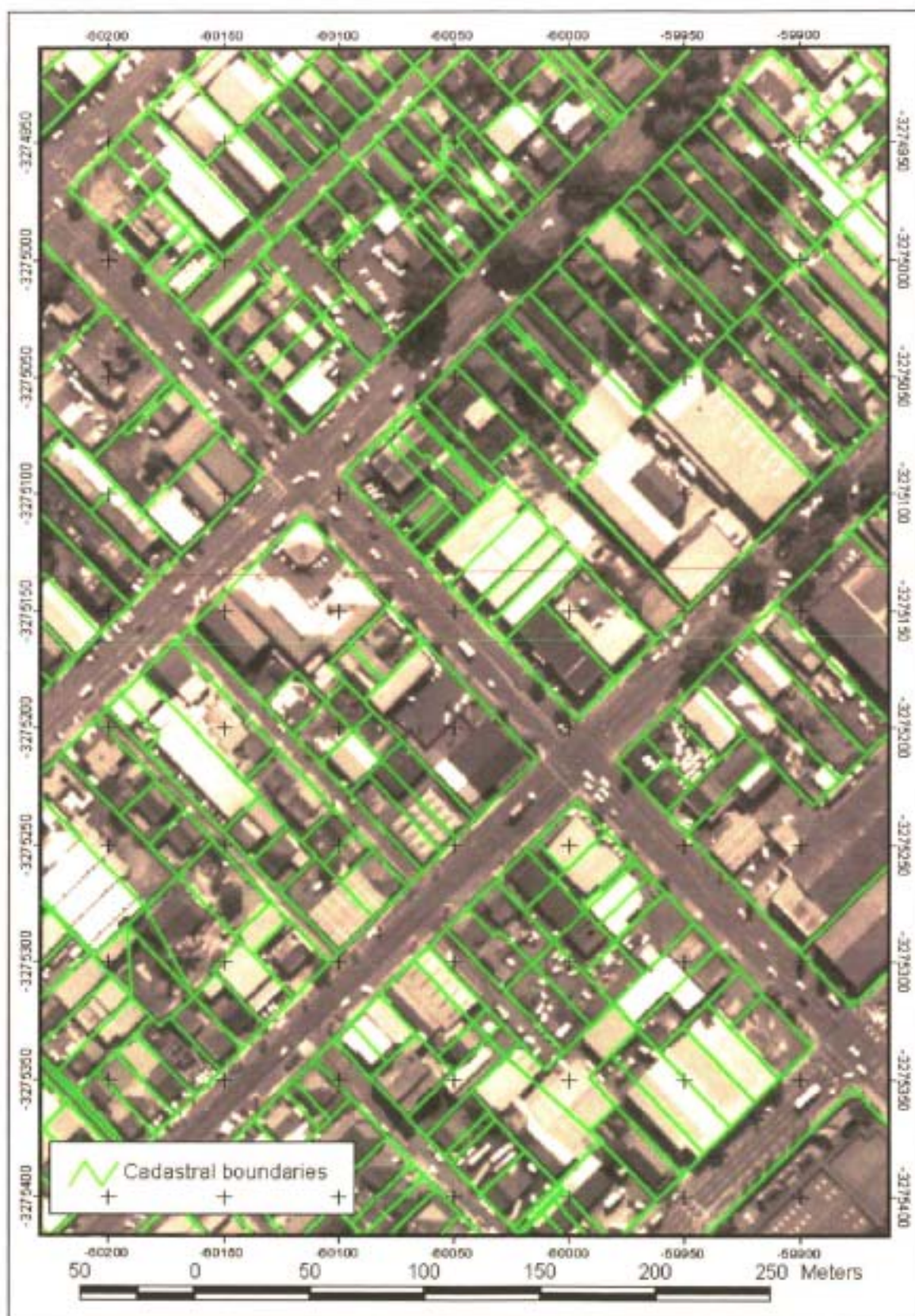


Figure 35: Example 4 of cadastral boundaries overlaid on digital camera orthophotographs.

Analysis of the digital camera orthophotos with the Pietermaritzburg cadastral boundary data overlaid indicated that the orthophotos were planimetrically accurate to an average of 5 to 10m. The maximum error encountered was 14m within the demarcated circular area 'a' in Figure 32. Based on the limited number of tie points used in the bundle block adjustment and the non-metric nature of the digital camera, these results were considered to be good. Imagery of this planimetric spatial accuracy would be suitable for many resource management applications, such as land use mapping, mapping of informal settlements, farm and area resource assessments, alien vegetation mapping and management, and forest fire damage assessment. If these images were used as base maps in a GIS for the mapping of land use and other data, the resulting GIS coverage would certainly be considerably more accurate than the 20 to 50m accuracy achievable with MBB's video based system. The timeliness of producing the end product would also be increased as discussed previously.

These results confirm the potential of using digital camera imagery for mapping and management applications where small areas are involved and a moderate spatial accuracy of 5 to 10m is required. Further improvements to the in-flight system, such as the incorporation of a tip roll sensor, and further experimentation with the use of digital camera images in Orthobase or similar software could produce even more favourable results.

## 7. DISCUSSION AND CONCLUSION

To determine whether the system developed was a success and could account for all the factors that could affect the capturing of high quality digital imagery, an evaluation of the complete system was performed. From the evaluation some recommendations for future improvements to the system were highlighted and final conclusions were drawn.

The pre-flight planning system was a vast improvement over the existing system. It provided an automated means of quickly and accurately calculating a flight plan of an area of interest for various camera and lens combinations. The number of flight lines and associated flying time for each combination could be calculated and the most appropriate option for a particular application could be selected. Variations in the terrain altitude could be accounted for by employing a DEM or by simply entering maximum, minimum and average altitudes for the area concerned. Situations where data could be lost due to the flight lines beginning or ending in the incorrect place were accounted for. The pre-flight system thereby contributed significantly to ensuring that the in-flight system captured imagery at the correct resolution and with the required percentage forward and side overlap. To further enhance the pre-flight system's efficiency and applicability the following possible improvements were identified:

- 1) Provide a means for the user to add and delete cameras and lenses, or change the specifications of the cameras and lenses currently available. This may take the form of a look up table in which the user can specify a particular camera's CCD size and number of pixels, or a lens's focal length, for example. This would make the program more universally applicable and avoid the need to adjust the actual program code when new cameras and/or lenses are purchased.
- 2) Add an algorithm that will allow the user to specify the flight strip spacing and hence calculate the remaining parameters relating to flying altitude, swath width, average pixel resolution, etc. The flight strip spacing, rather than the pixel resolution, was sometimes used by MBB as the main criterion in planning an aerial videographic survey.
- 3) Enhance the photograph spacing algorithm by excluding photographs within a particular flight strip that do not contain information pertaining to the area of interest. However, if the images were to be processed using a photogrammetric software package then

excluding images in the middle of a flight line may not be beneficial. Excluding these photographs will break up an otherwise continuous photograph/image block and increase the complexity of the bundle block adjustment process.

- 4) Improve the program's versatility by allowing the user to open files of the area's boundary with formats other than the generate file format currently supported. This will avoid the need for the user to have Arcview or ArcInfo software in order to create a generate file. Other formats which need to be considered include CAD formats such as dxf.
- 5) As an alternative to recommendation 4 above, the option of inputting a scanned, geographically referenced 1:50 000 topographical map into the pre-flight program and then digitising the area of interest's boundary from this map could be introduced. A generate or an equivalent file of the boundary could then be created within the pre-flight planning program and Arcview or ArcInfo would not be required
- 6) Include an estimate of the time to reach the survey area from a particular airport in the time summary form. This would aid the user in establishing the cost and time frame of a survey.
- 7) Add functionality to allow the user to define his/her own flight lines rather than the program simply calculating them without any user interaction. This would be useful when a line-type feature such as a river or road needs to be surveyed and a series of parallel, equally spaced flight lines is not the most economical means of obtaining imagery of the feature. To allow for such functionality, a scanned, geographically referenced map would be required and the user could then interactively click at intervals along the feature to be surveyed. The program would then attempt to optimise the number and direction of flight lines that would best achieve full coverage of the feature at the required resolution.

Examining the in-flight system, there were several factors which could affect the acquisition of high quality digital imagery. These factors could be divided into image sensor, GPS and operational factors and are listed below:

- 1) Image sensor - resolution, storage of imagery, camera response time and time to store imagery, the choice of lens, exposure control, and mounting of the camera.
- 2) GPS - accuracy and obtaining differential correction.
- 3) Operational - tip/roll and yaw of the aircraft, pilot error, flying height above ground level

and terrain altitude, ground speed of aircraft, and system power requirements.

While many of these factors have been discussed in detail in previous chapters, it is important to summarise how they have been accounted for in the system.

By incorporating the Kodak DCS420 digital camera, the resolution of the system developed was significantly better than the existing system. For a particular ground pixel resolution the Kodak DCS420 could offer approximately four times the area coverage per image when compared with the video-based system. This could dramatically reduce the post-flight processing and overall cost per survey since far fewer images are required to provide coverage of a particular area. However, it is recommended that to optimise the reduction in cost and turn-around time offered by digital cameras over a video-based system, a digital camera with the maximum possible resolution be used for a commercial system. The Kodak DCS460 would be such a camera, although other higher resolution cameras are likely to become available within the next 5 years.

The high resolution imagery captured by the Kodak DCS420 camera is stored on removable PCMCIA cards which can easily be replaced during flight. These cards are capable of storing upwards of 100 images per card, thereby ensuring that the in-flight operation will not be hampered by continuously having to change these cards. Replacing these cards on a regular basis would dramatically increase the flying time and reduce the cost effectiveness of the survey since turns would have to be made each time a card is to be replaced. The format in which the camera stores the images on the card also assists in reducing the memory requirements and intervals at which PCMCIA cards have to be changed. For each pixel of an image only one of the red, green and blue spectral bands is stored on the card. When downloading the images from the card after the flight the other two spectral bands are interpolated from the surrounding pixels. By storing the images in this manner the storage capacity required per image is reduced by a factor of 3.

The SLR functionality of the Kodak DCS420 allowed for different lenses to be used and permitted control over the exposure of the imagery. Narrow angle lenses would be required for mountainous areas to minimise the distortion in the imagery due to changes in terrain altitude, while wide angle lenses would be employed where maximum area coverage per flight line is required. Exposure control could be important when operating under broken cloud conditions where the contrast

between areas shadowed by cloud and sunlit areas could result in over or under exposure of sections of an image. This could lead to loss of data and may result in the survey having to be re flown.

The camera response time or, in other words, the delay between sending a signal to the camera to trigger and the camera actually capturing an image could not be accounted for. No data regarding this delay was available and no method of measuring the delay could be established. Similarly, the time required to store an image before another image can be captured could not be accounted for or removed in the in-flight system. This would have to be considered as a major limitation of currently available digital cameras for use in aerial surveying. To avoid situations where the continuous capture rate of a camera is likely to be exceeded it is recommended that the pre-flight planning program be altered to warn users of such situations. However, it is anticipated that as digital camera technology continues to improve and evolve this limitation will be addressed.

In terms of the camera mount, the ultimate would have been to have a gyro-stabilised mount that maintained the camera in a vertical plane regardless of tip and roll of the aircraft. Unfortunately, no such mount was available that could accommodate the Kodak DCS420 and developing a gyro-stabilised mount would have been too costly. Consequently, a simple mount that maintained the camera in a stable position and that limited the vibration that could affect the capturing of good quality imagery was designed and built. This mount was designed specifically for the Piper Twin Comanche used by MBB for their video surveys. This was not ideal since other aircraft might need to be used when the Piper Comanche is grounded or unavailable and not all aircraft would have a similar port to the Piper Comanche suitable for mounting cameras with an unobstructed view of the ground. The development of a 'universal' camera mount is therefore recommended. One possibility would be to build an adjustable mount that could be fitted in the luggage port present towards the rear of most light aircraft.

The GPS was to be an integral part of the system and a vital consideration was the GPS's spatial accuracy. A standard GPS was unsuitable since it could only offer an accuracy of 50m horizontally. After considering the advantages and disadvantages of differential and carrier phase GPS, differential GPS (DGPS) was chosen. The documented 2 to 5m accuracy of DGPS was considered to be suitable for the purposes of the system. Having identified DGPS as the system

of choice, the methods of obtaining the differential signal had to be considered. Obtaining the differential signal in real-time was a pre-requisite to allow accurate triggering of the camera at the pre-calculated positions. While the Real-Time Correction Message (RTCM) could be sent via radio link from a base station to the aircraft, this would require the establishment and running of one's own base station for each survey performed. Since the base station should be within 300 km of the rover station at all times, this would require moving the base station at regular intervals which would be both costly and time-consuming. Furthermore, finding a site where the base station could transmit the RTCM to the aircraft without any interference could be difficult. Consequently, the Trimble Pro-XRS GPS with its integrated GPS and satellite RTCM receiver was chosen. Using the Pro-XRS unit it was possible to receive the RTCM, which is generated from data obtained from permanent base stations situated in several South African towns, via satellite. This removed the need to set up a base station or purchase expensive radio transmission equipment.

There were also several operational factors which had to be considered and accounted for. Tip and roll of the aircraft could affect the acquisition of imagery with the required forward and side overlap and could also cause geometric distortions in the imagery. As previously mentioned the ideal solution to this problem would be to place the camera in a gyro-stabilised mount. However, this was not feasible and other possibilities would have to be considered. To remove the geometric distortions caused by aircraft tip and roll, two options exist. If photogrammetric software is used for post-flight image rectification then the geometric distortions caused by aircraft tip or roll are removed during the process of image rectification. However, as discovered if the tip and roll are excessive then the automation of the photogrammetric process is not possible. Therefore, the alternative of incorporating a low cost, reliable tip/roll sensor into the in-flight system needs to be investigated in future research. The tip and roll of the aircraft and camera at the time of exposure could then be recorded and the geometric distortions subsequently removed by implementing an affine transformation. To minimise the potential for loss of data due to tip and roll the pre-flight planning program could be used to plan the survey with an additional 5 or 10% overlap to that required. The additional cost associated with flying the survey with extra overlap and processing a greater number of images would have to be considered.

The error introduced due to the pilot not being able to fly exactly along a planned flight line could never be completely removed, however it could be minimised. The existing Garmin GPS provided a simple error bar display to assist the pilot in navigating along a flight line, but due to this GPS's limited accuracy of 50m the pilot could at best fly within an average of 50m of the flight line. Development of a unit that could provide a 'heads-up' display based on the sub-metre accuracy output from the Trimble Pro-XRS should therefore be considered. The NMEA strings from the Pro-XRS could be used in a program to calculate the distance left or right of the planned flight line and this information could then be displayed on a flat panel VGA display mounted on the aircraft dashboard. Alternatively, a dashboard mounted strip of different coloured LEDs could be used. By using the Trimble Pro-XRS output for both camera control and navigation the Garmin GPS would not be required and the manual input of way point coordinates would also not be necessary. A further refinement in this regard would be to log the flightpath flown either on a computer or on the GPS itself. Having the flightpath would further assist in post-flight analysis of the survey and in the process of image rectification. Areas where image overlap may be minimal could also be immediately identified.

The flying height above ground level affects the percentage forward and side overlap achieved. Maintaining a constant height above ground level while flying is impractical and consequently the effect of variation in terrain altitude on the percentage overlap had to be accounted for in the pre-flight planning system. The user had the option to use a DEM to calculate maximum, minimum and average altitudes for the survey area or input these figures manually. The program then used these altitudes to calculate the minimum, maximum and average percentage overlaps for the survey area and insured that the flight line spacing and photograph spacing used was such that the minimum percentage overlap specified by the user was not exceeded. In this manner the effect of a variable flying height AGL could be accounted for.

The ground speed of the aircraft could also affect the percentage forward overlap between consecutive photographs. At higher ground speeds the time between consecutive photograph or image centres is reduced. If a simple timer was used to trigger the camera at regular intervals along a flight line then the percentage forward overlap between images could vary due to variable wind speeds and directions. However, the in-flight system developed made use of one second updates of position and speed from the GPS to calculate when to trigger the camera. In so doing,



the effect of wind speed and direction on the aircraft's ground speed, and hence the forward overlap between images, was minimised. The only other consideration would be situations where a strong tail wind increases the aircraft's ground speed to such an extent that the continuous capture rate of the camera is exceeded. Such a situation was not accounted for in the system developed. To account for such situations the ground speed output from the GPS would have to be monitored and a warning given if the speed increased to a pre-calculated threshold value. The aircraft would then have to be slowed down to compensate for the tail wind or the flight line would have to be flown in the opposite direction, in other words, into the prevailing wind.

A final in-flight operational issue was the electrical power requirements of the system. A shortage of power had been encountered when operating the videographic system with two cameras and two VCRs and it had to be insured that similar problems were not encountered with the system developed. All components of the in-flight system developed could be run off their own battery power. The Kodak DCS420 had sufficient battery power for capturing 1000 images, while the Trimble GPS could operate for approximately 5 hours on one set of rechargeable batteries. The camera would therefore be able to capture 1m pixel resolution imagery with 60% forward overlap and 30% sidelap of an area of approximately 400km<sup>2</sup> before a new battery would be required. The GPS batteries would have to be replaced after surveying an area of approximately 600km<sup>2</sup>. This was deemed to be acceptable, particularly considering the ease with which the camera and GPS batteries could be replaced during flight. A laptop running the in-flight camera control software could be operated off battery power, although it would probably be limited to shorter periods of use than the camera or GPS. The inclusion of a DC-AC inverter would be advisable in order for the laptop to be operated for longer periods off the 12V aircraft battery.

Evidently most factors affecting the in-flight system were accounted for or could be accounted for through future refinement of the system. Furthermore, all requirements for the system as set out by MBB at the start of the project were met.

The system developed was certainly more automated and could produce imagery with an improved spatial resolution when compared with the videographic system. These aspects have been discussed above. Whether the cost of performing a survey and producing maps of the resource of interest would be reduced is difficult to determine. The cost-benefit analysis suggested

that the digital camera system was more cost-effective than a video-based system, however it should be remembered that MBB's post-flight system did not involve production of digital imagery or geographical referencing of the imagery. Mapping was done off the raw video data onto base maps in a GIS, thereby reducing the post-flight map production costs to the R/h cost of a technician to perform the mapping and the cost of purchasing or producing geographically referenced base maps. This methodology would result in similar or lower R/ha costs to those obtained for the DCS420 digital camera system at 1m pixel resolution.

In terms of the spatial accuracy of mapping, the digital camera system developed would produce maps with significantly improved spatial accuracy. The video system's spatial accuracy was estimated at 20 to 50 metres and would depend to a large extent on the experience of the technician. On the other hand, mapping directly off digital camera images rectified using photogrammetric software would increase the spatial accuracy to approximately 5-10 metres. Furthermore, the mapping process would in all likelihood become more timely since the visual transfer of data from the raw image data to a base map in a GIS would be eliminated. The time required to collect the GCPs for image rectification may influence the overall timeliness of the new system, though. This would be particularly true in inaccessible or mountainous areas.

While it was clear from the cost-benefit analysis that the resolution of digital cameras will have to increase substantially to become cost-effective and timely alternatives to 9" photography, the rate at which digital camera technology is currently evolving suggests that they may become an option as an airborne sensor within the next 10 years. A few of the limitations of high resolution digital cameras, such as the poor continuous image capture rate and large storage capacity requirement of high resolution imagery, will have to be overcome if they are to be used effectively for aerial survey applications though.

A further consideration is the anticipated establishment of a low level satellite network that will produce high resolution, multispectral imagery with a wide area coverage. While the details and costs of such a system were not available, it is conceivable that low cost, sub-metre resolution satellite imagery could become a reality within the next decade. If this satellite system does materialise then digital cameras may not be the best alternative to 9" photography, particularly if one considers that imagery of the same area could be captured at regular intervals using these

satellites. In addition, the availability of multispectral imagery without the need to purchase several sensors or fly an area several times with a single sensor and different filters could make satellite imagery a very attractive option. The factors that will determine the possibility of satellite imagery being used extensively will be the cost of the satellite imagery and the speed with which data from the satellites would be available for use.

Present satellite systems offer only modest resolutions of 10m or coarser and the imagery is expensive on a cost per area basis. The imagery from these newer low level satellite systems would therefore be expected to be more expensive. However, if several companies or organizations required the same image data then they could collaborate to buy the data. An added advantage of a higher resolution satellite system becoming a reality would be that the data from the poorer resolution satellite systems would have to become cheaper in order to remain competitive. This lower resolution imagery would then become a more viable and cost-effective alternative than it is at present for applications requiring lower resolution imagery such as large-scale hydrological modelling.

The speed with which the satellite data could be made available will also be very important for resource management applications requiring solutions in a short period of time. These applications would include crop disease detection, fire damage assessment and water pollution evaluation. The volume of data produced by a high resolution satellite network, particularly if it offers multispectral capabilities, will require a significant amount of processing and quality checking prior to the imagery becoming available. This may make this system unsuitable for quick turn-around applications and would leave digital cameras to fill this niche market.

In conclusion it can be surmised that the future of digital cameras in airborne remote sensing is uncertain. If digital cameras can improve to closely match the resolution of 9" photography then the use of traditional air photography in a GIS-based management system will decrease considerably. However, at all times the advancements in satellite technology will have to be monitored. Similarly, the improvements in the precision and widespread availability of GPS will have to be continuously reviewed. Due to these rapid improvements and changes in the technology associated with the components of an airborne remote sensing system, the cost effectiveness and applicability of any system developed will have to be examined on a continuous basis through

research on the internet and via consultation with experts in the field of airborne remote sensing and GIS-based management. While it would be ideal to replace a component of the system as soon as a better alternative became available on the market, this would not be feasible in terms of integrating the new component into the existing system, nor cost effective. Consequently, it is the author's opinion that the components of a system should remain unchanged for a period of 3 to 5 years, whilst always keeping track of technological developments. After this 3 to 5 year period the decision to replace or keep a component should be based on similar analyses to those described in the previous chapters.

## 8. REFERENCES

- Ackermann, F., 1996. Digital photogrammetry: challenge and potential. Commentary in *Photogrammetric Engineering and Remote Sensing*, June, pp. 679.
- Ackermann, F. and Schade, H., 1993. Application of GPS for aerial triangulation. *Photogrammetric Engineering and Remote Sensing*, 59 (11): 1625-1632.
- Anon, 1999a. Kodak DCS260 FAQ and technical information [Internet]. Available from: <<http://www.trix.com/dc260/#6.reaction-time>> [Accessed February 1999].
- Anon, 1999b. [Internet] Available from: <<http://www.ipi.uni-hannover.de/serv/bluh.htm>> [Accessed 1 May 1999].
- Becker, R.D. and Barriere, J.P., 1993. Airborne GPS for photo navigation and photogrammetry: an integrated approach. *Photogrammetric Engineering and Remote Sensing*, 59 (11): 1659-1665.
- Benkelman, C., 1999. Personal communication. Positive Systems, Inc., 250 Second Street East, Whitefish, Montana 59937. E-mail: [positive@possys.com](mailto:positive@possys.com).
- Bobbe, T., 1992. Real-time differential GPS for aerial surveying and remote sensing. *GPS World*, July/August: 18-22.
- Bobbe, T., Reed, D. and Schramek, J., 1993. Georeferenced airborne video imagery. *Journal of Forestry*, August: 34-37.
- Brodie, J.R., 1998. Personal communication. Formerly of MBB Consulting Engineers, Inc., 165 Boom Street, Pietermaritzburg, 3100, South Africa. Now of Land Resources International, PO Box 252, Pinetown, 3600, South Africa. E-mail: [jbrodie@lri.co.za](mailto:jbrodie@lri.co.za).

- Brodie, J.R., 1999. Personal communication. Formerly of MBB Consulting Engineers, Inc., 165 Boom Street, Pietermaritzburg, 3100, South Africa. Now of Land Resources International, PO Box 252, Pinetown, 3600, South Africa. E-mail: jbrodie@lri.co.za.
- Brownlie, R.K., Firth, J.G. and Hosking, G., 1996. Potential of airborne video for updating forest maps. *New Zealand Forestry*, May: 37-40.
- Burnside, C.D., 1979. Mapping from aerial photographs, p. 93. Granada Publishing Limited - Technical Books Division, 3 Upper James Street, London W1R 4BP, England.
- Colombo, O.L. and Peters, M.F., 1992. Precision long-range DGPS for airborne surveys. *GPS World*, April: 44-50.
- Colomina, 1993. A note on the analytics of aerial triangulation. *Photogrammetric Engineering and Remote Sensing*, 59 (11): 1619-1624.
- Corel, 1997. Corel WordPerfect Suite 8 - Academic package. Corel Corporation, 1600 Carling Avenue, Ottawa, Ontario, Canada, K1Z 8R7.
- Cosandier, D., Chapman, M.A. and Ivanco, T., 1993. Low cost attitude systems for airborne remote sensing and photogrammetry. *Proceedings of the GIS'93 Conference*, Ottawa, Canada, March, 1993, pp. 295-303.
- Craigie, D., 1999. Personal communication. GIMS Photogrammetry, PO Box 652, Halfway House, South Africa, 1685. E-mail: dcraigie@gims.com.
- Craigie, D., 2000. Personal communication. GIMS Photogrammetry, PO Box 652, Halfway House, South Africa, 1685. E-mail: dcraigie@gims.com.
- Curry, S. and Schuckman, K., 1993. Practical considerations for the use of airborne GPS for photogrammetry. *Photogrammetric Engineering and Remote Sensing*, 59 (11): 1611-1617.

- Erdas, 1999. IMAGINE Orthobase User's Guide. ERDAS, Inc., 2801 Buford Highway, NE, Suite 300, Atlanta, Georgia 30329-2137 USA.
- Esri, 1998. Arcview GIS version 3.0a. Environmental Systems Research Institute, 380 New York Street, Redlands, CA 92373-8100, USA. <<http://www.esri.com>>
- Evans, D.L., 1992. Using GPS to evaluate aerial video missions. *GPS World*, July/August, pp. 24-29.
- Fogler, H.S. and LeBlanc, S.E., 1995. Strategies for creative problem solving. Prentice Hall PTR, Prentice-Hall, Inc., Englewood Cliffs, New Jersey, 07632, USA.
- Fraser, C.S., 1997. Digital camera self-calibration. *ISPRS Journal of Photogrammetry and Remote Sensing*, 52: 149-159.
- Garmin, 1999. Garmin Corporation home page [Internet]. Available from: <<http://www.garmin.com>> [Accessed February 1999]
- Graham, L.A., 1993. Airborne video for near-real-time vegetation mapping. *Journal of Forestry*, August: 28-32.
- Gruen, A., Cocard, M. and Kahle, H.G., 1993. Kinematic GPS: Results of a high accuracy test. *Photogrammetric Engineering and Remote Sensing*, 59 (11): 1643-1650.
- Heipke, C., 1995. State-of-the-art of digital photogrammetric workstations for topographic applications. *Photogrammetric Engineering and Remote Sensing*, 61 (1): 49-56.

- Hoppus, M. and Evans, D., 1997. Using videography and digital cameras for aerial applications. Notes from the workshop entitled "Aerial videography and digital cameras for resource applications" held at the *1997 ASPRS/ACSM Annual Convention*, Seattle, Washington, USA, April 7-10. American Society for Photogrammetry and Remote Sensing, 5410 Grosvenor Lane, Suite 210, Bethesda, Maryland 20814-2144, USA.
- Horita, 1998. Horita home page [Internet]. Horita Co., Inc., PO Box 3993, Mission Viejo, California, 92690, USA. Available from: <<http://www.horita.com>> [Accessed February 1998]
- Hurn, J., 1989. GPS: A guide to the next utility. Trimble Navigation Limited, 645 North Mary Ave., P.O. Box 3642, Sunnyvale, California 94088-3642, USA.
- Hurn, J., 1993. Differential GPS explained. Trimble Navigation Limited, 645 North Mary Ave., P.O. Box 3642, Sunnyvale, California 94088-3642, USA.
- Jadkowski, M.A., Convery, P., Birk, R.J. and Kuo, S., 1994. Aerial image databases for pipeline rights-of-way management. *Photogrammetric Engineering and Remote Sensing*, 60 (3): 347-353.
- Johnston, C.A., Bonde, J., and Sersland, C.A., 1997. Development of a GIS-linked airborne video system for the construction of georeferenced GIS databases [Internet]. Available from: <<http://www.nrri.umn.edu/video/airvideo.ms>> [Accessed September 1997].
- King, D.J., 1995. Airborne multispectral digital camera and video sensors: a critical review of system designs and applications. *Canadian Journal of Remote Sensing*, 21 (3): 245-273.
- King, D.J., 1997. Low cost multispectral digital camera imaging for forest modelling and topographic mapping. *Proceedings of Third International Airborne Remote Sensing Conference and Exhibition*, 7-10 July, Copenhagen, Denmark.



- King, D.J., 1999. Personal communication. Department of Geography and Environmental Studies, Carleton University, 1125 Colonel By Drive, Ottawa, Ontario, K1S 5B6, Canada. E-mail: doug\_king@carleton.ca.
- King, D.J., Armenakis, C. and Chichagov, A., 1995. The use of airborne digital frame camera imagery for DEM generation. *Geomatica*, 49 (4): 489-497.
- King, D.J., Haddow, K. and Pitt, D.G., 1997. Evaluation of CIR digital camera imagery in regeneration assessment: research design and initial results. *Proceedings of 1<sup>st</sup> North American Symposium on Small Format Aerial Photography*, Cloquet, Minnesota, USA, October, pp. 186-195. Hosted by ASPRS, Bethesda, Maryland, USA.
- King, D.J., Walsh, P. and Ciuffreda, F., 1994. Airborne digital frame camera imaging for elevation determination. *Photogrammetric Engineering and Remote Sensing*, 60 (11): 1321-1326.
- King, D.J., 1999. Personal communication. Department of Geography and Environmental Studies, Carleton University, 1125 Colonel By Drive, Ottawa, Ontario, K1S 5B6, Canada. E-mail: doug\_king@carleton.ca.
- Kodak, -. Kodak Professional EOS-DCS1 and DCS 460 digital cameras product brochure. Eastman Kodak Company, 343 State Street, Rochester, New York, 14650, USA.
- Kodak, 1998. Eastman Kodak home page [Internet]. Eastman Kodak Company, 343 State Street, Rochester, New York, 14650, USA. Available from: <<http://www.kodak.com>> [Accessed 20 February 1998]
- Kodak, 1999. Personal communication. Eastman Kodak Company, 343 State Street, Rochester, New York, 14650, USA.

- Krzystek, P., Heuchel, T., Hirt, U. and Petran, F., 1999. An integral approach to automatic aerial triangulation and automatic DEM generation [Internet]. INPHO GmbH, Smaragdweg 1, D-70174, Stuttgart, Germany. Available from: <[http://www.inpho.de/pk/v10\\_www.html](http://www.inpho.de/pk/v10_www.html)> [Accessed 13 January 1999] E-mail: [inpho@inpho.de](mailto:inpho@inpho.de).
- Lang, L., 1996. Geotechnology use grows in California's ag community. *Earth Observation Magazine*, October, pp. 17-20.
- Light, D.L., 1996. Film cameras or digital sensors? The challenge ahead for aerial imaging. *Photogrammetric Engineering and Remote Sensing*, 62 (3): 285-291.
- Light, D.L., 1997. A digital 3K x 2K array camera for reconnaissance and mapping. For presentation at the *1997 ASPRS/ACSM Annual Convention*, Seattle, Washington, USA, April 7-10. American Society for Photogrammetry and Remote Sensing, 5410 Grosvenor Lane, Suite 210, Bethesda, Maryland 20814-2144, USA.
- Linden, D.S., Hoffer, R.M., Pywell, H.R., Paschke, J.L. and Bobbe, T.J., 1996. Automated digital mosaicing of airborne videography. Forest Health Technology Enterprise Team - Fort Collins, 3825 East Mulberry, Fort Collins, Colorado, 80524, USA.
- Maas, H. and Kersten, T., 1997. Aerotriangulation and DEM/orthophoto generation from high resolution still-video imagery: On the potential of digital cameras onboard an aircraft. *Photogrammetric Engineering and Remote Sensing*, 63 (9): 1079-1084.
- Mason, S., 1997. Low cost information technology options for tackling South Africa's housing problems. *IMIESA: Official journal of the Institution of Municipal Engineering of Southern Africa*, 22 (11): 3-8. E-mail: [mason@engfac.uct.ac.za](mailto:mason@engfac.uct.ac.za).
- Mason, S., Ruther, H. and Smit, J., 1997. Investigation of the Kodak DCS460 digital camera for small-area mapping. *ISPRS Journal of Photogrammetry and Remote Sensing*, 52: 202-214.

- Mausel, P.W., Everitt, J.H., Escobar, D.E. and King, D.J., 1992. Airborne videography: current status and future perspectives. *Photogrammetric Engineering and Remote Sensing*, 58 (8): 1189-1195.
- Meisner, D.E. and O.M. Lindstrom, 1985. Design and operation of a color infrared aerial video system. *Photogrammetric Engineering and Remote Sensing*, 51 (5): 555-560.
- Merchant, D.C. and Tudhope, R.L., 1994. Demonstration of selected aspects of a utility mapping system (UMS). Internal Report: Topo Photo Inc., Upper Arlington, Ohio, USA; Ontario Hydro, Surveys and Mapping Division, Toronto, Ontario, Canada, pp. 18.
- Mills, J.P. and Newton, I., 1996. A new approach to the verification and revision of large-scale mapping. *ISPRS Journal of Photogrammetry and Remote Sensing*, 51: 17-27.
- Monday, H.M., Urban, J.S., Mulawa, D. and Benkelman, C.A., 1994. City of Irving utilizes high resolution multispectral imagery for N.P.D.E.S. compliance. *Photogrammetric Engineering and Remote Sensing*, 60: 411-416.
- Moore, I.D., Grayson, R.B., and Ladson, A.R., 1991. Digital terrain modelling: a review of hydrological, geomorphological, and biological applications. *Hydrological Processes*, 5: 3-30.
- Myhre, R.J., Graham, L.A. and Sumpter, C.W., 1990. Airborne video technology. *Proceedings of 3<sup>rd</sup> Forest Service Remote Sensing Applications Conference*, Slidell, Mississippi, pp. 242-252.
- Olthof, I. and King, D.J., 1997. Evaluation of textural information in airborne CIR digital camera imagery for estimation of forest stand leaf area index. *Proceedings of 1<sup>st</sup> North American Symposium on Small Format Aerial Photography*, Cloquet, Minnesota, USA, October, pp. 154-164. Hosted by American Society for Photogrammetry and Remote Sensing, 5410 Grosvenor Lane, Suite 210, Bethesda, Maryland 20814-2144, USA.

- Oltman, D., 1996a. Lofty image. *California Farmer*, January, pp. 8-9, 44 .
- Oltman, D., 1996b. Vine spacing. *California Farmer*, April, pp. 8-9, 79-80, 82, 84.
- Omnistar, 1998. Omnistar GPS technical discussion [Internet] OmniSTAR, Inc.  
8200 Westglen, Houston, TX 77063. Available from: <<http://www.omnistar.com/tech.html>> [Last accessed 15 Nov 1999].
- Positive Systems, 1996. *The Digital Flyer* brochure, Summer 1996. Positive Systems, 250 Second Street East, Whitefish, Montana, 59937, USA. E-mail: [positive@possys.com](mailto:positive@possys.com)
- Positive Systems, 1997. *The Digital Flyer* brochure, Winter 1997. Positive Systems, 250 Second Street East, Whitefish, Montana, 59937, USA. E-mail: [positive@possys.com](mailto:positive@possys.com)
- Positive Systems, 1998. Personal communication. Positive Systems, 250 Second Street East, Whitefish, Montana, 59937, USA. E-mail: [positive@possys.com](mailto:positive@possys.com)
- Pywell, H.R. and Myhre, R.J., 1992. Monitoring forest health with airborne videography. Proceedings of IUFRO Conference, Canberra, Australia. IUFRO Secretariat, c/o Federal Forest Research Institute, Seckendorff-Gudent-Weg 8, A-1131 Vienna, Austria.
- Schenk, T., 1996. Current status and future directions of digital photogrammetry: a personal view. Commentary in *Photogrammetric Engineering and Remote Sensing*, June 1996, pp. 682.
- Scion, 1998. Scion Image acquisition and analysis software [Internet]. Scion Corporation, 82 Worman's Mill Court, Suite H, Frederick, Maryland 21701, USA. Available from: <[http://www.scioncorp.com/frames/fr\\_scion\\_products.htm](http://www.scioncorp.com/frames/fr_scion_products.htm)> [Last accessed September 1998].
- Schwarz, K.P., Chapman, M.A., Cannon, M.W. and Gong, P., 1993. An integrated INS/GPS approach to the georeferencing of remotely sensed data. *Photogrammetric Engineering and Remote Sensing*, 59(11): 1667-1674.

- Seed, E.D. and King, D.J., 1997. Determination of mixed boreal forest stand biophysical structure using large scale airborne digital camera imagery. *Proceedings of the International Symposium on Geomatics in the Era of Radarsat*, Ottawa, Canada, May, paper no.75.
- Smith, M., 1998. Personal communication. Optron, P.O. Box 1858, Westville, 3630, South Africa. E-mail: mark@optron.com.
- Tang, L., Braun, J. and Debitsch, R., 1997. Automatic aerotriangulation - concept, realisation and results. *ISPRS Journal of Photogrammetry & Remote Sensing*, 52: 122-131.
- Thomas, M., 1996a. The development and assessment of a GPS integrative technique for georeferencing video remote sensing imagery through trials. FOR-650, unpublished CSIR report. CSIR, PO Box 395, Pretoria, 0001, South Africa.
- Thomas, M., 1996b. Georeferencing airborne video imagery independently from maps using differentially-corrected global positioning coordinates. *South African Journal of Geo-information*, 17(2): 27-34.
- Topolniski, K. and Roussell, T.G., 1994. Evaluation of spatially referenced video technology for forest database updating. Fraser Inc., 27 Rice Street, Edmunston, N.B., E3V 1S9.
- Toth, C.K., 1997. Airborne Integrated Mapping System. *Proceedings of the 1997 ASPRS-ACSM Annual Convention*, Seattle, USA, vol 3, pp. 674-680. E-mail: toth@cfm.ohio-state.edu
- Toth, C.K. and Krupnik, A., 1996. Concept, implementation, and results of an automatic aerotriangulation system. *Photogrammetric Engineering and Remote Sensing*, 62 (6): 711-717.
- Trimble, 1997. A new level of accuracy for differential GPS mapping applications using EVEREST™ multipath rejection technology. Trimble Navigation Limited, Mapping and GIS Systems Division, 645 North Mary Avenue, Sunnyvale, CA 94088-3642, USA.

- Trimble, 1998. GPS Pathfinder Pro XRS [Internet] Trimble Navigation Limited, Mapping and GIS Systems Division, 645 North Mary Avenue, Sunnyvale, CA 94088-3642, USA. Available from: <[http://www.trimble.com/products/catalog/gis/pro\\_xrs.htm](http://www.trimble.com/products/catalog/gis/pro_xrs.htm)> [Last accessed 05/06/2000]
- Tsai, R.Y., 1987. A versatile camera calibration technique for high-accuracy 3D machine vision metrology using off-the-shelf TV cameras and lenses. *IEEE Journal of Robotics and Automation*, RA-3 (4), August: 323-344.
- Tsai, R.Y., 1998. Tsai camera calibration software [Internet] Available from: <<http://www.cs.cmu.edu/afs/cs.cmu.edu/user/rgw/www/TsaiCode.html>> [Accessed 25/2/99].
- TurboPower, 1998. Async Professional Reference Guide. TurboPower Software Company, PO Box 49009, Colorado Springs, CO, 80949-9009, USA. See <[www.turbopower.com](http://www.turbopower.com)>.
- Will, J.D., 1999. Personal communication. E-mail: [esq@ews.uiuc.edu](mailto:esq@ews.uiuc.edu).
- Wilson, D.L., 1999. GPS accuracy web page [Internet] Available from: <<http://users.erols.com/dlwilson/gps.htm>> [Accessed 6/12/99].
- Wood, G.A., 1999. Personal communication. Institute of AgriTechnology, Cranfield University, Silsoe, Bedfordshire MK45 4DT. E-mail: [g.a.wood@cranfield.ac.uk](mailto:g.a.wood@cranfield.ac.uk).
- Wooding, R., 1998. Personal communication. Rob Wooding and Associates, 21 Pearson Road, Everton, 3610, Kwazulu-Natal, South Africa.
- Wunneberger, D.F., 1992. Automating geographically referenced digital mosaics from aerial videography with area based feature matching. Ph.D. Thesis, Texas A&M University, College Station, TX. 77845, USA. E-mail: [douglas@rsgis4.tamu.edu](mailto:douglas@rsgis4.tamu.edu).